ENVIRONMENTALLY TUNING ASPHALT PAVEMENTS USING PHASE CHANGE MATERIALS: BENEFITS, DESIGN, AND CHALLENGES

by

Miguel A. Montoya

A Dissertation

Submitted to the Faculty of Purdue University

In Partial Fulfillment of the Requirements for the degree of

Doctor of Philosophy

Lyles School of Civil Engineering

West Lafayette, Indiana

December 2021

THE PURDUE UNIVERSITY GRADUATE SCHOOL

STATEMENT OF COMMITTEE APPROVAL

Dr. John E. Haddock, Chair

Lyles School of Civil Engineering

Dr. Jan Olek

Lyles School of Civil Engineering

Dr. Luna Lu

Lyles School of Civil Engineering

Dr. Jusang Lee

Indiana Department of Transportation

Approved by:

Dr. Dulcy Abraham

To my parents Carlos and America,
and to the Alpha and the Omega,
the First and the Last, the Beginning and the End

ACKNOWLEDGMENTS

First, I would like to express my sincere gratitude to my academic advisor and mentor, Dr. John E. Haddock. The completion of this study could not have been possible without Dr. Haddock's immense knowledge and plentiful experience. His unparalleled support, patience, and advice have encouraged me throughout the research and writing of this Ph.D. dissertation and made my time at Purdue incredibly satisfying and enriching.

I would like to express my most profound appreciation to my examination committee members, Dr. Jan Olek, Dr. Luna Lu, and Dr. Jusang Lee, for serving on my Ph.D. committee and their assistance at every stage of this doctoral work and insightful comments and suggestions. I am deeply grateful to Dr. Rebecca McDaniel for her valuable support toward developing this research and lasting impression on this journey.

I would like to acknowledge the financial support of the Indiana Department of Transportation (INDOT) under the SPR-4335 Joint Transportation Research Program (JTRP) project and Partnership to Enhance General Aviation Safety, Accessibility and Sustainability (PEGASAS), a Federal Aviation Administration (FAA) Center of Excellence for General Aviation, under Project 27, Heated Pavements Phase Change Materials. I also wish to thank all the researchers within the Innovative Materials and Pavements Group, Lyles School of Civil Engineering, and Purdue College of Engineering, with whom I have had the pleasure to work on completing the projects mentioned above.

Special thanks go to my colleagues and friends at Purdue University. I would also like to extend my deepest gratitude to my God and family for their unconditional love, encouragement, support, and prayers, especially to my parents, Carlos and America, siblings, Carlos, Arturo, and Herta, and grandmother, America.

TABLE OF CONTENTS

LIST OF TABLES

LIST OF FIGURES

LIST OF ABBREVIATIONS

APE	Absolute Percentage Error
V_a	Air Voids Content
AASHTO	American Association of State Highway and Transportation Officials
P_b	Asphalt Binder Content
AADT	Average Annual Daily Traffic
BBR	Bending Beam Rheometer
G_{sb}	Bulk Specific Gravity
G*	Complex Shear Modulus
CPCM	Composite Phase Change Material
S_{app}	Cyclic Fatigue Index Parameter
ΔT_c	Delta Tc
DSC	Differential Scanning Calorimeter
DW	Durbin-Watson
DBR	Dust-to-Binder Ratio
DSR	Dynamic Shear Rheometer
P_{be}	Effective Asphalt Binder Content
ESAL	Equivalent Single Axle Load
FAA	Federal Aviation Administration
FHWA	Federal Highway Administration
FEM	Finite Element Model
AR(1)	First-Order Autoregressive
FTIR	Fourier-Transform Infrared Spectroscopy
INDOT	Indiana Department of Transportation
JTRP	Joint Transportation Research Program
LCD	Local Climatological Data
LWA	Lightweight Aggregate
LAS	Linear Amplitude Sweep
MAPE	Mean Absolute Percentage Error

μPCM	Microencapsulated Phase Change Material
μPCM-43	Microencapsulated Phase Change Material with a Transition Temperature of 43°C
MADM	Multiple Attribute Decision Making
MSCR	Multiple Stress Creep Recovery
NAPA	National Asphalt Pavement Association
NMPS	Nominal Maximum Particle Size
N_{des}	Number of Design Gyrations
OLS	Ordinary Least Squares
PEGASAS	Partnership to Enhance General Aviation Safety, Accessibility and Sustainability
PCM	Phase Change Material
PAV	Pressure Aging Vessel
PCS	Primary Control Sieve
PVD	Probability of Volumetric Discrepancy
QA	Quality Assurance
QC	Quality Control
QQ	Quantile-Quantile
SEM	Scanning Electron Microscope
SCS	Secondary Control Sieve
SURE	Seemingly Unrelated Regression Equations
SCB	Semi-Circular Bend
SSPCM	Shape-Stabilized Phase Change Material
SHRP	Strategic Highway Research Program
SGC	Superpave Gyratory Compactor
RAP	Reclaimed Asphalt Pavement
RAS	Reclaimed Asphalt Shingles
RTM	Road Temperature-Adjustment Material
RTFO	Rolling Thin-Film Oven
TOPSIS	Technique for Ordering Preference by Similarity to Ideal Solution
TCS	Tertiary Control Sieve
G_{mm}	Theoretical Maximum Specific Gravity
TES	Thermal Energy Storage

TGA	Thermogravimetric Analysis
TEM	Transmission Electron Microscope
US	United States
VFA	Voids Filled with Asphalt
VMA	Voids in the Mineral Aggregate
XRD	X-Ray Diffraction

ABSTRACT

The vulnerability of highway infrastructure to changes in environmental conditions is becoming a topic of concern, and the effects of climate on pavement performance need to be better mitigated. Abrupt environmental fluctuations can detrimentally affect pavement performance and service conditions. Moreover, noticeable temperature fluctuations, coupled with heavy vehicles and ample rainfall and snow precipitations, can cause pavements to reach their limiting performance criteria rapidly.

Asphalt materials must balance the need for thermal management with mechanical resistance to maximize pavement performance in such unpredictable environments. The ability to endow asphalt pavements with thermal energy storage capacities based on environmental conditions will enhance their life cycle performance. Phase Change Materials (PCMs) have demonstrated ideal characteristics as thermoregulating agents for various engineering applications. PCMs are substances that absorb and release thermal energy as they liquify and solidify, depending on pavement temperature. Accordingly, this study investigates the environmental tuning of asphalt pavements using PCMs. This dissertation presents four thematic research efforts that intend to: (1) reveal the benefits of modifying asphalt pavements with PCMs to lessen the appearance of low and high temperatures in roads, (2) develop characterization and design techniques to aid the tuning of asphalt pavements with Microencapsulated PCMs (μPCMs), (3) illustrate the challenges of implementing new paving technologies, and (4) propose a statistical approach to predict the volumetric, mechanical, and thermal properties of asphalt mixtures simultaneously.

The findings of this dissertation corroborate through experimental and computational results that, indeed, PCMs can enhance the thermal response of asphalt pavements to adverse freezing temperatures, leading to a considerable reduction in snow accumulation and ice formation at the pavement's surface. A prototype PCM asphalt pavement slab shows that, over a year and across 100 locations in the United States, the exposure of asphalt pavements to freezing temperatures could be reduced up to 29.1% by taking advantage of the thermal effect of PCMs. Additionally, μPCM modified asphalt mixtures demonstrate that high temperatures (above 43°C) in asphalt pavements could be alleviated, reducing the contributions of roads to the urban heat island effect.

Thermal cycling results suggest that μPCM tuned asphalt mixture specimens can experience temperature reductions between 1.8 and 10.3°C, as compared to non-μPCM modified asphalt mixture specimens subjected to the same ambient temperatures. However, this outcome depends on the amount and characteristics of μPCMs, asphalt mixture materials, ambient temperature, phase change transition (liquification or solidification), depth from the pavement surface, and density of the compacted asphalt mixture specimens. Thus, to systematize this tuning effect, a portion of this study focuses on developing a rheological approach for identifying the μPCM latent heat effect and a design approach for reproducing asphalt mixtures with μPCM in large quantities. A Complex Shear Modulus (G*) Change Rate emerges as one of the most interesting findings of this dissertation and as a novel parameter to detect the μPCM latent heat effect using rheological measurements. The G* Change Rate links well with the Differential Scanning Calorimetry results of μPCM modified asphalt binders and thermal response of μPCM modified asphalt mixtures.

Although the design of μPCM modified asphalt mixtures is successfully demonstrated, mechanical testing results reveal that there are still several challenges to be addressed in the implementation of μPCM tuned asphalt pavements. As such, this dissertation presents a field demonstration project accompanied by a thorough statistical analysis that could assist in implementing asphalt pavements with PCMs. The proposed statistical approach could help adjust the volumetric, mechanical, and thermal properties of μPCM modified asphalt mixtures. Overall, the findings of this dissertation are worth further exploration to promote the adaptability of asphalt pavements to the environment through the utilization of thermal energy storage systems.

1. INTRODUCTION

1.1 Background

The United States (US) has over 3.7 million kilometers of paved roads and highways, approximately 96% of which have asphalt surfaces (Roberts et al., 2002), due primarily to the fact that asphalt pavements are easy to maintain, quick to construct, cost-effective, and provide a safe, smooth, quiet ride. The asphalt mixtures comprising an asphalt pavement have traditionally composed approximately 95% aggregates and 5% asphalt binder by total mixture mass. The asphalt binder acts as a bonding agent to hold the aggregate particles together (Brown, 2009). Asphalt mixtures are typically produced at a mixing facility known as an asphalt plant, where the aggregates and asphalt binder are heated, mixed according to predetermined proportions, and loaded into trucks for transport to the construction site. The United States has around 3,500 asphalt plants. Each year, these plants produce a total of about 400 million tons of asphalt pavement material worth in excess of US$30 billion (National Asphalt Pavement Association [NAPA], 2014).

The need for transportation agencies to achieve specific engineering performance objectives has significantly encouraged the use of modifiers for asphalt pavements over the last decades, as illustrated in Figure1.1. The modification of asphalt pavements has allowed transportation officials to methodically manage pavement systems and allocate limited funds for pavement construction, maintenance, rehabilitation, and reconstruction. Therefore, the inclusion of modifiers in asphalt pavement materials can be regarded as a sustainable engineering practice, as it helps to either (1) go above and beyond required regulatory minimums or standard practice or (2) provide innovation in meeting these minimums and standards (Federal Highway Administration [FHWA], 2016).

One of the earliest and most successful forms of enhancement for asphalt paving materials is polymer modification. Adding chains of repeated small molecules (or polymers) to asphalt began to be implemented in the US during the 1980s (Yildirim, 2007). However, the high initial expenses for polymer modified asphalt limited its use. The eventual appearance of more cost-effective polymers, better understanding of the polymerization process, and prevalence of a long-term economic outlook encouraged the polymer modification of asphalt in the US and elsewhere. By 1997, all but three states in the US were already using polymer modified binders or intended

to use them in the future, and federal regulations supported their use (Yildirim, 2007). Asphalt pavements with polymer modification generally show superior resistance to fatigue and thermal cracking, rutting, stripping, and temperature susceptibility than unmodified pavements (Yildirim, 2007; Brasileiro et al., 2019; Habbouche et al., 2020). Over the years, the polymerization of asphalt paving materials has evolved, overcoming several challenges and leading to significant economic, social, and environmental benefits (Brasileiro et al., 2019; Habbouche et al., 2020).

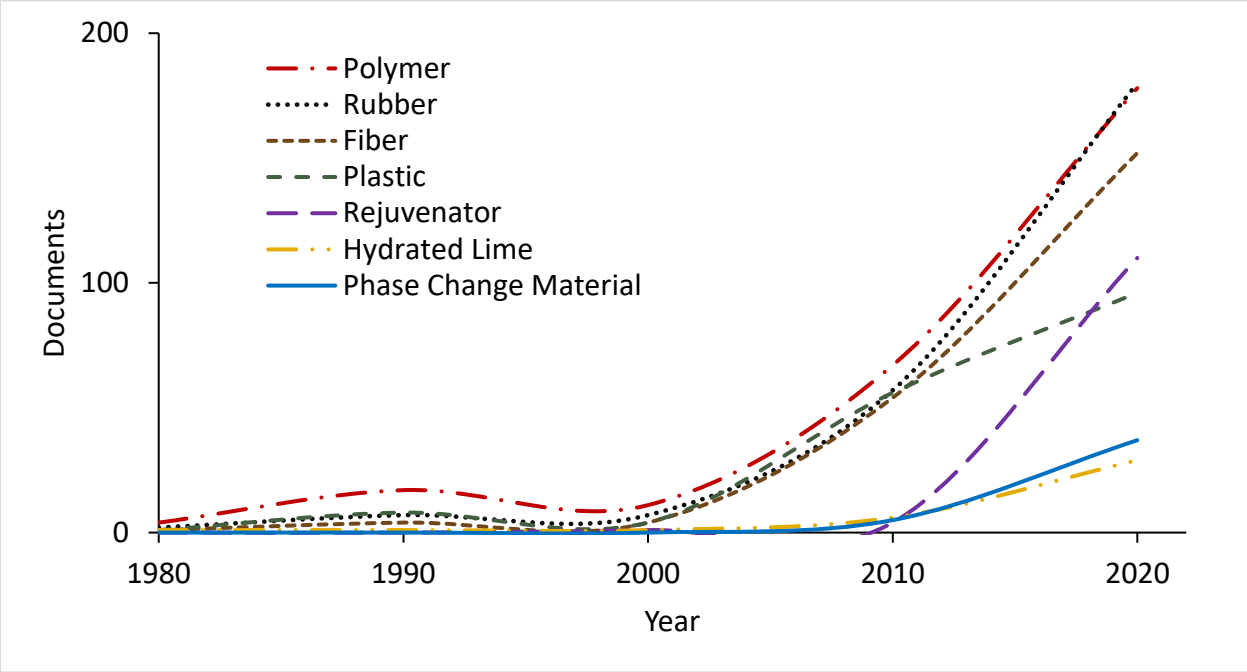

Figure 1.1. Trends of documents by year for common asphalt pavement modifiers (based on Scopus search).

The advantages of using rubber modified asphalt are becoming more widely recognized (Huang et al., 2007; Lo Presti, 2013). Incorporating recycled tire rubber into asphalt is perhaps the most common approach due to its stability and availability; about one billion tires worldwide reach the end of their useful lives each year (Brasileiro et al., 2019). Rubber modified asphalt paving materials have demonstrated better fatigue and thermal cracking resistance when compared to neat materials (Lo Presti, 2013; Brasileiro et al., 2019). This improvement in mechanical performance accompanied by environmentally friendly waste management has influenced the modification of asphalt with rubber. For example, in 2005, the state of California elaborated a government mandate that supports the adoption of rubber modified asphalt pavements. Since then, California

transportation officials have enforced the incorporation of minimum levels of recycled tire rubber into asphalt pavements (approximately 35% of the total mass of asphalt mixture) (Lo Presti, 2013).

Another method that has proved to be convenient for improving asphalt pavement performance is fiber reinforcement. This type of modification has been studied to a lower extent in comparison to polymer and rubber. Integrating fiber into asphalt materials has been demonstrated to enhance the resistance of pavements to various distresses, including reflective cracking, freeze-thaw, and moisture susceptibility (Abtahi et al., 2010). Fibers are also applied to asphalt pavements to accomplish specific purposes. For example, they are used to prevent excessive drain down of the asphalt binder in stone matrix asphalt mixtures, prepare electrically conductive paving materials, and manage waste fibers produced from manufacturing processes (Putman and Amirkhanian, 2004; Abtahi et al., 2010).

Evidently, a common trend in the pavement industry consists of using waste materials in paving applications to reduce the consumption of virgin and increasingly scarce materials and avoid landfilling. Such sustainable objectives have driven pavement engineers to investigate the use of recycled plastics as asphalt pavement modifiers. Recycled materials obtained from waste plastic bottles containing polymer chains have been introduced into asphalt mixtures. The modification of asphalt with recycled plastic has indicated positive effects on the properties of asphalt materials (Huang et al., 2007; Rahman et al., 2020; Santos et al., 2021). However, the past decade has seen a decreased attention across asphalt pavement scholars for plastic compared to other modifiers (including rejuvenators). Introducing plastics into asphalt pavement layers could potentially pose environmental concerns (i.e., contamination of air and water), hindering the long-term recyclability of asphalt materials (Santos et al., 2021).

Over the past decade, perhaps the most disruptive form of asphalt modification has been rejuvenators. A rejuvenating agent or rejuvenator is usually used to restore the properties of an aged Reclaimed Pavement Asphalt (RAP) binder to a condition that resembles the characteristics of an unaged asphalt binder (Baghaee Moghaddam and Baaj, 2016). Thus, asphalt mixtures containing a high RAP content typically embrace a rejuvenator as a modifier. Rejuvenators ensured excellent rutting resistance while providing a longer fatigue life (Zaumanis et al., 2014; Baghaee Moghaddam and Baaj, 2016); however, sometimes, they slightly reduce the moisture resistance of asphalt materials (Zaumanis et al., 2014). For the US, the total estimated tons of RAP used in asphalt mixtures was 89.2 million tons in 2019. This tonnage is a nearly 8.5% increase

from the 2018 construction season and represents a 59.3% increase from the total estimated tons of RAP used in 2009 (Williams et al., 2020). It should be highlighted that many state transportation agencies specifications allow up to 30% RAP in the surface layers (Mogawer et al., 2013).

A different substance use in small quantities to upgrade asphalt pavements is hydrated lime. This type of modification is seen as a multifunctional filler that increases the durability of asphalt mixtures (Little and Petersen, 2005; Gorkem and Sengoz, 2009; Lesueur et al., 2013). Due to its straightforward benefits, hydrated lime is highly applied in practice to asphalt materials. The field experience from several state agencies estimates that hydrated lime at the usual rate of 1.0 to 1.5% of total mixture mass increases the durability of asphalt pavements by 2 to 10 years (Lesueur et al., 2013). Hydrated lime treated asphalt pavements have shown greater resistance to low-temperature thermally induced cracking and fatigue damage (Little and Petersen, 2005; Gorkem and Sengoz, 2009). Understanding the behavior of hydrated lime modified asphalt materials is not simple; their performance depends on the physicochemical interaction that develops between the asphalt binder and hydrated lime (Little and Petersen, 2005). The complexity of this analysis has kept the investigations related to this topic to a minimum. Nevertheless, it is estimated that 10% of the asphalt mixtures produced in the US hold hydrated lime (Lesueur et al., 2013).

It is impossible to summarize all the information related to asphalt pavement modification. The asphalt pavement industry is versatile and vast, and modifiers are not the exception. Many modifiers in use or under investigation are not discussed in this introduction, such as nanomaterials (Li et al., 2017; Ezzat et al., 2016), warm-mix additives (Rubio et al., 2012), biobased materials (Yang et al., 2014), etc. Asphalt pavement modifiers can vary in size, shape, form, quantity, mixing process, purpose, performance, and cost-effectiveness, to name a few factors. The previous discussion has been provided to illustrate the circumstances that drive the modification of asphalt pavements and underline the surge of interest for incorporating Phase Change Materials (PCMs) into asphalt pavements. Although not yet partially or fully implemented in practice, PCMs have attracted considerable scholarly attention as an asphalt pavement modifier. In recent years, the amount of research work published is comparable to the documents available for a few traditional modifiers (i.e., hydrated lime).

The incorporation of PCMs into asphalt pavements has been primarily encouraged by the positive application of PCMs as a thermoregulating agent in numerous engineering fields (Agyenim et al., 2010; Anupam et al., 2020; Guo et al., 2020; Chen et al., 2020). PCMs are

substances that absorb or release thermal energy when they undergo a phase change from solid to liquid, liquid to gas, or vice versa (Dutil et al., 2011). This Thermal Energy Storage (TES) ability of PCMs allows them to maintain specific temperatures for extended periods, making them capable of helping tune the service temperature of asphalt pavements. As a result, the past decade has seen a proliferation in studies evaluating the thermoregulation of asphalt pavement with PCMs. A significant breakthrough that could occur from incorporating PCMs in asphalt pavements is to mitigate the appearance of temperature extremities that lead to pavement distresses or even sudden failure (Anupam et al., 2020; Guo et al., 2020; Chen et al., 2020). Thus, several researchers have realized that the modification of asphalt pavements with PCMs could prompt a great deal of change in the ultimate performance of roadways. However, despite the amount of information available, this area of research should be regarded as ongoing. There are still many benefits to quantify, design procedures to formulate, and challenges to overcome for successfully modifying asphalt pavements with PCMs.

1.2 Problem Statement

Over the years, roadway pavements have been designed and constructed to withstand the interacting damage effects of traffic and the environment. Traffic loads, primarily those from heavy trucks, causes stresses/strains in pavement structures, whose effects accumulate over time, resulting in pavement deterioration. Additionally, pavements are exposed to the environment, which has a significant impact on their performance. Two main environmental factors of concern are water and ice in the pavement layer and subgrade, and temperature variation throughout diurnal and seasonal cycles (Papagiannakis and Masad, 2008). Therefore, pavement engineering encompasses both pavement materials characterization and the pavement layer structural design to satisfy anticipated traffic and environmental demands.

The vulnerability of the US' roadway network to changes in environmental conditions is becoming a topic of concern (Mallick et al., 2014) and the effects of climate on pavement performance need to be better mitigated (Kodippily et al., 2018). Abrupt environmental fluctuations can detrimentally affect pavement performance and service conditions. Moreover, noticeable temperature fluctuations, coupled with heavy vehicles and ample rainfall and snow precipitations, can cause pavements to rapidly reach their limiting performance criteria (Papagiannakis and Masad, 2008; Mallick et al., 2014; Kodippily et al., 2018).

The importance of adequate design provisions to mitigate the effect of environmental conditions on pavement performance cannot be overemphasized (Papagiannakis and Masad, 2008). Environmental conditions are considered a critical factor influencing asphalt pavement durability. The addition of modifiers, both to the asphalt binder and the asphalt mixture, has attracted considerable attention in potentially alleviating environmentally induced pavement performance issues. Although many solutions have been developed and deployed, many asphalt pavements persist in failing prematurely due to environmental loading.

Asphalt pavements experience many different diurnal and seasonal temperature fluctuations and are exposed on multiple occasions to detrimental environmental conditions during their life cycles. For instance, extremely low temperatures in pavements cause freeze-thaw damage and low-temperature cracking (Brown, 2009). While elevated pavement temperatures contribute to the urban heat island effect and thermal distresses in pavements (Anupam et al., 2020). Although asphalt material selection is already systemized to withstand the appearance of extreme pavement temperatures, PCMs pose the ability to endow asphalt pavements with thermal energy storage functions like no other existing modifier. The capacity of moderating the excessive absence or presence of heat in asphalt pavements through the release or absorption of thermal energy could impose numerous benefits. However, such paradigm shift is inherently associated with risks and challenges that need to be managed using scientific knowledge and engineering.

1.3 Research Objectives

This dissertation experiments with the hypothesis that if asphalt materials are modified with PCMs, it should be possible to "tune" the resulting asphalt pavement to the environment, thereby mitigating or eliminating pavement damage due to the exposure of asphalt pavement layers to temperature fluctuations. The amount of research work required to validate this hypothesis fully is extensive, broad, and multidisciplinary. As shown in Figure 1.1, further studies are vital to warrant incorporating PCMs into asphalt pavements. For example, polymer modified asphalt pavements have been under investigation for decades, and still, new findings are brought out continuously (Habbouche et al., 2020). Thus, the scope of this dissertation is to demonstrate and evaluate aspects considered critical for the positive implementation of PCM modified asphalt pavements. This investigation's main purpose is to set out a solid stage that could drive the tuning of asphalt

pavements using PCMs. As a step toward this goal, the following specific objectives were identified as required for the accomplishment of this dissertation:

1. Conduct a literature review that summarizes the relevant information of PCM modified asphalt pavements. The available literature in this area of research has focused on formulating PCMs for paving purposes and demonstrating this concept's potential (Anupam et al., 2020; Guo et al., 2020; Chen et al., 2020). However, very little published research highlights the gaps related to the field implementation of PCM modified asphalt pavements. This investigation attempts to condense the progress made so far in this subject of study and reflect on the benefits and challenges linked to the modification of asphalt pavements with PCMs.
2. Demonstrate the potential of incorporating PCMs in asphalt pavements to melt snow and ice. The latent benefits of modifying asphalt pavements with PCMs are numerous and still unquantifiable to a great extent (Guo et al., 2020). Few studies have provided quantitative evidence of the advantages of including PCMs in asphalt pavements. As a result, an objective of this study was to estimate the thermal performance of asphalt pavement slabs containing ideal PCMs that prevent the appearance of freezing temperatures and assist in the melting of snow and ice from the pavement's surface.
3. Identify an approach that determines the Microencapsulated PCM (μPCM) effect in asphalt binders using rheological measurements. Asphalt binder performance grading system employs Dynamic Shear Rheometer (DSR) testing to determine high and intermediate temperature rheological properties, and recent equipment developments have allowed researchers to measure low-temperature binder properties as well reliably (Oshone et al., 2018). While some research has been carried out on the rheological behavior of μPCM modified asphalt binders, no single empiric or mechanistic method have been proposed to detect the latent heat μPCM effect in asphalt binders. This study examines the way in which DSR testing can be applied to determine the μPCM effect in asphalt binders.
4. Design an asphalt mixture containing a substantial amount of μPCM without compromising its volumetric and mechanical properties. The past decade has seen the rapid advancement of μPCMs for diverse engineering applications (Jamekhorshid et al., 2016), aiding the incorporation of this thermoregulating agent in asphalt materials.

However, the effects of different types and mass fractions of μPCMs on asphalt materials' thermal properties and mechanical performance have rarely been investigated. This dissertation seeks to establish a mixture design framework for dosing optimal amounts of μPCM into asphalt pavements.

5. Describe the production, placement, and compaction process of asphalt mixtures in the field. The direct incorporation of PCMs into asphalt pavements yields adverse effects. A form of encapsulation is necessary to benefit the final application of the core PCMs (Anupam et al., 2020; Guo et al., 2020). The high temperatures and mechanical forces experienced by asphalt materials during paving promote the leakage of PCMs from their carrying materials, making PCMs have direct contact with asphalt materials. Consequently, asphalt mixtures' production, placement, and compaction process have been singled out as a significant challenge for modifying asphalt pavements with PCMs. This dissertation discusses a case study that illustrates the procedures use for asphalt pavement construction. The field demonstration is intended to bridge the knowledge between PCM encapsulation methods and asphalt pavement technology. Thus, PCM encapsulation methods could be tailored for specific paving purposes, and paving procedures could be adapted to incorporate PCM materials during production and construction.
6. Evaluate the use of a statistical approach for the design and quality assurance of asphalt mixtures. Asphalt materials must balance the need for thermal management with mechanical resistance to maximize pavement performance under unpredictable environments. Hence, the tuning of asphalt pavements using PCMs will require methodologies that help analyze the trade-offs between different material components and mixture properties. Part of the aim of this dissertation is to demonstrate how a statistical technique can be used to estimate asphalt mixture volumetric properties using mixture design, material properties, and testing inputs. This technique can simultaneously predict various asphalt mixture properties; therefore, the findings can be extrapolated to adjust asphalt pavements using PCMs.

1.4 Organization of Dissertation

This dissertation is organized in a hybrid form, as shown in Figure 1.2. The overall structure of the study takes the form of seven chapters. Chapter 1 introduces the background, problem statement, and objectives for this research effort. Chapter 2 presents a chronological literature review investigating the technical publications and research articles concerning the modification of asphalt pavements with PCMs. The significant findings available in the literature are presented, and research needs are identified. Then, the methods, results, and discussions parts of this dissertation are divided into four thematic chapters. Chapters 3 and 4 draw out the key findings of this study directly related to the benefits, design, and challenges of PCM modified asphalt pavements. Chapter 3 presents a PCM modified asphalt pavement slab prototype tested under actual thermal cycles and snowfall events. Chapter 4 shows the tuning of asphalt pavements with μPCM, revealing a novel approach to determine when the μPCM effect occurs using rheological measurements. Additionally, the thermal and mechanical performances of μPCM modified asphalt mixtures are evaluated. An asphalt mixture design method is demonstrated to systematically incorporate a considerable portion of μPCM particles in a reference mixture.

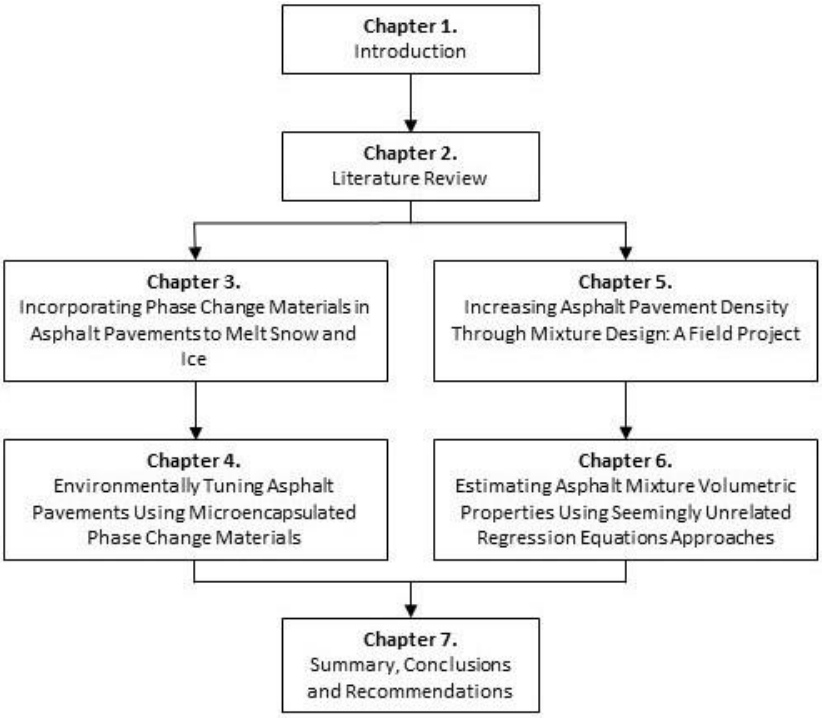

Figure 1.2. Organization of dissertation.

Chapters 5 and 6 can be considered research associated with this dissertation's title and main line of research. These chapters are included because they demonstrate case studies that have constrained the research process of this investigation. Additionally, these complementing portions provide information about methodologies and tools that could boost the tuning of asphalt pavements with PCMs, by controlling aspects related to the construction process and quality assurance of asphalt technology. Lastly, Chapter 7 summarizes the main findings of this dissertation, derives conclusions from work presented in previous chapters, and reflects on the implications of this dissertation and further areas of research.

2. LITERATURE REVIEW

PCMs have been extensively investigated as a thermoregulator for a wide variety of engineering applications, including electronics, spacecraft, solar energy, textiles, buildings, and construction materials, to name a few (Agyenim et al., 2010). Accordingly, the research studies about PCMs available in the literature are quantitatively vast. Regarding time, TES started to receive increased attention in the 1970 decade (Lane, 2018). Thus, most of the information on PCMs has been reported over the past 40 years (Zalba et al., 2003).

In the literature, the 'PCM' term is widely used to refer to a substance that absorbs or releases thermal energy when it undergoes a phase change from solid to liquid, liquid to gas, or vice versa (Dutil et al., 2011). This chapter summarizes the relevant information of PCMs relating to their general engineering applications. Then, the pertinent studies performed by various investigators are reviewed, along with the potential benefits of incorporating PCMs into asphalt binders and mixtures. Finally, the chapter appraises critical events in the investigation of PCM modified asphalt pavements to narrow the research scope for this dissertation.

2.1 General Review of Phase Change Materials

The main purpose of PCMs is the storage of thermal energy in a latent form (Baetens et al., 2010). It is well known that latent heat storage can be achieved through changes in the state of matter (Incropera, 2007; Lane, 2018). If a PCM change from solid to liquid (liquification, melting) or from liquid to vapor (vaporization, evaporation, boiling), the latent energy of a given system increases, absorbing a large amount of heat from its surrounding environment. Conversely, if the phase change is from vapor to liquid (condensation) or from liquid to solid (solidification, freezing), the latent energy of a given system decreases, releasing a significant amount of heat to its surrounding environment. If no phase change occurs, there is no change in latent energy (Incropera, 2007). A proper understanding of the fundamental concepts and principles that underlie PCM incorporation into any system is required for its optimization (Oro et al., 2012).

2.1.1 Phase change materials for thermal energy storage

In general, there are three methods of storing thermal energy: (1) sensible, (2) latent, and (3) thermochemical heat storage (Incropera, 2007; Lane, 2018). They differ in the amount of heat stored per unit mass or volume of storage medium, in the time-temperature history of the medium during heat storage and retrieval. In sensible heat storage, thermal energy is stored by changing the temperature of the storage medium. As shown in Equation 2.1, the amount of heat stored depends on the heat capacity of the medium, the temperature change, and the amount of storage material. Sensible heat storage is the least efficient method of storing heat since much less thermal energy is involved in raising the temperature of a material than in melting a crystalline compound or in breaking and reforming chemical bonds (Lane, 2018).

$$Q = \int_{T_i}^{T_f} mc_p dT = m\,\bar{c}_p(T_f - T_i) \qquad \text{(Eq. 2.1)}$$

where:

Q = quantity of heat stored,

T_i = initial temperature,

T_f = final temperature,

m = mass of heat storage medium,

c_p = specific heat, and

$\bar{c}_p$ = average specific heat between T_i and T_f.

In latent heat storage, thermal energy is stored applying a reversible change of state, or phase change, in the storage medium, as shown in Equation 2.2. Solid-liquid transformations are most commonly utilized, though solid-solid transitions have been investigated. Liquid-gas or solid-gas phase changes involve the most energy of the possible latent storage methods. However, storage of the gas phase is complicated and bulky. Latent heat storage has the advantages of higher heat capacity, allowing a reduction in size and weight of the thermal storage unit; lower storage temperature, permitting the use of less insulation, and letting higher solar collection efficiency; and largely isothermal operation, requiring more straightforward controls, and rendering broader design opportunities (Lane, 2018).

$$Q = ma_m \Delta h_m + \int_{T_i}^{T_m} mc_{p_s} dT + \int_{T_m}^{T_f} mc_{p_l} dT \quad \text{(Eq. 2.2)}$$

where:

a_m = fraction melted,

Δh_m = heat fusion per unit mass,

T_m = melting temperature,

c_{p_s} = specific heat between T_i and T_m, and

c_{p_l} = specific heat between T_m and T_f.

Thermochemical systems rely on the energy absorbed and released in breaking and reforming molecular bonds in an entirely reversible chemical reaction. In this case, the heat stored depends on the amount of storage material, the endothermic heat of reaction, and the extent of conversion, as shown in Equation 2.3. Thermochemical heat storage has the advantages of a more compact system, long-term storage with minor loss, and room temperature storage without insulation. However, the selected chemical reactions must have a high selectivity, no by-products, and be completely reversible. Reactants and products must not be corrosive to construction materials, and all the chemicals used must be safe and environmentally appropriate (Lane, 2018).

$$Q = ma_r \Delta h_r \quad \text{(Eq. 2.3)}$$

where:

a_r = fraction reacted, and

Δh_r = heat of reaction per unit mass.

2.1.2 Classification of phase change materials

Many researchers have presented well-documented classifications for PCMs, which may be used for several TES engineering applications (Oro et al., 2012). In 1983, Abhat (1983) provided a helpful classification for the PCM substances used for TES. As shown in Figure 2.1, Abhat (1983) divided PCMs into two main groups, organic and inorganic materials. Organic materials are further classified as paraffin and non-paraffins (i.e., fatty acids, eutectics, and mixtures) (Baetens et al., 2010). Melting and freezing cycles experimenting these materials showed that they crystallize with little or no subcooling and are usually non-corrosive and very stable. Inorganic materials are assigned as eutectics and mixtures. A eutectic material is a composition of two or more components,

which melts and freezes congruently, forming a combination of crystals during crystallization. Eutectics nearly always melt and freeze without segregation, leaving little opportunity for the individual components to separate. Eutectic mixtures melt almost at a constant temperature. The main inorganic mixture compounds are salts, salt hydrates, aqueous solutions, and water (Oro et al., 2012).

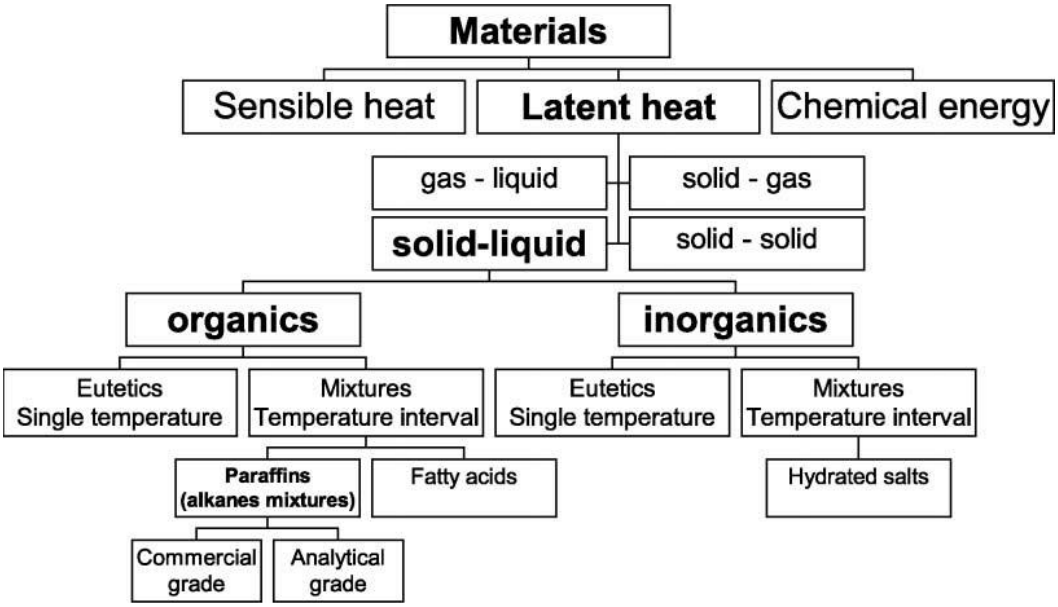

Figure 2.1. Classification of phase change material substances according to Abhat (1983).

Although PCMs are typically classified based on their chemical composition, Figure 2.2 shows that PCMs can be grouped as a function of the ranges of their phase transition temperature and melting enthalpy, or latent heat (Baetens et al., 2010). As a result, PCMs are divided into three main groups based on the temperature ranges over which the phase transition occurs: (1) low-temperature PCMs – with phase transition temperatures below 15°C, usually used in air conditioning applications and the food industry; (2) mid-temperature PCMs, the most popular – with phase transition temperatures in the range of 15 to 90°C, with solar, medical, textile, electronic and energy-saving applications in building design; and (3) high-temperature PCMs – with a phase transition above 90°C developed mainly for industrial and aerospace applications (Pielichowska and Pielichowski, 2014).

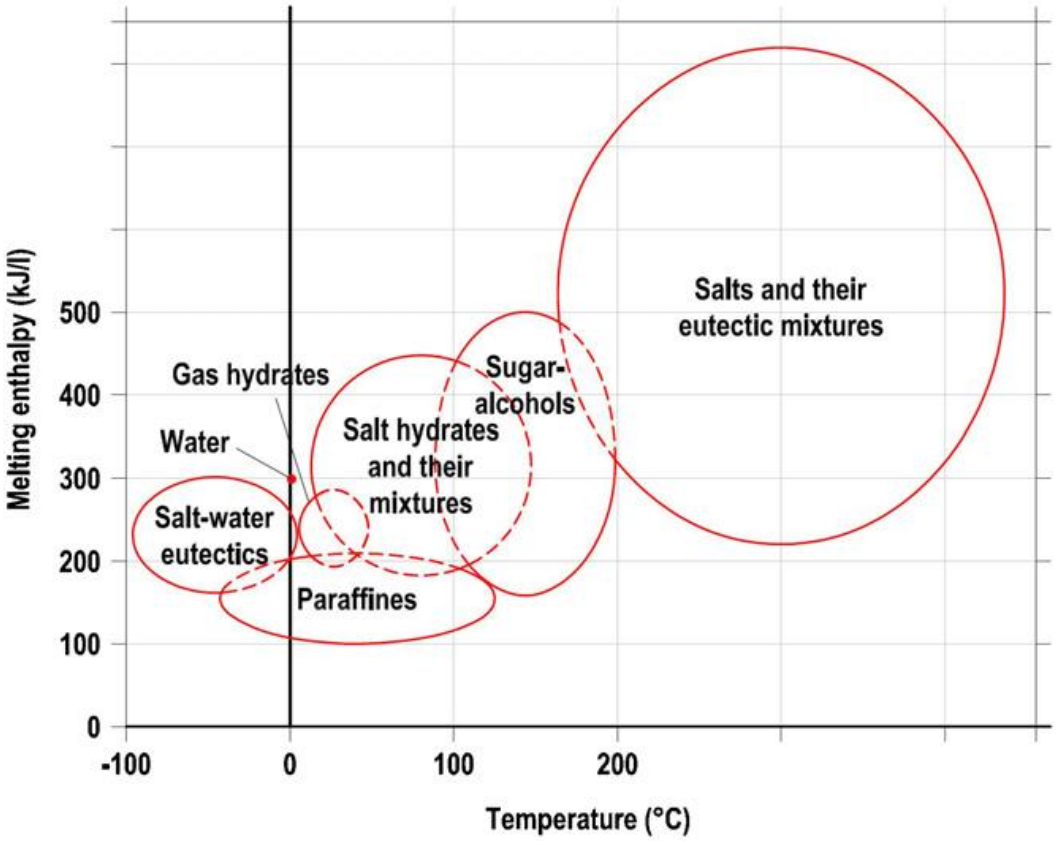

Figure 2.2. Classification of phase change material substances based on transition temperature (Baetens et al., 2010).

Additionally, PCMs are sometimes classified by their mode of phase transition: (1) gas-liquid, (2) solid-gas, (3) solid-liquid, and (4) solid-solid systems (Abhat, 1983). Over the years, new groups, substances, and formulations of PCMs have appeared. On many occasions, PCMs have been re-engineered to enhance their overall performance and safety significantly. Thus, PCMs can be graded due to various factors, such as thermal conductivity, encapsulation method, and shape stabilization procedure (Pielichowska and Pielichowski, 2014). The number of commercially available PCMs is over 160,000 (Wei et al., 2018). Each PCM group has its characteristics, applications, advantages, and limitations (Rathod and Kanzaria, 2011).

2.1.3 Criteria used for selecting phase change materials

Although there is an innumerable number of substances, compounds, and mixtures that can be considered as PCMs for engineering purposes, most of them can be rejected for a specific application from considerations of economics, safety, or general physical, chemical, and thermal

properties. As a result, several investigators have proposed different selection criteria for an extensive range of PCM applications (Lane, 2018; Rothan and Kanzaria, 2011; Wei et al., 2018). Telkes (1949, as cited in Lane, 2018), a pioneer of TES systems, outlined five main requirements for PCM selection: (1) supercooling, (2) segregation, (3) corrosion, (4) volume change, and (5) mass production of filled containers (or capsules). Historically, these factors have been the center of attention in PCM development programs. In 1983, Lane provided a complete review of the selection criteria for PCMs. Table 2.1 shows the list outlined by Lane (2018), which can be generalized for almost every PCM engineering application.

Table 2.1. Requirements for practical application of phase change materials (Lane, 2018).

General Attribute	Requirements
Thermal Properties	Suitable phase transition temperature High latent heat of transition Good heat transfer
Physical Properties	Favorable phase equilibria Low vapor pressure Small volume change High density
Kinetic Properties	No supercooling Sufficient crystallization rate
Chemical Properties	Long-term chemical stability Compatible with materials of construction Non-toxic No fire hazards No nuisance factor
Economics	Abundant Available Cost-effective

However, even after applying a thorough selection process, a reasonable number of PCM formulations can remain as candidates (Lane, 2018). Many different methods are available to measure or analyze the TES characteristics of PCMs, including theoretical calculations, experimental methods, and numerical simulations. However, no matter which approach is used, the obtained storage characteristics of the investigated PCMs should be comprehensively assessed by evaluating as many properties as possible (Wei et al., 2018). Thus, the PCM selection process is generally described as a Multiple Attribute Decision Making (MADM) problem where several factors should be considered in decision making among a set of available alternatives. Inherently, this process contains subjectivity, uncertainty, and ambiguity. Designers and engineers must consider numerous material selection criteria depending upon the application. However, no single

material can have all the required properties for an ideal TES system. As a result, the PCM which will give the desired thermal performance at a minimum cost is typically selected (Rothan and Kanzaria, 2011).

2.1.4 Optimization methods for phase change material selection

The selection of a suitable PCM in each design plays an essential role in the thermal efficiency, economic feasibility, and utility of TES systems (Oro et al., 2013). Over the last decade, many researchers have proposed systematic approaches to narrow down the number of PCM alternatives for a specific application.

Rathod and Kanzaria (2011) proposed two MADM methods to systemize the PCM selection process. These two methods are described as Technique for Ordering Preference by Similarity to Ideal Solution (TOPSIS) and fuzzy TOPSIS method that uses linguistic variable presentation and fuzzy operation. Both methods use an analytic hierarchy process method to determine the weights of the criteria. Rathod and Kanzaria (2011) evaluated the best choice of PCM used in a solar domestic hot water system. Empirical results showed that the proposed methods are viable approaches in solving PCM selection problems. TOPSIS is suitable for using detailed performance ratings, while the fuzzy TOPSIS is preferred when the performance ratings are vague and inaccurate.

Rastogi et al. (2015) attempted to extend the MADM approach for ranking and selecting PCMs for domestic heating, ventilation, and air-conditioning applications. In this study, the performance of PCMs was simulated using PCMExpress, a planning and simulation program for buildings that are temperature controlled with PCM. It was observed that the results obtained by simulation are in good agreement with those obtained using a MADM approach. The candidates with the best ranks showed significant improvement in ameliorating the temperature conditions. Thus, Rastogi et al. (2015) concluded that implementing the MADM into practice for PCM selection would prove an economical and swift alternative technique for ranking and screening PCMs. Xu. et al. (2017) verified the MADM approach to systematically select PCM for latent heat TES in solar air conditioning applications. The results obtained showed that MADM could be a valuable and efficient tool in the design process of PCM modified solar air conditioning systems.

Although multiple criteria approaches seem suitable for PCM selection, other methods have also been explored in the literature. Oro et al. (2013) studied PCM selection for low-

temperature applications, such as those of refrigerated trucks, domestic freezers, and commercial freezers. In the study conducted by Oro et al. (2013), the design of experiments methodology was used as an optimization tool to determine the additive concentration to provide a constant phase transition temperature, maximize the latent heat, and deliver suitable physical, technical, and economic properties after many thermal cycles. Oro et al. (2013) determined that using the design of experiment analysis, an equation for each PCM additive can be developed to predict the material phase transition temperature as a function of the concentration of the components in its formulation.

Wei et al. (2018) reviewed the selection process for high-temperature PCMs. This type of thermoregulating agent is widely used in concentrated solar power projects whose operating temperatures are above 300°C. Wei et al. (2018) suggested that using digital selection tools, such as databases and software packages, can improve the comprehensiveness of any comparison between available PCMs and make the selection process more efficient. Such software packages integrate various information in a single tool and achieve a progressive method to select materials. The software packages allow users to choose materials using diagram methods based on design process parameters. This study noted that the data stored in the digital tools must be accurate enough to ensure the accuracy of the selection. As a result, whenever a set of data is provided, objective conditions such as the test method and the material's sources should be provided to maintain and ensure rigorous data accuracy (Wei et al., 2018).

Dutil et al. (2011) presented an exhaustive review of numerical methods used to simulate PCMs and latent heat energy storage systems for optimal design and material selection. Dutil et al. (2011) suggested that numerical analysis is generally required to obtain appropriate solutions for the thermal behavior of PCM systems. Consequently, this study concluded that models are desired for most applications of PCMs. In many cases, simplified models, analytic expressions, or correlation functions have been developed for practical guidance in optimizing the design of TES systems. Additionally, the work done by Dutil et al. (2011) highlighted the need to match experimental investigations with recent numerical analyses. In recent years, models mainly rely on other models in their validation stages. Conversely, other researchers have used laboratory and field experiments to optimize PCM systems. Gil et al. (2013) proposed to select the best PCM for real solar cooling applications based on Differential Scanning Calorimeter (DSC) analysis and pilot plant scale experiments at a specific location.

2.2 Chronological Review of Phase Change Materials Incorporation into Asphalt Materials

In comparison to other engineering applications, few comprehensive literature reviews are available regarding the use of PCM in asphalt pavement materials. The continuous appearance of new potential PCM formulations for asphalt pavement materials has hindered the amalgamation of previous studies. Intrinsically, researchers have typically investigated the effect of a specific PCM, making it difficult to generalize the findings from one study to another. This section provides a chronological summary of the previous research related to this topic to consolidate the critical events in the investigation of PCM modified asphalt materials.

2.2.1 Early phase change material formulations assessed on asphalt materials

During the last decade, PCMs have been investigated as a potential thermoregulator for asphalt pavement materials. In 2011, the first research studies related to PCM incorporation into asphalt materials became available in the literature. Chen et al. (2011) studied the feasibility of using a paraffin/expanded graphite Shape-Stabilized PCM (SSPCM) with a phase transition temperature between 40 and 50℃ to develop a temperature self-control asphalt pavement to prevent rutting. A control mixture without SSPCM and a test mixture with SSPCM were exposed to a solar simulator (produced by a 300 W metal halide lamp). The specimen preparation process and percentage of SSPCM modification used were not reported by the authors. The mixtures were subjected to a heating process for about 125 minutes. The initial temperature for both specimen types was nearly 18℃. The maximum temperatures achieved for the control and test mixtures were approximately 50 and 48℃, respectively. Chen et al. (2011) reported that it is feasible to control the temperature-rising of asphalt pavement materials using SSPCMs.

In the same vein, Guan et al. (2011) investigated the temperature change rate of asphalt mixtures with and without PCMs under temperature cycles. The purpose of this research effort was to demonstrate that PCMs can be used to regulate the temperature change of asphalt mixtures. A commercially available Composite PCM (CPCM), which is a PCM formulation composed of a based material matrix carrying a PCM, was used to dope an asphalt mixture. This type of CPCM formulation is mainly used for building applications, and it has a phase transition temperature of 17°C. The asphalt mixtures specimens were CPCM modified at five different percentages, 0, 3, 20, 30, and 50%, by total mixture mass. Guan et al. (2011) indicated that CPCMs could regulate

the temperature change of asphalt mixture under fluctuating environmental conditions. However, Guan et al. (2011) did not discuss the optimum CPCM modification percentage.

To formulate CPCMs for asphalt mixture applications, Ma et al. (2011) compared the performance of different PCM carrier materials and packing methods. The study's objective was to identify CPCM carrier materials that prevent PCM leaks within the asphalt mixture. A tetradecane with a phase transition temperature of 2℃ was used as PCM. The carrier materials used were activated carbon and sol-gel, silica and sol-gel, and silica and ethyl cellulose. The CPCM microscopic characteristics and thermophysical properties were analyzed by Scanning Electron Microscope (SEM) and DSC. Ma et al. (2011) concluded that a proper combination of carrier material and packing method could prevent PCM leaking within the asphalt mixture at typical service temperatures between -30 to 40℃. However, CPCM modified asphalt materials were not evaluated. The experimental matrix just included testing on CPCMS.

Chen et al. (2012) investigated the performance of CPCMs above 40°C, and reported that CPCM modified asphalt materials might experience PCM leakage at temperatures higher than 40°C. This caused an adverse effect of the CPCM on the asphalt mixtures tested, affecting their indirect tensile strength, low-temperature cracking resistance, and high-temperature rutting performance. However, thermal performance tests confirmed that CPCMs in the asphalt mixtures absorbed and released latent heat to control temperature. The CPCMs used by Chen et al. (2012) were two commercially available CPCMs with nominal phase transition temperatures of 45 and 50℃. The amounts of CPCM applied were 5% by mass of aggregate.

Bian et al. (2012) also compared the thermal performance of asphalt mixtures with and without CPCMs. The PCM examined was a palmitic acid with a phase transition temperature between 61 and 64°C. Pottery sand and diatomite powder were employed as carrier materials. To prepare the CPCM modified mixture, the fine aggregate particles between 1.18 and 0.600 mm were substituted with the same volume of corresponding CPCM carried by pottery sand. Meanwhile, the mineral filler was replaced with the same volume of CPCM carried by diatomite powder. The CPCM modified asphalt mixture obtained a maximum temperature reduction of about 7.6 and 3.4℃ under transient laboratory and field scenarios, respectively. The asphalt mixture specimens were tested in the laboratory from room temperature to 80°C. In the field, the temperature of the compacted mixtures with and without CPCMs fluctuated between 32 and 58°C.

In 2013, He et al. (2013) claimed that SSPCM showed a broad application foreground in asphalt materials to regulate pavement temperature using latent heat, lessen the asphalt pavement temperature-related distresses, enhance the performance, and prolong the service life of asphalt pavements, lower repair and maintenance costs, and enhance driving safety. The analysis done by He et al. (2013) highlighted that SSPCM must resist very high temperatures during the asphalt mixing to consider PCMs as a pavement modifier. Thus, the thermal stability of SSPCM modified asphalt binders was investigated by Thermogravimetric Analysis (TGA), along with their chemical stability characterized by Fourier-Transform Infrared Spectroscopy (FTIR). He et al. (2013) reported that SSPCM modified asphalt binders could have a satisfactory phase enthalpy of fusion (or latent heat), thermal stability, and chemical compatibility.

Ma et al. (2014) combined various unsaturated organic acids to formulate a CPCM that released and absorbed thermal energy between a broad temperature range from -27.4 to 26.0°C. This type of CPCM formulation was referred to as Road Temperature-Adjustment Material (RTM). In the research performed by Ma et al. (2014), the effect of the RTM on the temperature profile of a modified asphalt mixture was analyzed by monotonic cooling, cooling-heating cycle, and experimental field tests. The cooling-heating cycle tests indicated that the RTM in the modified asphalt mixture reduced temperature variations and postponed the appearance of extreme temperatures over time. The experimental field results showed that the RTM helped decrease the highest temperature during the heating moment and increase the lowest temperature during the cooling moment, reducing the environment's adverse impact on the modified asphalt mixture specimen. Ma et al. (2014) used indices analyzing the temperature difference, cooling and heating rates, and lag time to compare the mixtures' thermal responses. The amount of CPCM added to the modified asphalt mixture was equivalent to 0.30% of the total asphalt mixture mass.

Leng et al. (2014) formulated a CPCM for asphalt paving applications using lauric acid as PCM and organophilic montmorillonite as carrier material. The proportion of CPCM components was optimized by conducting DSC, FTIR, SEM, X-Ray Diffraction (XRD), and Transmission Electron Microscope (TEM) methods. The experimental results showed the formation of hydrogen bonds between the CPCM components, core PCM, and carrier material. Leng et al. (2014) concluded that such hydrogen bonds could help prevent the leakage of liquid lauric acid during the phase change process. However, no inferences were reported about PCM leakage over the asphalt mixing course.

It took few studies for researchers to recognize the importance of tailoring suitable PCM compounds for asphalt paving applications. Ren et al. (2014) continued to address this concern by reviewing several CPCM preparation methods, including direct immersion, melt blending, graft polymerization, intercalation, microencapsulation, sintering, and sol-gel techniques. Due to its moderate reacting process and easiness, Ren et al. (2014) decided to investigate the sol-gel preparation method and formulate CPCMs that could withstand the high asphalt mixture mixing temperatures and required demands during pavement service life. Four different kinds of CPCMs were prepared by Ren et al. (2014) via the sol-gel method using pure and silica powder, floating bead, and activated carbon adsorbed PCM approaches. SEM results showed that a silane coupling agent delivered positive impacts on particle distribution of CPCMs in comparison to the other formulations. However, SEM analysis suggested that activated carbon adsorbed PCM can achieve a more considerable sol-gel coating effectiveness than the other materials explored. Likewise, DSC results revealed that activated carbon adsorbed PCM exhibited a superior latent heat storage capacity and thermal stability. However, further investigations were recommended to validate the preparation of CPCMs developed with activated carbon adsorbed PCM.

In 2015, Kheradmand et al. (2015) assessed the feasibility of impregnation and encasement of PCMs in Lightweight Aggregates (LWAs). Two types of paraffins were enclosed in four different LWAs of inorganic and organic compositions. The paraffins had phase transition temperatures of approximately 3 and 5°C. The application of PCMs into asphalt pavements was targeted to reduce freeze-thaw cycles. Thus, the phase transition temperatures were chosen slightly above 0°C to attenuate freezing temperatures within environmentally tuned asphalt pavements. Four different coating materials encased the PCMs in the porous structure of the LWAs and worked to prevent PCM leakages. A total of 40 treatments were prepared by combining two PCMs, four LWAs, and five coating options (including four coating materials and no coating or reference). The testing matrix was extensive, comprising SEM, DSC, particle density, PCM absorption, and oven drying tests on LWAs with PCMs. Kheradmand et al. (2015) confirmed that minimal leakage of PCM from LWA is experienced with coating and that the mass loss is dependent on the type of coating technique. However, the mass loss of the composites was tested up to 40°C, which is a temperature significantly lower than those used for mixing and compaction of conventional asphalt mixtures.

2.2.2 Development of phase change materials for paving applications

One of the firsts lists of technical requirements for PCMs to be used in asphalt pavements was provided by Si et al. (2015). The technical specifications of PCMs for asphalt pavement purposes were grouped into seven categories: (1) adequate thermal conductivity, (2) enough heat storage capacity, (3) suitable phase transition temperature, (4) entirely reversible phase change, (5) harmless chemical properties, (6) high-temperature performance and durability, and (7) simple incorporation process. Additionally, Si et al. (2015) considered critical the proper selection of PCM transition temperature and relevant to the pavement temperature region and typical distresses. Three types of PCM combinations, namely low-temperature (-5 to 5°C), intermediate-temperature (5 to 35°C), and high-temperature (35 to 50°C), were formulated by Si et al. (2015). The raw PCMs used to develop the PCM compounds were tetradecane, 58# paraffin, and liquid paraffin. Finally, Si et al. (2015) recommended PCM mass ratios to assemble PCM combinations with different phase transition temperatures.

In 2016, a study carried by Ma et al. (2016) stressed that conventional asphalt methods could not fully capture the thermoregulation mechanism of CPCMs on asphalt mixtures. Ma et al. (2016) emphasized that to properly understand the thermal response of CPCM modified asphalt mixture specimens, their specific heat capacity should be measured under induced endothermic and exothermic reactions. A temperature gradient between the specimen surface and the specimen center can lead to unreliable experimental results without setting consistent testing boundaries. Therefore, Ma et al. (2016) proposed a heat exchange system to test real-time temperature change behaviors and calculate the specific heat capacities of raw CPCM (or 100% CPCM) and CPCM modified asphalt mixture specimens. The CPCM applied for this study had a phase transition temperature and latent heat of about 5°C and 80 J/g, respectively. The raw CPCM and CPCM modified asphalt mixture specimens were examined from -20 to 60°C (endothermic reaction). The specimens had a 70 mm diameter and 35 mm height and were prepared using a geotechnical mold. The CPCM was added to the asphalt mixtures at four different levels, 0.6, 1.2, 1.8, and 2.4%, by total mixture mass. The experimental results demonstrated that the raw CPCM specimen temperature rise curve had an evident thermal lag, while the temperature change obtained for the CPCM modified asphalt mixture specimens showed a more subtle temperature plateau. The low dosage of CPCM on the asphalt mixture specimens was attributed as the main factor for the minor thermal lag achieved.

Athukorallage and James (2016) conducted a heat transfer numerical analysis to better understand the incorporation of different PCM dosages on the surface layer of an asphalt pavement structure. The PCM fractions modeled ranged between 0 and 100% by total pavement layer volume. The PCM transition temperature and latent heat were assumed to be 43°C and 200 J/g, respectively. The study done by Athukorallage and James (2016) underlined that heat transfer in PCMs is a transient, non-linear phenomenon with a moving solid-liquid interface, generally referred to as the Stefan problem. During the phase change transformation, the liquid and solid fractions of PCMs depend on several parameters, such as temperature, solidification speed, nucleation rate, and cooling and heating rates. For modeling purposes, a set of thermal conductivity values, specific heat capacities, and densities were assumed by Athukorallage and James (2016) for both PCM phases, solid and liquid. As expected, the PCM volume fraction significantly affected the rate of change in temperature in the PCM modified pavement. Overall, the simulation results obtained by Athukorallage and James (2016) suggested that a PCM volume fraction between 30 and 40% can be considered the optimal amount of PCM modification to improve the pavement's thermal response. However, no experimental validation or mechanical performance analysis was provided by Athukorallage and James (2016).

In 2017, Lin et al. (2017), in brief, reviewed the available literature till that point and found evidence to support the incorporation of PCMs into asphalt pavements. Lin et al. (2017) provided a concise list of potential CPCMs to adjust asphalt pavement temperatures. A study developed by Jin et al. (2017) prepared three kinds of mineral-supported polyethylene glycol as CPCMs for paving purposes. The three minerals used were diatomite, expanded perlite, and expanded vermiculite. The microstructure and chemical structure of the CPCMs were characterized by SEM, FTIR, and XRD, while TGA and DSC determined the thermal properties. The phase transition temperatures of the CPCMs were between 52 and 55°C, with latent heats ranging from 100 to 115 J/g. The CPCM prepared using expanded perlite showed the best thermal performance and chemical stability. Thus, asphalt mixture specimens were fabricated using this CPCM formulation. The fine aggregates between 0.300 and 0.150 mm of a reference mixture were substituted with the corresponding particle size of expanded perlite CPCM, at a replacement level of 50% by mass of fine aggregate substituted. The maximum surface temperature difference between the reference and CPCM modified asphalt mixture specimens under transient laboratory and field conditions reported by Jin et al. (2017) were 7.0 and 4.3°C, respectively.

Kumalasari et al. (2018) confirmed that the temperature management of asphalt pavements using PCMs is promising. However, the mechanical performance of PCM modified asphalt materials could be compromised and should be further explored. Kumalasari et al. (2018) also made other interesting observations regarding the suitable types, incorporation methods, and phases transition temperatures of PCMs for pavement engineering applications. The research performed by Kumalasari et al. (2018) reported that paraffins and fatty acids had been the most studied PCM types for paving purposes. The key advantages of these PCM types are that their phase transition temperatures lie in the service temperature range of pavements, latent heat amounts are considerable, and volume change is minimal when changing phase. Kumalasari et al. (2018) noted that the direct incorporation of PCMs affects the asphalt penetration, softening point, and ductility properties. However, adequately encapsulated PCMs can postpone the appearance of critical temperatures, such as the temperatures that trigger the softening point of asphalt materials.

Athukorallage et al. (2018) conducted experimental work to develop heat transfer models for PCM modified asphalt materials, expanding the knowledge provided by Athukorallage and James (2016). In the experimental setup operated by Athukorallage et al. (2018), the heat conduction through a μPCM modified asphalt binder and base binder were determined. The PCM encompassed paraffin as core PCM and a polymer shell as encapsulating form. The μPCM modified asphalt binder and base binder were poured into a cylindrical container that was insulated from the bottom and rectangular faces. Thermocouples were inserted at the bottom, middle, and top of the specimens along their central axis. Then, the binder specimens were placed in an environmental chamber programmed to run a thermal cycle between 20 and 60°C in 24 hours. The experimental results were used to simulate the thermal response of μPCM modified asphalt binders through computational models. The binder simulations were further by Athukorallage et al. (2018) to predict the thermal behavior of asphalt pavement systems having μPCM modified surface layers between 25 and 50 mm. The computational effort done by Athukorallage et al. (2018) demonstrated that incorporating μPCMs into a pavement system could yield better temperature management compared to a conventional pavement.

Zhang et al. (2018) prepared an SSPCM with expanded graphite and polyethylene glycol. Thorough examinations were performed on the morphological, chemical, and thermophysical properties of the SSPCM produced by Zhang et al. (2018). XRD and DSC results indicated that polyethylene glycol's crystallization ability and phase change behavior were hindered using higher

doses of expanded graphite. In addition, nitrogen adsorption experiments revealed that the expanded graphite supporting matrix had an adsorptive limitation of polyethylene glycol. Porous characterization tests indicated that the maximum mass ratio of expanded graphite to polyethylene glycol to minimize PCM leakage is 1:7. SEM images and FTIR spectrum tests also proved that the 1:7 mass ratio was appropriate to formulate suitable SSPCMs made of expanded graphite and polyethylene glycol. TGA examined the viability of the SSPCM to withstand the mixing process of asphalt mixture at high temperatures. Overall, the study presented by Zhang et al. (2018) concluded that the produced SSPCM could reduce the thermal sensitivity of asphalt binders, decreasing its temperature variation rate. However, Zhang et al. (2018) suggested that further work is required to study the rheological properties and ultimate pavement performance of SSPCM modified asphalt materials.

Like Zhang et al. (2018), Jin et al. (2018) conducted a systematic study, analyzing the microstructure, chemical compatibility, and thermal properties of CPCMs. Two kinds of PCM, polyethylene glycol and ethylene glycol distearate, were combined with ceramsite to obtain CPCMs by vacuum impregnation. The ceramsite had a particle size between 4.75 and 9.5 mm. To prevent PCM leakage, the CPCMs were encapsulated with a epoxy resin. The CPCMs had phase transition temperatures of 54.3 and 56.1°C. The experimental results suggested that the CPCM with polyethylene glycol possesses better morphological, chemical, and thermal properties than the CPCM with ethylene glycol distearate. Thus, one-quarter of the aggregate between 4.75 and 9.5 mm of a reference mixture was substituted with CPCM containing polyethylene glycol. The reference and CPCM modified asphalt mixtures were exposed to a radiant lamp. First, the compacted mixture specimens were stabilized at room temperature. Then, both specimens were exposed to an irradiance of 800 W/m² until their temperature reached equilibrium at about 75°C. Temperature sensors were placed at the top and bottom surfaces of the asphalt mixture specimens. The maximum top and bottom temperature differences obtained during testing between the reference and CPCM modified specimens were 9.1 and 10.3°C, respectively.

Refaa et al. (2018) developed a numerical model to study the transient heat conduction in asphalt pavements with μPCMs. The investigation done by Refaa et al. (2018) was conceptually similar to the work done by Athukorallage and James (2016) and Athukorallage et al. (2018). Refaa et al. (2018) considered the volumetric heat capacities of the μPCM modified asphalt pavements as a function of the volumetric heat capacities of the μPCM and asphalt mixture.

Throughout the transient simulation, the properties of the core PCM in the μPCM were divided into liquid, mushy and solid fractions. The PCM assessed by Refaa et al. (2018) was an alkaline eicosane with a phase transition temperature of 36.5°C and latent heat of 247 J/g. A preliminary model was validated using actual climatic conditions for a conventional asphalt pavement in a dry zone climate. Then, Refaa et al. (2018) applied the prior model to study the effect of μPCM volume fraction on the thermal behavior of μPCM modified asphalt pavements. It was found that the thermal response of asphalt pavements could be tailored using μPCMs. As a result, Refaa et al. (2018) concluded that the mechanical performance of asphalt pavements might be enhanced by incorporating μPCMs into asphalt materials.

In 2019, Kakar et al. (2019a) made an effort to understand the direct interaction of tetradecane with asphalt binder. Tetradecane is a low-temperature PCM having a phase transition temperature of about 5°C. Kakar et al. (2019a) used three different penetration grade asphalt binders: (1) 10/20, (2) 70/100, and (3) 160/220. Penetration and softening point parameters were utilized to assess the physical effects of the PCM on the base binder. Temperature sweep tests were conducted by Kakar et al. (2019a) using a DSR to analyze the rheological response of tetradecane modified asphalt binders. In addition, the thermal properties of the base and modified binders were evaluated by applying DSC measurements. The tetradecane was directly incorporated into the base binders at three levels, 1, 5, and 10%, by binder mass. The results suggested that the PCM increased penetration and decreased both softening point and complex shear modulus. The rheological data was analyzed using black diagrams, which indicated that the PCM softened the asphalt binders. The DSC results showed that the tetradecane did not solidify during cooling. Therefore, no PCM latent heat storage properties were observed. Kakar et al. (2019a) concluded that a suitable encapsulation method must be applied to tune asphalt materials with PCMs.

Wei et al. (2019a) synthesized a CPCM by means of a two-step condensation reaction. The CPCM had a polyurethane as PCM, which has a solid-solid transformation. The CPCM synthesized by Wei et al. (2019a) showed a phase transition temperature range between 10.9 and 46.8°C, and latent heat of approximately 72 J/g. The CPCM demonstrated good thermal stability up to 320°C. Therefore, Wei et al. (2019a) manually stirred a base binder with the CPCM at 160°C for 30 minutes. The CPCM was incorporated into the asphalt material at three dosages, 3, 5, and 7%, by binder mass. Then, the CPCM modified binders were agitated at 170°C for 50 minutes under 5000 rpm to ensure a reasonable homogeneity. The viscosity of all the CPCM modified

binders was lower than 2000 cP at 120°C. Penetration and softening point tests performed by Wei et al. (2019a) suggested that the base binder is hardened as the CPCM content increases. Moreover, Wei et al. (2019a) proved that the ductility at 10°C is adversely affected as the CPCM content rises. As explained by Wei et al. (2019a), the base asphalt binder hardened because of some residual products from the synthesis process.

The work presented by Jin et al. (2017) and Jin et al. (2018) on CPCMs was complemented by the investigation published in Jin et al. (2019). A diatomite was selected by Jin et al. (2019) as a carrier material to vacuum impregnate a eutectic binary fatty acid composed of stearic acid and palmitic acid. The synthesized CPCM showed good morphological, thermal, and chemical stability. Jin et al. (2019) validated that proper quantification of thermal parameters (i.e., albedo) can help understand the variation in temperature for mixtures with and without CPCMs. Thermal performance tests revealed that a CPCM modified asphalt mixture specimen held a maximum temperature reduction of 8.11°C relative to a reference specimen. However, the CPCM modified asphalt mixture failed in high-temperature mechanical performance and moisture stability tests.

2.2.3 Microencapsulated phase change materials for asphalt pavement tuning

The research work done by Athukorallage et al. (2018) and Refaa et al. (2018) made μPCMs gain prominence as a PCM formulation suitable for paving applications. Thenceforth, most of the attention has been drawn to μPCMs over SSPCMs and CPCMs. μPCMs are PCMs with a liquid-solid transformation enveloped within a polymer or inorganic shell (Jamekhorshid et al., 2014). The existence of a shell material can prevent PCM leakage and restrict the PCM when it liquifies. To address the concerns reported by Kakar et al. (2019a), Wei et al. (2019b) fabricated a μPCM through in situ-polymerization using melamine-formaldehyde resin as shell and tetradecane as core PCM. The prepared μPCM showed a latent heat of 100.3 J/g at a phase transition temperature of about 4°C. The theoretical and measured microencapsulation ratio by mass of tetradecane were 43 and 39%, respectively. SEM images obtained by Wei et al. (2019b) indicated that the μPCM had spherical profiles, smooth surfaces, and particle diameters ranging from 0.100 to 0.200 mm. FTIR and TGA tests suggested that the μPCM experienced minimal PCM leakage up to 235°C. Wei et al. (2019b) also modified an 80/100 penetration graded asphalt binder with the μPCM at three different levels, 1, 3, and 5%, by base binder mass. Thermal cycle tests showed that the μPCM modified asphalt binders exhibited a lower temperature change rate. However, Wei et al. (2019b)

demonstrated that μPCM modified asphalt binders could be susceptible to storage stability problems.

In an attempt to build standardization across research studies, Ma et al. (2019) proposed two indices to evaluate the thermal effect of μPCM on asphalt mixtures. Based on the theory of latent heat, Ma et al. (2019) defined the accumulation of temperature difference between two asphalt mixtures in a time range as Latent Heat Accumulated Temperature Value (LHATV). While the completion degree of latent heat in unit time and the unit temperature was referred to as Latent Heat Thermoregulation Index (LHTI). Ma et al. (2019) embedded temperature sensors at various vertical and horizontal depths on a reference and μPCM modified asphalt mixture slabs to capture their thermal response. After monitoring multiple cooling and heating moments under field conditions, Ma et al. (2019) demonstrated that the proposed indices could quantify the thermal effect of the μPCM in the modified asphalt mixture slab. However, the solar radiation intensity was a key factor affecting the temperature variation of the slabs in the field. The uncontrolled environmental conditions made the LHATV and LHTI vary significantly, making it impossible to support standardization. Further studies are required to explore the proposed indices by Ma et al. (2019) more in-depth under controlled environmental conditions.

Kakar et al. (2019b) studied the aging effect on base and μPCM modified asphalt binders to determine the feasibility of this modification method. The μPCM used by Kakar et al. (2019b) consisted of melanime-formaldehyde as polymer shell and tetradecane as core PCM. Two types of microcapsules with average particle sizes of 0.007 and 0.021 mm were employed. Three asphalt binders with different penetration grades (i.e., 10/20, 70/100, and 160/220) were mixed using a speed mixer with 25% of μPCM by binder mass. Kakar et al. (2019b) found that the latent heat effect of μPCMs reduces upon aging. The results also suggested that the survival of μPCM in asphalt binder depends on the type of binder and μPCM size. By plotting master curves, Kakar et al. (2019b) observed an improved performance for the μPCM modified asphalts compared to the base binders. The study completed by Kakar et al. (2019b) concluded that the DSR could be a helpful tool to detect the thermal effect of μPCMs on the mechanical properties of modified asphalt binders, particularly during the melting and crystallization of PCMs. Kakar et al. (2019b) emphasized that this area of study needs further detailed investigations.

Kakar et al. (2019c) continued the assessment of μPCM modified binders using mechanical and thermal tests. The asphalt binders and μPCM evaluated by Kakar et al. (2019c) were similar

to the materials reported previously in Kakar et al. (2019a) and Kakar et al. (2019b). Asphalt binders with penetration grades of 160/220, 70/100, and 10/20 were analyzed at three concentrations of μPCM and lime mineral filler, 0, 1, and 3%, by base binder mass. The μPCM had a measured density and average particle size of 0.899 g/cm³ and 0.007 mm, respectively. In comparison, the lime mineral filler showed a measured density and average particle size of 2.780 g/cm³ and 0.019 mm, respectively. The temperatures used to mix the materials were 120°C for 160/220 binder, 130°C for 70/100 binder, and 140°C for 10/20 binder. DSR and DSC tests indicated that while blending, the μPCMs were damaged with both 70/100 and 10/20 asphalt binders and survived with the 160/220 asphalt binder. The μPCM modified 10/20 asphalt binders showed a much softer behavior than base and lime filler modified 10/20 asphalt binders. The expected and DSC-measured latent heat effects for the μPCM modified 160/220 asphalt binders were in good agreement, meaning minimal PCM leakage. However, no latent heat effect was captured by Kakar et al. (2019c) performing DSR measurements. Thus, Kakar et al. (2019c) encouraged using higher concentrations of μPCMs in asphalt binders to store a more considerable amount of thermal energy that could be detectable through rheological measurements.

In 2020, Ma et al. (2020) conducted a series of tests to enhance the selection process of μPCMs for asphalt pavement modification at a given location. Latent heat storage capacity tests were used to explore the heat transfer characteristics of μPCMs. The μPCMs used by Ma et al. (2020) had various tetradecanes as core PCMs and phase transition temperatures of -5, 0, and 5°C. The latent heats of the μPCMs were about 93 J/g. Ma et al. (2020) conducted an outdoor experiment to explore the variations in temperature of seven asphalt pavement slabs. Two slabs contained the μPCM with a -5°C phase transition temperature. Another two slabs were prepared with the μPCM having a 0°C phase transition temperature. Two other slabs were elaborated with the μPCM that transitioned at 5°C. For each μPCM type, the μPCM was incorporated by substituting an equivalent amount of mineral filler at the dosages of 0.3 and 0.5% by total slab mixture mass. Ma et al. (2020) fabricated a final slab without μPCMs that was used as reference. Temperature sensors were installed in the center, as well as the surfaces of each slab. Considering that the ambient temperature range studied by Ma et al. (2020) was between 0 and 10°C, the μPCM transitioning at 5°C showed the best temperature management response; also, the μPCM effect was more pronounced for the slab containing a 0.5% μPCM dosage, rather than slab with a 0.3%

μPCM dosage. The maximum ambient air and asphalt pavement slab temperature change rates observed by Ma et al. (2020) were approximately 0.01 and 0.02 °C/h, respectively.

Bueno et al. (2019) studied the use of μPCMs to regulate the temperature of road surfaces and avoid low-temperature damages when asphalt materials become brittle and prone to cracking. A reference asphalt mixture was modified with a μPCM transitioning near 6°C and with a latent heat and average particle size of about 195.5 J/g and 0.021mm, respectively. Bueno et al. (2019) investigated the impact of replacing mineral filler with μPCMs on mechanical and thermal performances. Bueno et al. (2019) also paid attention to dry (i.e., added to the aggregate blend and then mixing with binder) and wet (i.e., merged to binder before mixing with the aggregate blend) modification processes for incorporating the μPCM particles into the mixtures. In both scenarios, the μPCM was integrated at a ratio of 50% by binder mass. The results gathered by Bueno et al. (2019) demonstrated that μPCM add-ons are indeed able to slow down pavement cooling and prevent temperatures below zero. A maximum temperature offset of 2.5°C was achieved by the μPCM modified asphalt mixture specimen while cooling from 10 to -10°C compared to the non-μPCM modified specimen. However, Bueno et al. (2019) also suggested that the μPCM incorporations significantly reduce the modified mixtures' stiffness compared to the response observed for the reference mixture. Minimal differences were noticed by Bueno et al. (2019) when adding the μPCM through a wet or dry mixing process.

2.3 Summary of Literature Review

In general, the incorporation of PCMs into asphalt pavement materials has been primarily motivated by the successful application of PCMs in a wide variety of engineering fields. The challenges currently faced by asphalt pavement scholars to understand this topic overlap with the obstacles experienced by scholars in other engineering applications. Several approaches could be used for the proper selection and optimization of PCM for asphalt pavement purposes. A fundamental understanding of PCMs' latent heat storage capacities is essential to promote PCM tuned asphalt pavements.

The relevant literature in PCM modified asphalt pavements research has focused on demonstrating this concept's practical potential. A large and growing body of literature has investigated numerous PCM formulations' morphological, thermal, and chemical performance for asphalt pavement purposes. SEM, FTIR, XRD, DSC, and TGA have been the most common tests

used for such analyses (Ma et al., 2011; He et al., 2013; Leng et al., 2014). In most cases, comparative test inputs are used across studies. These studies suggest that morphological, thermal, and chemical tests are appropriate to determine the feasibility of using a PCM formulation in asphalt pavement materials. However, initial studies have been primarily concerned with SSPCM and CPCM, some of the earliest PCM formulations appraised for paving purposes. SSPCMs and CPCMs can be described as composite materials consisting of a dispersed PCM material (i.e., paraffin) supported by a carrier material, for instance, activated carbon, sol-gel, and silica (Ma et al., 2011; Si et al., 2015; Kheradmand et al., 2015). There are differences between SSPCMs and CPCMs, but frequently the terms are used interchangeably due to their similarities. These types of PCMs are found defective for asphalt material modification mainly because of PCM leakage issues. Such findings led to the consideration of μPCMs for the thermal adjustment of asphalt binders and mixtures. While proper test methods to evaluate PCM formulations' toughness and abrasion characteristics are missing, μPCMs have demonstrated a more viable approach for tuning asphalt pavements to the environment than SSPCMs and CPCMs.

One body of literature is concerned with developing computational models to predict the heat transfer and temperature variations in PCM modified asphalt pavements (Athukorallage and James, 2016; Athukorallage et al., 2018; Refaa et al., 2018). Similar volume-averaged energy governing equations have been applied to estimate the transient response of PCM modified asphalt pavement structures. Conversely, a volume of published studies reports the results of PCM modified asphalt pavement slabs exposed to controlled and uncontrolled environmental conditions (Jin et al., 2018; Ma et al., 2019). A wide range of experimental setups has been employed to investigate the temperature variations of PCM modified asphalt mixture specimens. A few measuring indices have been proposed to quantify the extent to which μPCMs change temperature profiles of asphalt pavements (Ma et al., 2019). The experimental and computational results show enough evidence to support the thermoregulation of asphalt pavements with μPCMs. Still, some disagreement exists between the experimental and numerical results obtained across the studies available in the literature. Computational studies tend to underestimate the μPCM effect in comparison to experimental results. Simulations typically yield a lower temperature difference between reference and PCM modified asphalt pavements. Few models have been calibrated and validated using relatable experimental data.

The past decade has seen the rapid development of μPCMs for diverse engineering applications (Jamekhorshid et al., 2014), aiding the incorporation of this thermoregulating agent in asphalt materials. As a result, more recent attention has focused on conducting mechanical performance tests for μPCM modified asphalt binders and mixtures. The rheological behavior of μPCM modified asphalt binders has been studied using conventional and unconventional testing protocols (Wei et al., 2019b; Kakar et al., 2019b; Kakar et al., 2019c). In contrast, μPCM modified asphalt mixtures' mechanical performance has been mainly examined by conducting standard test protocols (Bueno et al., 2019), relinquishing the thermal effect of μPCMs on the engineering behavior of compacted asphalt mixture specimens unexamined. Further studies are required to fully quantify the μPCM latent heat effect on the performance of asphalt pavements. Several questions regarding the mechanical characterization of μPCM modified asphalt materials remain to be addressed. For example, the thermomechanical response of μPCM modified asphalt materials evaluated under contiounous loads when the core PCM is in solid or liquid phase. There is a lack of standard methods for assessing the suitability of a given μPCM formulation to a specific asphalt pavement environment or target asphalt mixture distress. An investigation is needed to develop procedures that allow comparison and evaluation for μPCM modification in asphalt paving materials. Given such information, this dissertation seeks to obtain data that will help to address these research gaps. Therefore, a series of theoretical, experimental, statistical, and computational approaches are demonstrated, the results of which can be instrumental in extending the knowledge of PCM tuned asphalt pavements.

3. INCORPORATING PHASE CHANGE MATERIALS IN ASPHALT PAVEMENTS TO MELT SNOW AND ICE[a]

[a]This Chapter is extracted from the draft manuscript "Incorporating Phase Change Materials in Asphalt Pavements to Melt Snow and Ice", to be submitted for publication.

3.1 Introduction

The snow accumulation and ice formation in asphalt pavement riding surfaces plays a critical role in the direct contact of the roadway with vehicle traffic. Considering the importance of this matter to vehicle transportation safety and other pavement performance concerns, PCMs have emerged as a potential solution to make snow and ice removal more accessible. The ability of PCMs to dissipate and store thermal energy shows promise to reduce snow accumulation and ice formation on the surface of pavements (Farnam et al., 2017; Esmaeeli et al., 2018). However, the potential benefits of their incorporation into asphalt pavements under actual thermal cycles and snowfall events have yet to be understood. The formulation of PCMs and their addition to asphalt pavements has been primarily researched in a generalized fashion, rather than targeting specific purposes, such as snow and ice melting.

The work reported in this chapter investigates the snow and ice melting processes of a PCM modified asphalt pavement slab using laboratory experiments and numerical simulations. The snow accumulation and ice formation on roadways cause unsafe conditions primarily due to the reduction of road surface friction. The most common de-icing agent is sodium chloride, commonly used preemptively when wet, freezing temperatures, or snow is forecasted. However, due to the adverse environmental effects and high costs of de-icing agents, highway transportation agencies seek to decrease the use of chemicals while maintaining traffic safety and road accessibility (Riehm et al., 2012).

In recent years, several different techniques have been developed with the specific objective of melting snow and ice from pavement surfaces without using conventional de-icing agents or methods, such as sand, grit, and snow plowing. In addition, intrinsic resistance to snow accumulation and ice formation on asphalt pavements has been investigated to minimize the spread of large amounts of de-icing agents along roads. One study proposed the direct addition of a synthetic filler during the production of asphalt mixtures (Giuliani et al., 2012). This filler consists

of a combination of inorganic materials whose main component is sodium chloride. Compared to traditional limestone asphalt mixture fillers, the anti-icing filler considerably delays ice formation on the pavement surface, accelerating the snow and ice melting process and reducing the adhesion between snow and ice and the pavement surface. However, the inclusion of sodium chloride in the asphalt pavement structure can negatively impact both the environment and pavement structure.

A different approach to solving snow accumulation and ice formation on asphalt pavement surfaces involves using an asphalt solar collector (Chen et al., 2011). In this method, fluid is circulated through a series of pipe circuits laid below the pavement surface, acting much like a geothermal cooling-heating system. The pavement absorbs solar radiation transferring it to fluid in the embedded pipes. During the warmer months, this heat is stored in the surrounding soil. When snow and ice are forecast, the stored energy is then used to warm the pavement surface, thereby inhibiting snow accumulation and ice formation. A small-scale study demonstrated this type of snow melting system and concluded that an asphalt pavement solar collection could be helpful for snow melting purposes (Chen et al., 2011). The investigation done by Chen et al. (2011) showed that such a hydronic snow melting system could function at a fluid (i.e., water) temperature of about 25°C, a temperature favorable to asphalt pavements, which are susceptible to permanent deformation if exposed to relatively high temperatures (above 45°C). Such a condition has precluded snow melting systems that use electric heating wire buried in the pavement, as have been successfully implemented in concrete pavements for anti-icing and de-icing (Sassani et al., 2018).

A methodology that has evidenced the ability to melt snow and ice on the surface of concrete slabs is placing PCMs inside the concrete. A previous study demonstrated that when a PCM modified concrete slab was exposed to an ambient temperature above the transitioning temperature of the PCM before a snow event, a latent heat release beneficial for melting snow and ice can be obtained by embedding pipes containing PCMs in the concrete (Farnam et al., 2017). The work reported herein demonstrates the incorporation of PCMs in embedded metallic pipes inside an asphalt pavement slab. First, reference and PCM modified asphalt pavement slabs were tested in a thermally controlled environmental chamber. This experimental work aimed to characterize the latent heat release capacity of the PCMs during freezing and melting moments, as well as under snow events. Additionally, numerical simulations were performed to predict the TES effect of PCMs on improving the freeze-thaw performance of asphalt pavements exposed to

realistic thermal conditions at various locations throughout the United States. The contributions of the work should be of broad interest to those wishing to implement TES systems for low-temperature management and to melt snow and ice from asphalt pavement surfaces, and any other engineering applications that require such TES properties.

3.2 Methodology

The methodology for this portion of the dissertation consisted of three parts: (1) thermal cycling of asphalt pavement slabs, (2) snow melting evaluation of asphalt pavement slabs, with and without PCMs, and (3) finite element simulations of asphalt pavement slabs exposed to representative environmental conditions.

3.2.1 Materials

The asphalt pavements slabs were prepared using a 9.5-mm hot-mixed asphalt mixture, PCMs, and low-carbon steel pipes. The asphalt mixture was plant-produced and composed of a PG 70-22 asphalt binder, coarse dolomite aggregate, fine dolomite aggregate, fine Reclaimed Asphalt Pavement (RAP), and mineral filler. The asphalt mixture was laboratory-designed using 50 gyrations of the Superpave Gyratory Compactor (SGC), choosing optimum binder content at 5% air voids content. The asphalt binder content to achieve the target air voids content was 6.2% by total mixture mass. The coarse dolomite aggregate possessed high crushed angularity properties; at least one fractured face and at least two fractured face percentages were 100 percent. The fine dolomite aggregate angularity was 46 percent. The fine RAP aggregate provided a 17.6% asphalt binder replacement. The asphalt mixture Voids in the Mineral Aggregate (VMA), Voids Filled with Asphalt (VFA), and Dust-to-Binder Ratio (DBR) were 16.5, 69.7, and 1.0%, respectively. The tensile strength ratio obtained for the asphalt mixture was 83.8 percent. The asphalt mixture production temperature was approximately 157°C.

Two fatty acid methyl esters were used in the study, a methyl laurate (C12:0, 95% pure, CAS: 111-82-0) and a binary methyl laurate/myristate (CAS: 67762-40-7) comprised of methyl laurate (C12:0, 70.5-74.5% pure) and methyl myristate (C14:0, 24-29% pure). The fatty acid methyl esters were reported to have specific gravities of 0.900, vapor pressures less than 0.01 mm Hg, and viscosities of 4 cp at 20°C. Both PCMs have a boiling temperature above 204°C. The

melting points (or phase transition temperatures) specified by the methyl laurate and methyl laurate/myristate supplier were 5 and 7°C, respectively.

In general, fatty acid methyl esters show solid-liquid phase transitions with desirable thermal properties within a narrow temperature range. This type of PCM can be tailored to include a phase transition temperature that differs from the pure material for the required temperature, slightly above 0°C, and high latent heat (>150 J/g), making them ideal for low-temperature management (Liston et al., 2016). Additionally, their physical properties include low vapor pressure and small volumetric changes during phase transition. Fatty acid methyl esters are chemically stable, non-toxic, and non-flammable. They are commercially available and sustainably derived from common vegetable and animal oils providing a renewable supply without relying on petroleum (Liston et al., 2016). However, they might cause damage to pavement materials upon direct contact (Kakar et al., 2019a; Jin et al., 2017). Thus, the PCMs were contained in low-carbon steel tubes, grade 008-1010, and yield strength of 30,000 psi. The low-carbon steel pipes' outer diameter, inner diameter, and wall thickness dimensions were approximately 32, 28, and 2 mm, respectively.

3.2.2 Fabrication of slabs

Figure 3.1a shows a schematic of the experimental setup used to compare the thermal performance of Reference (without PCM) and PCM (with PCM) asphalt pavement slabs. The Reference slab consisted of a 76.2 mm thick asphalt mixture structure. The Reference slab was fabricated in two lifts, a 25.4 mm thick bottom layer and a 50.8 mm thick top layer. The plant-produced asphalt mixture was heated in a laboratory oven at 135°C for two hours. Once heated, the required amount of mixture to achieve a specific compacted lift thickness was placed into the slab mold. The material was spread evenly and leveled using a carbon steel 203.2 mm x 203.2 mm tamper. Ten tamper blows were applied evenly to level the material. A 101.6 mm diameter manual Marshall hammer was then used, in a tamping fashion, to increase the asphalt mixture layer density. A total of 50 Marshall hammer blows were applied uniformly across the top surface of each layer. Lastly, ten tamper caron steel tamper blows were again used to remove any marks left by the Marshall hammer and produce a smooth surface. The top layer was placed 24 hours after the bottom layer was cast.

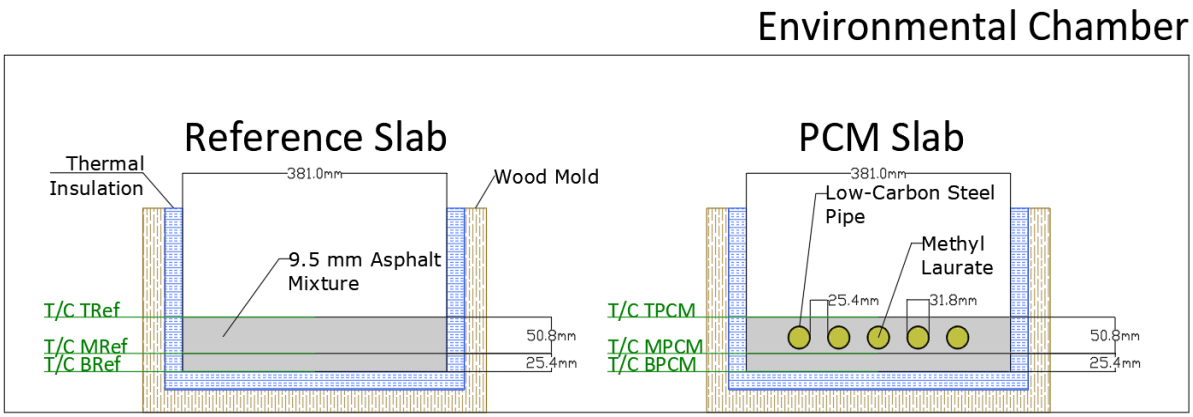

(a)

(b)

Figure 3.1. (a) Schematic of asphalt pavement slabs with and without PCM and (b) PCM slab fabrication.

For measuring purposes, type T thermocouples were placed at the bottom of the slab, between layers, and at the top surface, referred to as T/C BRef, T/C MRef, and T/C TRef, respectively. The T/C BRef was placed before laying the bottom layer of material, T/C MRef was placed after compacting the bottom layer and before placing the top layer, and the T/C TRef was attached after compacting the top layer. The bottom and lateral surfaces of the slab were insulated using a 25.4 mm thick thermal insulation board. The insulating composite has a service temperature range between -40 and 135°C, making this insulation board suitable for casting asphalt mixtures. The lateral sides of the asphalt pavement slabs had a length of approximately 381 mm. An insulating foam sealant was applied at the slab's top surface between the asphalt pavement edges and the insulation board to minimize heat losses. The slab mold was made of 38.1 mm thick wood.

The PCM slab was fabricated and dimensioned the same as the Reference slab. However, five evenly spaced low-carbon steel pipes were seated above the asphalt mixture bottom layer and embedded within the top layer, as shown in Figure 3.1b. The distance between the outer surfaces of the pipes was 25.4 mm. About 50.8 mm of pipe projected out of the slab mold from both ends of the pipes. The pipes were filled entirely with PCM and carefully sealed using thread seal tape and steel caps. The portions of pipe that projected out of the slab mold were thoroughly insulated with the same composite used to protect the asphalt material. The type T thermocouples placed at the bottom of the PCM modified slab, between both layers, and at the top surface are referred to as T/C BPCM, T/C MPCM, and T/C TPCM, respectively. In terms of volume proportions, the asphalt mixture, PCM, and steel pipe account for approximately 86, 11, and 3% of total PCM slab volume, respectively.

3.2.3 Thermal cycling experiments

The Reference and PCM asphalt pavement slabs were placed in a thermally controlled environmental chamber for the thermal cycling experiments. The environmental chamber temperature was varied between 10 and -10°C to capture the PCM effect. The test's initial temperature was set to remain at 10°C for 24 hours to allow the slabs to equilibrate thermally. Then, a cooling-heating cycle was applied: (1) the temperature in the chamber was cooled from 10 to -10°C at a prescribed rate, (2) once the environmental temperature reached -10°C, the temperature of the chamber was kept constant for 24 hours, (3) the temperature was then increased to 10°C at a predetermined rate, and (4) after reaching 10°C, the temperature was kept constant for 24 hours. The time taken to increased and decreased the temperature was the same for each experiment. A total of three rates for cooling and heating were employed for this study, 0.6, 4.0, and 8.0 °C/h. The temperature profile of the asphalt pavement slabs was captured from the thermocouples using a data logger. The temperature measurements were taken at 10-second intervals. Both PCM substances were tested under thermal cycling experiments.

3.2.4 Snow melting experiments

The ability of a methyl laurate modified asphalt pavement slab to melt snow was determined by performing snow melting experiments. For comparison purposes, the Reference and PCM slabs

were tested concurrently. Artificial snow (i.e., shaved ice) was made using cubic ice at -4°C and a commercial ice shaver machine, and applied to the surface of the asphalt pavement slabs. The snow was gently distributed and leveled while the slabs were in the thermally controlled environmental chamber. A total of 1000 g of artificial snow were applied, achieving an approximately 25.0 mm thick layer of snow on top of the asphalt pavement slabs. A time-lapse camera capturing photos at one-minute intervals was used to record the snow melting behavior. Each slab was tilted slightly (about 15°) to allow melted snow (water) to flow off the asphalt pavement slab surfaces and drain through a plastic tube. The tubes were placed at the lowest corner of the slabs and connected to a beaker sitting on a scale. The mass change of the beakers was recorded every two minutes. The slabs' temperature was also recorded at 10-second intervals at three different locations, as previously described in Figure 3.1a.

Two tests were used with different temperature sequences. In the first test, Procedure A, the maximum ambient temperature was kept at 5°C, while the minimum ambient temperature was maintained at 0°C. In the second experiment, Procedure B, the maximum ambient temperature was held at 8°C, while the minimum ambient temperature was kept at 3°C. The minimum temperature for Procedure B was controlled above the freezing temperature of the PCM (about 2°C for methyl laurate as determined through thermal cycling experiments). In contrast, the maximum and minimum temperatures for Procedure A were kept above and below the freezing temperature of the PCM. This methodology was done to assess the capability of the PCM to melt snow under different environmental temperature scenarios.

Snow melting experiments consisted of: (1) equilibrating the slab temperature at the maximum ambient temperature for 48 hours, (2) decreasing the ambient temperature in the thermally controlled environmental chamber to the minimum ambient temperature in 1 hour, (3) keeping the temperature at the minimum temperature for 7 hours, (4) then, adding 1000 g of snow on the top of the slab in less than 5 minutes, (5) keeping the temperature at the minimum temperature for 41 hours, (6) increasing the temperature to the maximum temperature in 1 hour, and (7) keeping the temperature at the maximum temperature for 48 hours.

3.2.5 Finite element simulations

To better understand the thermal response of PCM modified asphalt pavements under transient environmental conditions, two-dimensional finite element simulations were conducted using the

ABAQUS commercial software. Heat transfer models of the Reference and PCM asphalt pavement slabs were developed and calibrated using the experimental results. The software considers that a liquid-solid phase change is usually abrupt and is accompanied by a robust latent heat effect and consequently defines this case as a two-dimensional Stefan problem (Smith, 2009; Athukorallage and James; 2016). A brief overview of the mechanisms governing this latent heat energy storage system is given below.

Governing equations

Heat transfer Finite Element Models (FEMs) are built upon thermodynamics' first law over a time interval (or the law of conservation of energy). This principle states that the increase in the amount of thermal energy stored in the control volume must equal the amount of thermal energy that enters the control volume, minus the amount of thermal energy that leaves the control volume, plus the amount of thermal energy that is generated within the control volume (Incropera, 2007). As shown in Figure 3.2, the modes of heat transfer considered for this finite element analysis are conduction and convection. The heat transfer mechanisms can be explained in a model using the primary energy balance equation, Equation 3.1.

$$\int_V \rho \dot{U} dV = \int_S q dS + \int_V r dV \qquad \text{(Eq. 3.1)}$$

where:

V = volume of solid material,

S = surface area of solid material,

ρ = density of the material,

$\dot{U}$ = material time rate of the internal energy,

q = heat flux per unit area of the body, flowing into the body, and

r = heat supplied externally into the body per unit volume.

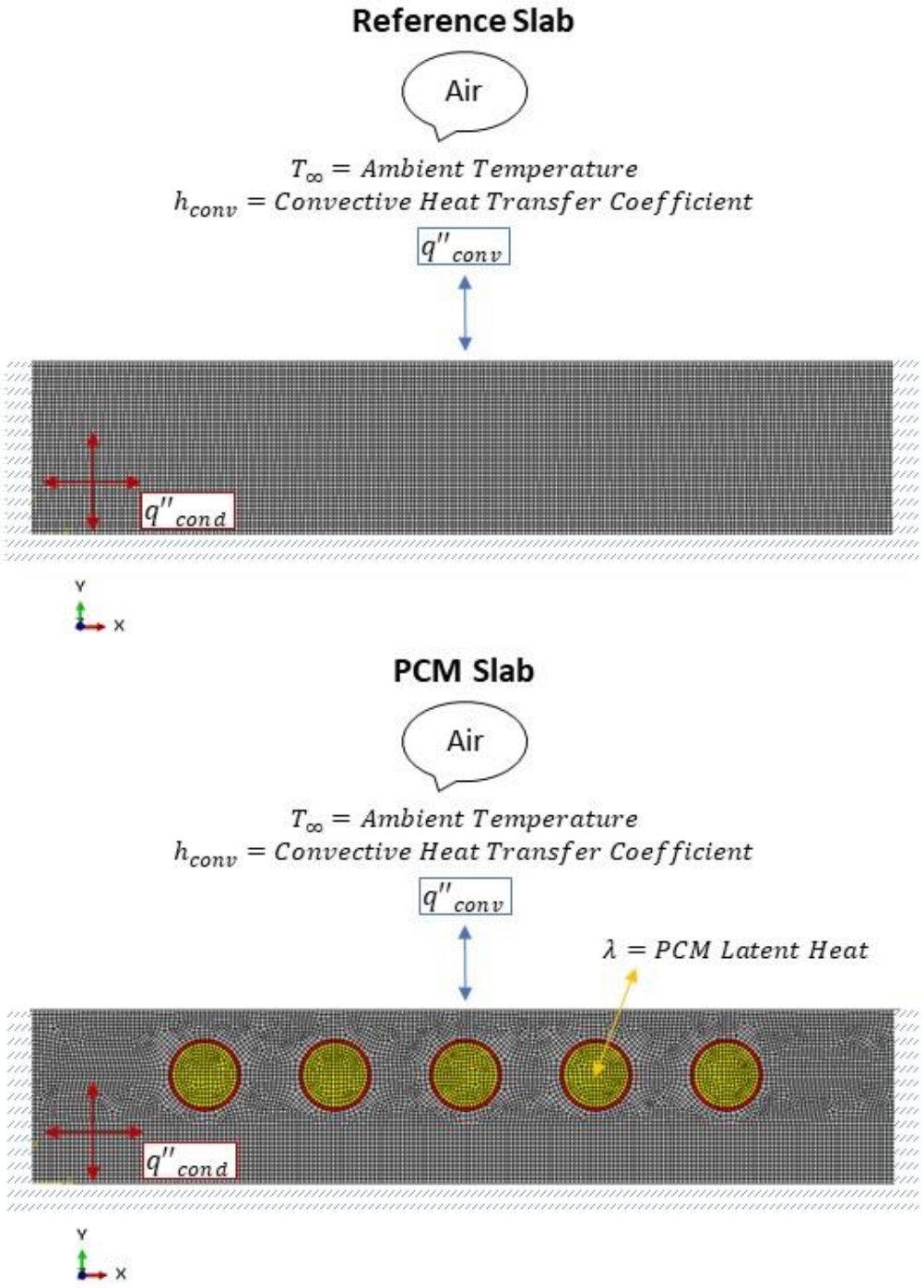

Figure 3.2. Schematic of finite element analysis.

Heat conduction is assumed to be governed by the Fourier Law, and the constitutive relationship is written as an expression of specific heat when latent heat is not present and neglecting the coupling between mechanical and thermal problems. However, when a latent heat

effect is present, the released and absorbed energy is assumed to be in addition to the specific heat effect. In the model, latent heat effects at phase changes are given separately in terms of solidus and liquidus temperatures (the lower- and upper-temperature bounds of the phase change range) and the total internal energy associated with the phase change (Smith, 2009). The latent heat material is analyzed by conducting a two-dimensional Stefan problem, as described by (Beckett et al., 2001). Let $\Omega \in \mathbb{R}^2$ be a bounded polygonal domain and $T > 0$. Set $Q := \Omega \times (0, T)$. It is well known that a substance of constant conductivity and unit density satisfies the heat formula, as shown in Equation 3.2.

$$\frac{\partial u}{\partial t} = \frac{\partial^2 \theta}{\partial x^2} + \frac{\partial^2 \theta}{\partial y^2} + f(x, y, t) \qquad \text{(Eq. 3.2)}$$

where:

θ = temperature,

$u(\theta)$ = enthalpy, and

$f(x, y, t)$ = any body heating or cooling sources.

For this study, the body source is represented by the conditions imposed by the pipe containing the PCM. If a pure substance with constant specific heats c_1 and c_2 undergoes a change of phase at the temperature $\theta = \theta_m$, then the enthalpy may be written as displayed in Equation 3.3.

$$u(\theta) = \begin{cases} c_1(\theta - \theta_{ref}), & \theta < \theta_m \\ u(\theta_m^-) + \lambda + c_2(\theta - \theta_m), & \theta_m \leq \theta \end{cases} \qquad \text{(Eq. 3.3)}$$

where:

$u(\theta_m^-) = lim_{\delta \to 0^-} u(\theta_m + \delta)$,

θ_{ref} = any reference temperature below θ_m, and

λ = PCM latent heat.

The following assumptions considerably simplify the latent heat transfer analysis: (1) The properties of the materials undergoing melting or freezing can be satisfactorily described by not more than two sets of properties, one for the liquid state and one for the solid state; the properties of both phases are assumed to be the same in the neighborhood of the interface (in this study, nominal phase transition temperature of PCM), and (2) the liquid melt remains stationary so that heat is transferred through it only by conduction (Lazaridis, 1970).

Finite element models

Two-dimensional finite element modeling was performed on the asphalt pavement slabs to evaluate their thermal responses. The presence of a PCM in the models required a transient heat transfer analysis. The geometric properties of the asphalt pavement slabs were used to assemble the FEMs. The assemblage of the asphalt pavement slabs with and without PCM was discretized into a total of 8904 and 9118 first order 4-noded quadrilateral elements (DC2D4), respectively (see Figure 3.2). This element type allows for heat storage, including specific heat and latent heat effects and heat conduction, and provides temperature output. The mesh was refined to avoid distorted element shapes and generate temperature output at the exact coordinates where the thermocouples were placed during the laboratory investigation.

Furthermore, to develop the models, it was assumed that: (1) all material (asphalt mixture, steel pipe, and PCM) parts are homogenous and isotropic, (2) thermal properties of asphalt mixture and steel pipes are constant and temperature-independent, (3) convective flow, if any, inside the liquid PCM is ignored, (4) there is no interfacial resistance between the asphalt mixture and steel pipes, and between asphalt pavement layers, and (5) the lateral and bottom surfaces are perfectly insulated. The initial temperature (when the analysis starts) of the entire asphalt pavement slab is assumed to be the same as the initial temperature of the environmental chamber or initial ambient temperature when the models were running under representative climatic conditions.

First, the materials' thermal properties were verified and calibrated using data obtained from the thermal cycling experiments and literature. A convective heat transfer coefficient was established to proceed with the analysis. The temperature outputs obtained at the predetermined locations were compared to the laboratory experiments' temperature measurements to validate the models. Finally, the FEMs were employed to simulate the field performance of PCM modified asphalt pavements at various airport locations in the United States. The slabs were subjected to actual climatic data, including hourly averages of temperature for one year from May 2019 through April 2020 for each airport location. The climatic data were obtained from the Local Climatological Data (LCD) online platform. As shown in Table 3.1, a total of 100 airport locations were examined.

Table 3.1. Airport locations used for field simulations.

No.	FAA code	Location	No.	FAA code	Location
1	ABQ	Albuquerque, NM	51	JAX	Jacksonville, FL
2	ALB	Colonie, NY	52	LAS	Las Vegas, NV
3	ATL	Atlanta, GA	53	LAX	Los Angeles, CA
4	AUS	Austin, TX	54	LGA	Queens, NY
5	BDL	Windsor Locks, CT	55	LIT	Little Rock, AR
6	BGR	Bangor, ME	56	MAF	Midland, TX
7	BHM	Birmingham, AL	57	MCI	Kansas City, MO
8	BIL	Billings, MT	58	MDT	Middletown, PA
9	BIS	Bismarck, ND	59	MEM	Memphis, TN
10	BNA	Nashville, TN	60	MFR	Medford, OR
11	BOI	Boise, ID	61	MIA	Miami, FL
12	BOS	Boston, MA	62	MKE	Milwaukee, WI
13	BTV	Burlington, VT	63	MSN	Madison, WI
14	BUF	Buffalo, NY	64	MSP	Minneapolis–Saint Paul, MN
15	BWI	Baltimore, MD	65	MSY	Kenner, LA
16	BZN	Belgrade, MT	66	OKC	Oklahoma City, OK
17	CHS	North Charleston, SC	67	OMA	Omaha, NE
18	CLE	Cleveland, OH	68	ORD	Chicago, IL
19	CLT	Charlotte, NC	69	PDT	Pendleton, OR
20	CMH	Columbus, OH	70	PDX	Portland, OR
21	COS	Colorado Springs, CO	71	PHL	Philadelphia, PA
22	CPR	Casper, WY	72	PHX	Phoenix, AZ
23	CRW	Charleston, WV	73	PIA	Peoria, IL
24	CVG	Hebron, KY	74	PIT	Pittsburgh, PA
25	DCA	Arlington, VA	75	PNS	Pensacola, FL
26	DEN	Denver, CO	76	PSM	Portsmouth, NH
27	DFW	DFW Airport, TX	77	PVD	Warwick, RI
28	DLH	Duluth, MN	78	PWM	Portland, ME
29	DSM	Des Moines, IA	79	RAP	Rapid City, SD
30	DTW	Detroit, MI	80	RDD	Redding, CA
31	EKO	Elko, NV	81	RDU	Morrisville, NC
32	ELP	El Paso, TX	82	RIC	Richmond, VA
33	EWR	Newark, NJ	83	RNO	Reno, NV
34	FAR	Fargo, ND	84	ROW	Roswell, NM
35	FAT	Fresno, CA	85	SAN	San Diego, CA
36	FSD	Sioux Falls, SD	86	SAT	San Antonio, TX
37	GCK	Garden City, KS	87	SDF	Louisville, KY
38	GCN	Grand Canyon Village, AZ	88	SEA	SeaTac, WA.
39	GEG	Spokane, WA	89	SFO	San Francisco, CA
40	GJT	Grand Junction, CO	90	SGF	Springfield, MO
41	GPI	Kalispell, MT	91	SGU	St. George, UT
42	GRI	Grand Island, NE	92	SJC	San Jose, CA
43	GRR	Grand Rapids, MI	93	SLC	Salt Lake City, UT
44	IAH	Houston, TX	94	SMF	Sacramento, CA
45	ICT	Wichita, KS	95	STL	St. Louis, MO
46	IDA	Idaho Falls, ID	96	TLH	Tallahassee, FL
47	ILG	New Castle, DE	97	TUL	Tulsa, OK
48	IND	Indianapolis, IN	98	TUS	Tucson, AZ
49	JAC	Jackson, WY	99	TVC	Traverse City, MI
50	JAN	Jackson, MS	100	TYS	Alcoa, TN

3.2.6 PCM Effectiveness

The PCM Effectiveness parameter was employed to quantify the laboratory and field performance of the PCM modified slab. As shown in Equation 3.4, the PCM Effectiveness is the percentage difference of time below 0°C between the Reference and PCM slabs at a given pavement location (Esmaeeli et al., 2018). This study's PCM Effectiveness is the average percentage difference of time below 0°C obtained at three different locations (i.e., top surface, between pavement layers, and bottom surface).

$$t_{PCM-eff}\ (\%) = \frac{t_{ref}[T < 0\ (℃),\quad (x,y)] - t_{PCM}[T < 0\ (℃),\quad (x,y)]}{t_{ref}[T < 0\ (℃),\quad (x,y)]} \times 100 \qquad \text{(Eq. 3.4)}$$

where:

$t_{PCM-eff}$ = percentage difference of time within the pavement,

t_{ref} = number of hours that reference pavement experiences a freeze-thaw cycle at a given (x, y) coordinate, and

t_{PCM} = number of hours that pavement with PCM experiences a freeze-thaw cycle at a given (x, y) coordinate.

3.3 Results and Discussion

3.3.1 Thermal cycling experiments

The thermal response of the slabs without PCM and with methyl laurate/myristate is demonstrated in Figure 3.3. The slabs were subjected to cooling, heating, and dwelling moments between 10 and -10°C to evaluate the slabs' thermal characteristics during ambient temperature variations, as shown in Figure 3a. For the Reference slab without PCM, the temperature within the depth of the slab dropped and rose in conformity with the environmental chamber's thermal conditions. The Reference slab's temperature transitions are dramatic and linear (Figure 3.3b), meaning that it is easily induced to temperature fluctuations by the surrounding environment. A visual comparison of the contour plots reveals that the PCM slab shows a thermal resistance when transitioning between 10 and -10°C, and vice versa. This behavior is mainly due to PCM freezing and melting, which releases and absorbs thermal energy to provide more gradual temperature transitions. Looking at Figure 3.3c, it is apparent that the PCM effect occurs between 5 and 0°C. During the

cooling moment, the onset of the PCM heat can be seen at an approximate depth from the top surface of 50 mm, which is in good agreement with the steel pipes' location containing the PCM.

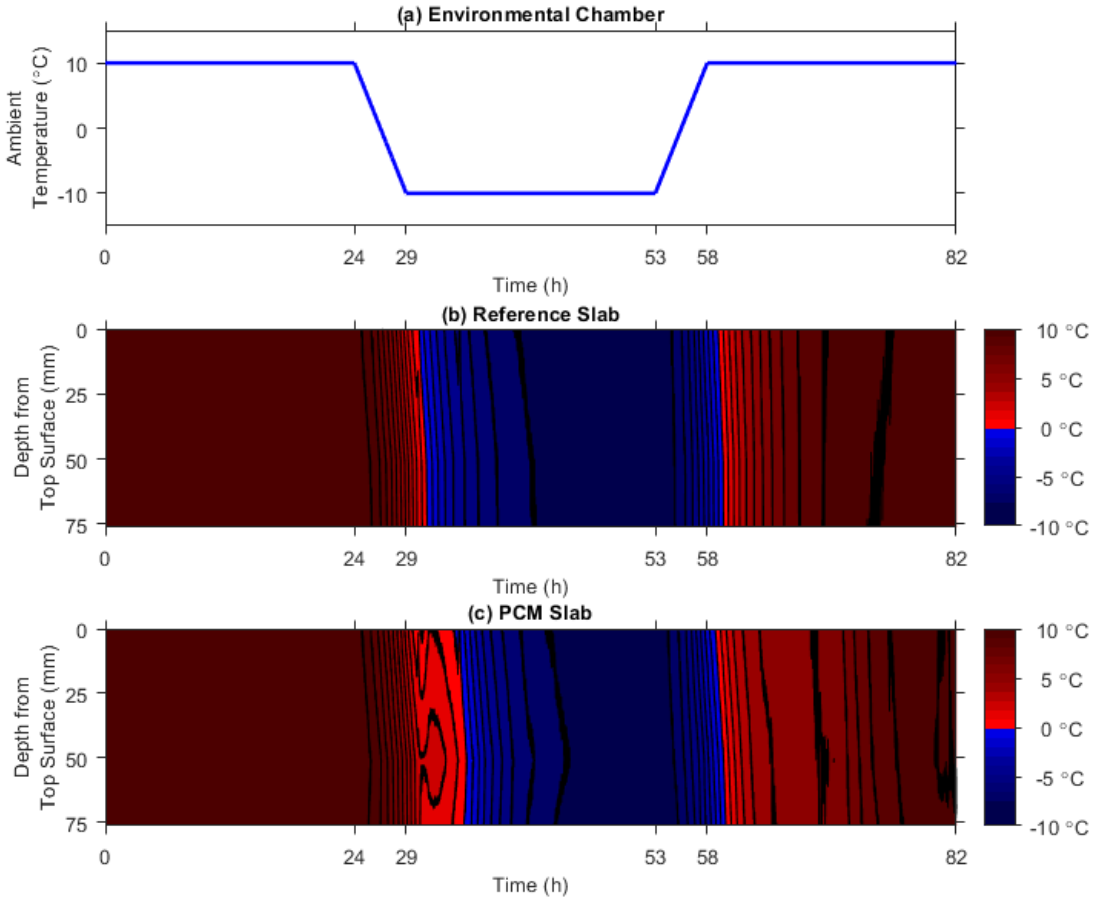

Figure 3.3. Thermal response of Reference slab and PCM slab with methyl laurate/myristate subjected to a rate of 4.0 °C/h for cooling-heating cycle between 10 and -10°C.

For the sake of brevity, the thermal cycling contour plots for each experiment combination are omitted. Table 3.2 reports the mean maximum temperature difference and PCM Effectiveness for the cooling moment of each experiment. As previously explained, the mean maximum temperature difference between the Reference and PCM slab was calculated by averaging the differences in temperature obtained at the three thermocouple locations. For both PCMs, the experimental data shows that the lowest mean maximum temperature difference was obtained for the 0.6 °C/h cooling rate. When these mean maximum temperatures occurred, the average PCM slab temperatures were 0.5 and 1.0°C for methyl laurate and methyl laurate/myristate, respectively. Additionally, during the melting moment of the thermal cycle, the PCM effect consistently

occurred above 0°C regardless of cooling rate, causing minimal consequences in the time to which the slab temperature was below 0°C. The results lend strong support to the argument that the PCM slab sustained a temperature above 0°C for more extended periods of time in relation to the Reference slab.

Table 3.2. Thermal cycling experimental results.

Experimental Result	Cooling Rate	PCM Type	
		Methyl Laurate	Methyl Laurate/Myristate
Mean Maximum Temperature Difference / Standard Deviation (°C)	0.6 °C/h	3.9 / 0.2	3.6 / 0.1
	4.0 °C/h	4.8 / 0.4	5.1 / 0.2
	8.0 °C/h	4.9 / 0.5	4.8 / 0.2
PCM Effectiveness / Standard Deviation (%)	0.6 °C/h	11.9 / 0.9	9.7 / 0.6
	4.0 °C/h	13.5 / 1.2	13.3 / 1.5
	8.0 °C/h	14.0 / 1.6	13.2 / 0.9

As previously stated, a PCM Effectiveness parameter was adopted to facilitate the quantitative analysis and gain insight into the reduced exposure in the PCM slab's time to freezing temperatures. A minimum and maximum PCM Effectiveness of 9.7 and 14.0% was attained for all thermal cycling scenarios. The main observation taken from the resulting PCM Effectiveness values is that the methyl laurate outperformed the methyl laurate/myristate in protecting the asphalt pavement slab from freezing temperatures. The PCM Effectiveness was higher for methyl laurate for all three cooling rates than the methyl laurate/myristate. The phase change transition temperature attribute is a possible explanation of why the methyl laurate better safeguards and enhances performance for the PCM slab. The methyl esters' manufacturer reported that the methyl laurate has a lower phase change transition temperature than the methyl laurate/myristate. This experimental finding laid out some initial evidence that proper phase change transition temperature selection could boost the PCM effect. Similar results have been found in previous studies (Liston et al., 2015; Esmaeeli et al., 2018).

3.3.2 Snow melting experiments

As shown in Figure 3.4a, this portion of the study's temperature profile was different from that used for thermal cycling experiments. Two approaches were employed to research the potential of a PCM to melt snow at different and representative temperature ambient profiles, according to the procedure suggested by Farnam et al. (2017). The temperature range for Procedure A was between

0 and 5°C, and for Procedure B was between 3 and 8°C. A similar rate for cooling and heating was applied for both procedures, 5 °C/h. Bearing in mind the thermal cycling results, methyl laurate was selected as PCM for snow melting experiments. It was assumed that the methyl laurate PCM could make faster the snow melting process in the PCM slab when compared to methyl laurate/myristate. A preliminary thermal cycle run without snow was performed for Procedure A to identify the most convenient time to add snow. It was determined that at approximately 7 hours after the environment was conditioned to 0°C, the PCM was activated (56 hours of total snow melting experiment time). At this point, a temperature difference started to build up between the Reference and PCM slab. The time for adding snow to Procedure B was kept the same, 7 hours after the environment reached 0°C.

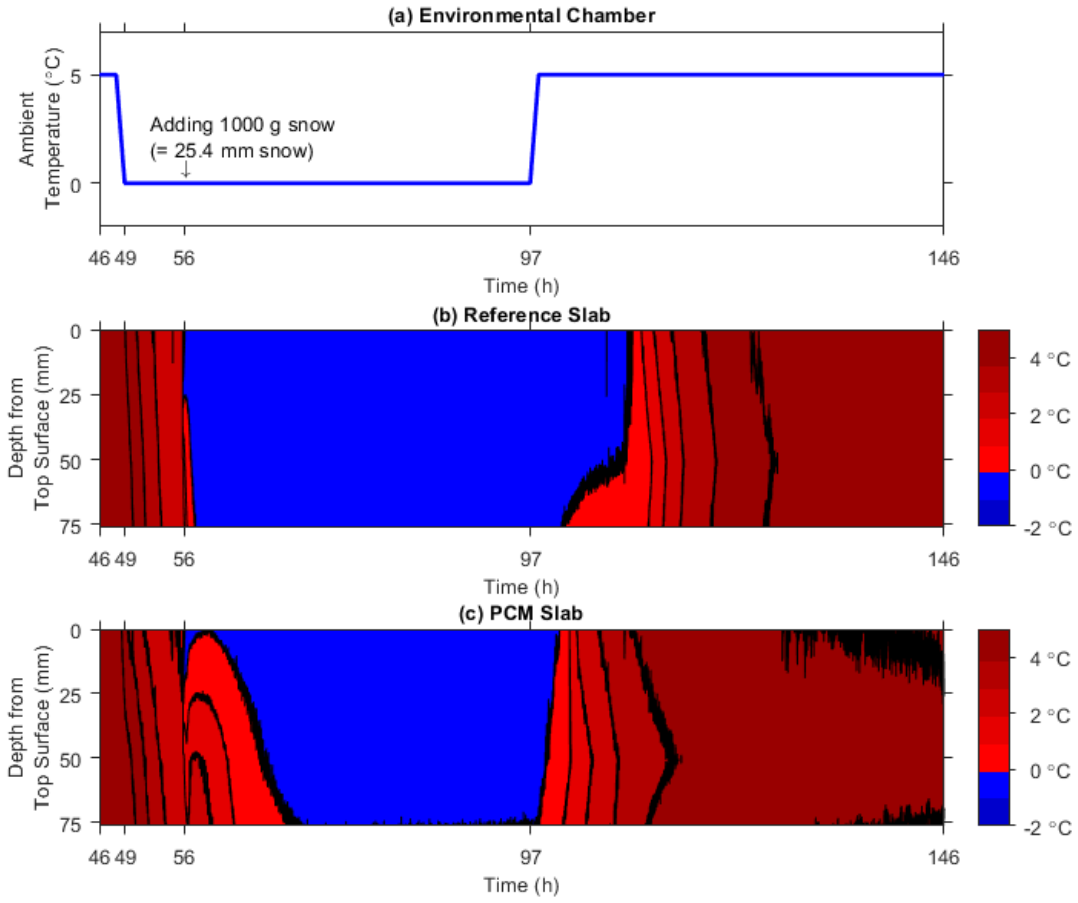

Figure 3.4. Snow melting cycle results for Procedure A.

Figures 3.4b and -c show that, indeed, the PCM shielded the asphalt pavement slab from experiencing freezing temperatures. As can be observed, although the temperature profile for Procedure A runs between 0 and 5°C, the addition of snow imposed new boundary conditions for the pavement systems, making them decrease their temperatures below 0°C (represented by the blue color in the contour figure). However, the PCM slab's decline in temperature is not as sharp as the Reference slabs. This behavior helped the PCM slab melt snow and ice and remove the water associated with the melting process more quickly. The latent heat effect helped the PCM slab recover faster from freezing temperatures than the Reference slab, which sustained unfavorable temperatures for a wider time interval. The PCM Effectiveness scores obtained for Procedure A and Procedure B were 31.3 and 82.7%, respectively. For Procedure B, the PCM slab recorded freezing temperatures only at the top surface.

Time-lapse images were taken every 1 minute as a qualitative observation, and a video was produced for each snow melting procedure. Table 3.3 reports the YouTube links for the time-lapse videos made for this study. Two videos are featured for each snow melting procedure, with and without seal coating. The reason for featuring two videos is that during the initial snow melting experiments (performed on slabs without asphalt seal coating) it was difficult to gather accurate data related to the mass of melted snow (i.e., water runoff), especially for the PCM slab. As shown in the time-lapse videos, snow was melting without seal coating. However, the mass of melted snow measurement was not fully capturing the PCM effect, primarily due to the asphalt pavement slabs' porosity; they were highly permeable to water. It is estimated that the asphalt pavement slabs were compacted at an average air voids content of about 10 percent. The air voids content at specific locations incredibly varied, depending on the closeness to the steel pipes and insulation board and lift thickness. Typically, as-constructed dense graded asphalt pavements, like the mixture type used for this study, have air voids contents between 5 and 7% (Brown, 2009) and are generally thought to be nearly impermeable. In comparison, the range of air voids content in porous asphalt pavements is between 15 and 25 percent (Wang et al., 2021). Such porous characteristics of the PCM slab prevented even more black ice formation on the top surface. As soon as the snow was melted, the water was evacuated through the pavement structure.

Table 3.3. Snow melting time-lapse videos.

Snow Melting Procedure	Slab Type	YouTube Link (unlisted)
Procedure A	Without seal coating	https://youtu.be/S8IjKCDgf3U
	With seal coating	https://youtu.be/j9WxjyMjE6w
Procedure B	Without seal coating	https://youtu.be/nmom3-0iB68
	With seal coating	https://youtu.be/Uo2fQTldGzo

For measuring purposes, each slab's top surface was thoroughly seal coated using a commercially available emulsified asphalt sealer. Similar temperature profiles were observed for both slabs with and without seal coating. As shown in Figure 3.5, an accurate representation of the mass of melted snow was obtained when the slabs were seal coated. To better visualize the results, the mass of melted snow data was normalized for each scenario by calculating the percentages of water runoff gathered over time from the total mass of melted snow obtained (slightly different ultimate total masses were found).

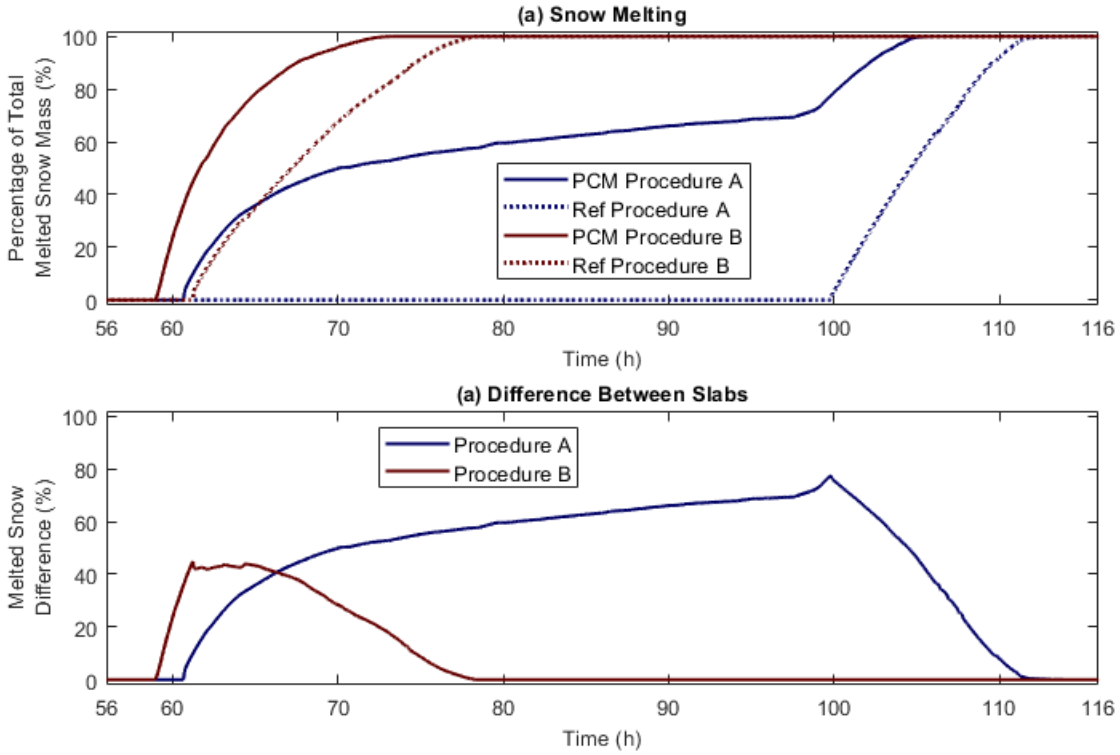

Figure 3.5. Melted snow mass data for snow melting procedures.

For Procedure A, snowmelt started to evacuate from the PCM and Reference slabs' top surfaces at about 5 and 44 hours after the snow was added. Closer inspection of the results suggests

that approximately 76% of melted snow mass was already collected from the PCM slab before any melted snow mass was recorded for the Reference slab, as shown in Figure 3.5b. For Procedure B, about 44% of melted snow mass was already gathered from the PCM slab before any melted snow mass had drained from the Reference slab. Adding PCM to the modified asphalt pavement slab augmented the system's snow melting capacity, evacuating more quickly snow than the Reference slab during experimental testing. These results contribute to the growing evidence suggesting that incorporating PCMs into pavements can provide temperature management (Anupam et al., 2020; Guo et al., 2020; Chen et al., 2020).

3.3.3 Finite element simulations

Turning to the computational effort, a conservative approach was taken for the two-dimensional finite element simulation of asphalt pavement slabs with and without PCM. A heat transfer FEM was developed and calibrated using the thermal cycling experiment's data with a cooling-heating cycle rate of 0.6 °C/h and methyl laurate/myristate. As already discussed, this experimental combination yielded the lowest PCM Effectiveness value and temperature difference between the Reference and PCM slabs (see Table 3.2). To accurately represent the transit of thermal energy between the pavement systems and their surroundings, the following steps were undertaken to procure adequate modeling parameters. First, explicit thermal conductivity and heat capacity values for compacted asphalt mixtures were obtained from Yavuzturk et al. (2005). The asphalt mixture density was assumed to be about 90% of the mixture's Theoretical Maximum Specific Gravity (G_{mm}) or theoretical maximum density.

The next step in the modeling process was to determine a convective heat transfer coefficient by calibrating the Reference slab data model. Consideration was given to the fact that typical values of the convection heat transfer coefficient for free convection, which is the case under the applicable data was gathered, are between 5 and 25 W/m²-K (Incropera, 2007). An estimated 10 W/m²-K was obtained as the heat transfer rate between the asphalt pavement slabs and ambient air. Once a rational convective heat transfer coefficient was attained, the PCM slab data model was developed. The thermal properties of the steel pipes were obtained from the manufacturer's specifications. A considerable amount of information is available in the literature related to the conductivity and generation of heat of methyl esters. Consequently, the methyl laurate/myristate's thermal properties were derived from several studies (Pratas et al., 2011; Pauly

et al., 2014; Liston et al., 2016; Fan et al., 2021). Finally, calibration of the FEM for the PCM slab proved that the phase change transition for the PCM occurred at approximately 3.5°C. Following software developer guidelines, the low and high end of the temperature range within which the phase change occurs were specified at 3.45 and 3.55°C, respectively. Table 3.4 reports the input parameters designated for each material component.

Table 3.4. Finite element modeling input parameters.

Property	Asphalt Mixture	Steel	Methyl Laurate/Myristate	
			Below Solidus Temperature = 3.45°C	Above Liquidus Temperature = 3.55°C
Thermal Conductivity (W/m²-K)	1.40	59.50	0.17	0.16
Volumetric Specific Heat (kJ/m³-K)	900	481	1775	1645
Density (kg/m³)	2242	7870	890	880
Latent Heat (J/g)	-	-	177.8	

Figure 3.6a illustrates the profile temperature to which the slabs were exposed to obtain the experimental and computational results; that is, a thermal cycle between 10 and -10°C with a rate of ambient temperature change of 0.6 °C/h at predetermined time intervals. Figures 3.6b and -c show that the correspondence between experimental and computational results is not necessarily straightforward. The temperature contour plots within the PCM slab are obtained by interpolating the corresponding recorded and predicted temperature values at the three thermocouple depths. As has already been noted, the temperature output for the finite element simulation was extracted at the very same locations where the thermocouples were placed during laboratory experiments. The observed variation in the contour lines between the experimental data and numerical results analysis can be primarily attributed to the time-step specified to conduct the finite element simulations. The time-step used for the numerical analysis was 1 hour, which is in stark contrast with the 10-second interval at which the experimental measurements were taken.

Indeed, the temperature contour plot for the computational results misses fully capturing the sudden heat release of PCM. However, the simulation is considered sufficient to predict slabs' freeze-thaw performance with and without PCM. The PCM Effectiveness obtained using the experimental and numerical results was the same, 9.7 percent. As can be observed, despite the systematic differences, the temperature contour plots exhibit quite parallel time intervals below 0°C (blue section). Overall, the results point to the idea that the proposed FEM is simple yet effective in explaining the heat transfer phenomenon under discussion. Thus, reliable predictions

can be made about the capability of PCMs to lessen freezing temperatures in asphalt pavements under realistic climatic conditions.

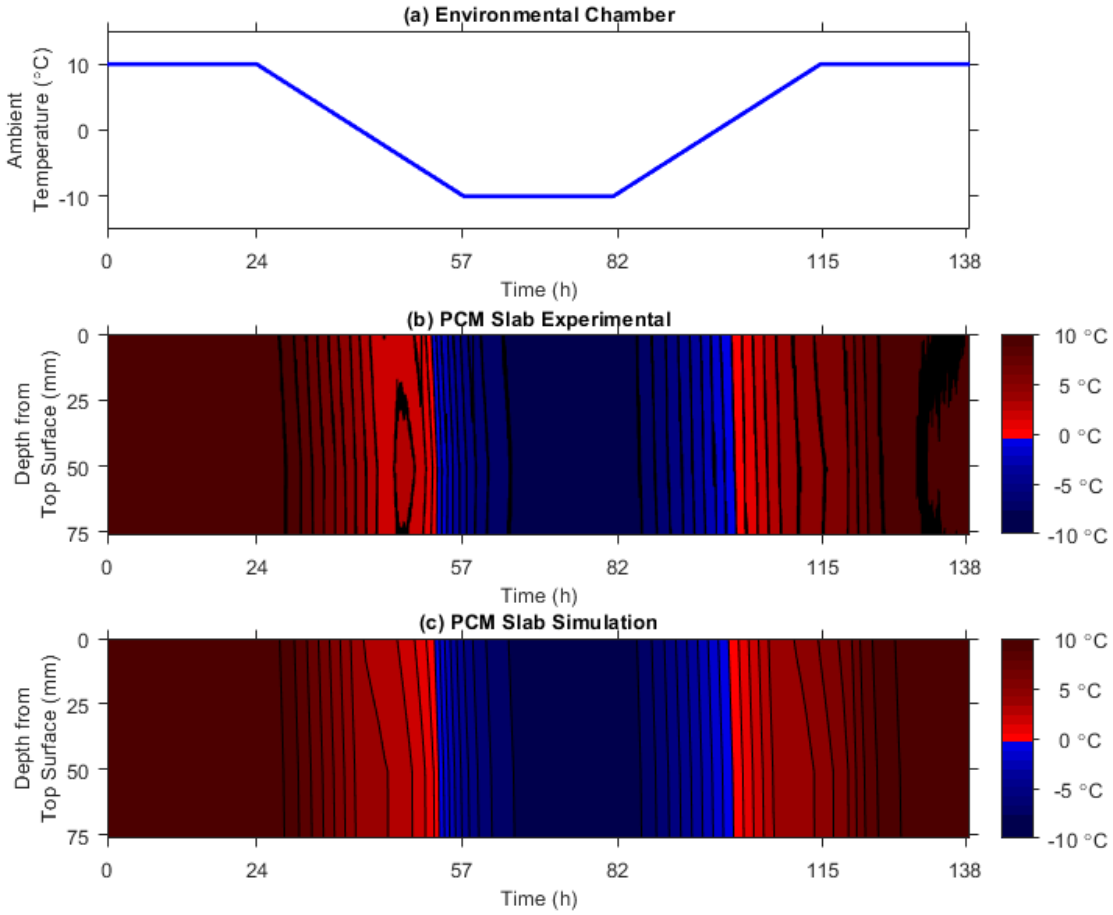

Figure 3.6. Experimental and computational analysis of asphalt pavement slab with methyl laurate/myristate.

3.3.4 Field simulation and prediction of PCM Effectiveness

Having developed a sound basis to perform temperature-based numerical simulations, evaluations were made of the effect of PCMs on improving the freeze-thaw performance of asphalt pavements under realistic ambient temperature profiles from various locations in the United States. To better comprehend the influence of PCM melting point, four simulations were performed at each airport location by adjusting the PCM phase transition temperature (i.e., 0.5, 1.5, 2.5, and 3.5°C) in the FEM. This approach is not new; previous studies have already demonstrated that slight changes in PCM properties (i.e., phase transition temperature) can significantly impact the thermal behavior

of concrete pavement slabs exposed to thermal cycles (Sakulich and Bentz, 2012; Esmaeeli et al., 2018). However, the temperature degree at which the PCM is induced to change from one phase to another has received little attention within the asphalt pavement community. Thus, besides predicting the field applicability of PCM modified asphalt pavements, this study also attempts to emphasize the importance of proper PCM selection.

Difficulties arise in evaluating the asphalt pavement slabs under realistic in-service conditions and capturing the effect of all the contributory factors. Before analyzing the results, it is worth noting that specific considerations were taken to simplify the analysis. First, the convective heat transfer coefficient remains constant throughout the simulation. Secondly, cloud-covered conditions obstruct radiation exchange between the pavement and sky, and no precipitation is contemplated to occur. In reality, asphalt pavements are not free of snow, ice, and rain. They experience solar radiation and are affected by weather conditions such as cloud cover, wind velocity, atmosphere, and transparency (Yavuzturk et al., 2005; Si et al., 2020). Thus, the results presented here set a starting point for further investigations.

For each location, PCM Effectiveness calculations were completed using the FEM temperature output. The investigations reveal that the PCM modification more effectively prevents freeze-thaw cycling when the PCM phase transition temperature is reduced from 3.5 to 0.5°C. As shown in Table 3.5, the highest mean PCM Effectiveness for all locations was obtained when the asphalt pavement modification included a PCM with a phase transition temperature of 0.5°C. Figure 3.7 identifies that the PCM incorporation is more advantageous in the east, central, and northwest regions of the United States. Whereas the PCM modification was less beneficial in warm areas where ambient temperatures rarely go below 0°C, or in regions so cold, ambient winter temperatures rarely cycle above 0°C. This graphical illustration of PCM Effectiveness correlates well with previous studies that predict the potential of PCM incorporation in pavements to reduce their time at freezing conditions (Sakulich and Bentz, 2012; Esmaeeli et al., 2018). Hence, the PCM effect exhibits superior performance at locations where the ambient temperature repeatedly fluctuates above and below 0°C, allowing the PCM to cyclically release a considerable amount of latent heat immediately before the pavement experiences freezing temperatures.

Table 3.5. Descriptive statistics of PCM Effectiveness as a function of phase transition temperature.

Description	Phase Transition Temperature			
	0.5°C	1.5°C	2.5°C	3.5°C
Locations where effective ≥ 0% and < 10%	23	25	34	51
Locations where effective ≥ 10% and < 20%	19	22	24	19
Locations where effective ≥ 20% and < 30%	19	13	14	13
Locations where effective ≥ 30%	39	40	28	17
Mean (%)	29.1	28.9	23.8	18.4
1st Quartile (%)	11.2	10.0	7.1	4.0
2nd Quartile (%)	23.7	21.9	16.1	9.8
3rd Quartile (%)	40.3	42.1	33.5	24.0

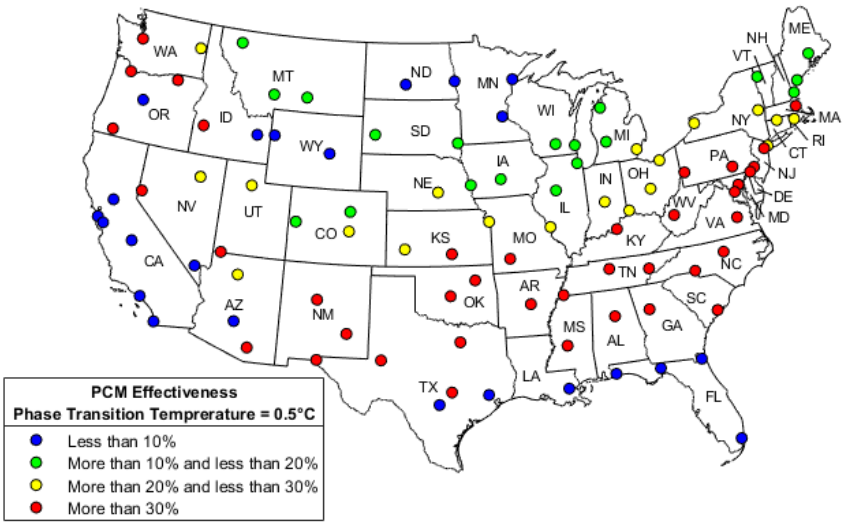

Figure 3.7. Map of locations where the incorporation of PCMs in asphalt pavements was investigated.

3.4 Summary and Conclusions

This chapter presents an effort to develop an asphalt pavement system that melts snow and ice based on the release of latent heat generated from PCMs embedded in the pavement structure. The development included designing and testing Reference and PCM asphalt pavement slabs in the laboratory under temperature-controlled scenarios. In addition, the study conducted finite element modeling to investigate the field performance of asphalt pavements subjected to genuine climatic conditions. The results suggest the efficacy of this methodology in melting snow and ice from pavement surfaces and reducing asphalt pavements' exposure to unfavorable temperatures.

This study's experimental and computational findings demonstrate that a PCM with a lower phase transition temperature, closer to 0°C (but not lower than 0.5°C), could yield a better PCM outcome to melt snow and ice and reduce pavement freezing time. The PCM Effectiveness parameter can be considered a practical method to quantify the PCM success in protecting the pavement structure from temperatures below a threshold. However, the PCM Effectiveness depends on the environmental and boundary conditions imposed on the asphalt pavement system. For thermal cycling experiments, the PCM Effectiveness varied between 9.7 and 14.0 percent. For snow melting experiments, the PCM Effectiveness for Procedure A and B was 31.3 and 82.7%, respectively. For the finite element simulations, the PCM Effectiveness ranged from 0 to 100 percent. The mean PCM Effectiveness across all locations fluctuated between 18.4 and 29.1%, when tuning the phase transition temperature of the PCM. Further parameters could be developed to better quantify the PCM potential to melt snow and ice and reduce freezing and thawing in asphalt pavements and determine the enhancements to transportation safety and pavement performance due to the inclusion of PCMs.

The experimental analysis revealed that asphalt pavement porosity could contribute to better evacuate melted snow from the pavement surface through the pavement structure. This practical outcome should lead to further detailed investigations. The combination of asphalt pavement and PCM properties could boost the TES system's capability to melt snow and ice and provide safer riding surfaces. In terms of modeling, the FEMs developed for this study show good agreement with the experimental results. In particular, the FEMs accurately compute the freezing time experienced by the asphalt pavement slabs. This computational outcome allows extending this investigation's findings using different modeling input parameters and pavement structure configurations. Nevertheless, work needs to be done to include other heat transfer mechanisms and other significant factors in the FEMs.

For this study, embedding pipes in the pavement structure has contributed toward a better understanding of PCM incorporation in asphalt pavement slabs. However, it should be stressed that the practical implementation of embedded pipes in the pavement poses significant issues, including from a highway construction and maintenance perspective. A much more adequate solution should be investigated for the long-term implementation of PCM modified asphalt pavements, such as μPCM. The findings of this study are worth further exploration to promote the adaptability of asphalt pavements to climate through the utilization of TES systems.

4. ENVIRONMENTALLY TUNING ASPHALT PAVEMENTS USING MICROENCAPSULATED PHASE CHANGE MATERIALS[b]

[b]This Chapter is adapted from the draft manuscript "Environmentally Tuning Asphalt Pavements Using Microencapsulated Phase Change Materials", to be submitted for publication.

4.1 Introduction

In recent years, the asphalt pavement industry has recognized the need for designing and constructing roadways that satisfy the requirements of macro and global trends, such as the connectivity, automation, and electrification of road transportation services, as well as conservation of raw materials, climate change and demographic shifts (Mallick et al., 2014; Asphalt Institute Foundation, 2017; Kodippily et al., 2018). As a result, the advancement of pavement engineering will require the utmost care and the use of state-of-the-art technology. The prominence of satisfactory design provisions to relieve the effect of environmental conditions on pavement performance cannot be overstressed (Papagiannakis and Masad, 2008). Asphalt binder viscoelastic properties determine the thermomechanical behavior of asphalt pavements. These binders have a complex chemical composition that exhibits both viscous and elastic properties, depending on temperature and loading time. The exposure of asphalt pavements to normal temperature fluctuations can result in pavement failures. For instance, pavement rutting typically occurs during high temperatures, when the binder stiffness is reduced, while thermal cracking is related to pavement contraction at low temperatures (Brown, 2009).

The ability of PCMs to maintain specific temperatures for extended periods of time can help tune the service temperature of asphalt pavements. Modifying asphalt pavements with μPCMs can provide desired engineering properties, such as increased shear modulus and reduced plastic flow at high and intermediate temperatures, and increased resistance to thermal cracking at low temperatures (Reefa et al., 2018; Kakar et al., 2019b; Kakar et al., 2019c; Wei et al., 2019b). However, the effects of different types and mass fractions of μPCMs on the properties and performance of asphalt materials have rarely been investigated. The advent of μPCMs to modify asphalt pavements can be a significant breakthrough for asphalt pavement performance. However, before the large-scale practical application of this technology, it is necessary to address numerous research and development stages (Sharma et al., 2009). An in-depth understanding of the effects

of μPCMs on the thermal and mechanical performance of asphalt binders and mixtures is still required. The continued existence of this need is likely to limit the application of μPCMs to enhance asphalt pavement materials, despite the potential advantages of their use.

By modifying asphalt materials with μPCMs, it should be possible to "tune" the resulting asphalt pavement to the environment, thereby mitigating or eliminating pavement damage due to the exposure of asphalt pavement surfaces to temperature fluctuations. Comprehensive thermal, rheological, and mechanical testing is hypothesized to characterize and optimize μPCM modified asphalt binders and mixtures. However, research to date has not yet determined rational tests and parameters that can be used to explain the performance of μPCM modified asphalt binders and mixtures, develop standard specifications, and link binder and mixture behavior. As a result, this chapter's overall research objective is to identify testing techniques that characterize the thermomechanical performance of μPCM modified asphalt binders and mixtures within the linear viscoelastic range. This chapter introduces a new approach to identify the μPCM effect in asphalt binders using rheological measurements. Additionally, the findings of this study corroborate experimental and numerical investigations showing that a reduction in pavement surface temperatures between 2 and 9°C can be obtained with μPCM modified asphalt materials, as compared to non-μPCM modified asphalt materials (Jin et al., 2017; Reefa et al., 2018). Finally, the re-design of an asphalt mixture with μPCM is demonstrated, and the mechanical performance implications of incorporating a significant portion of μPCM in the mixture are discussed.

4.2 Methodology

4.2.1 Microencapsulated phase change material

A commercially available μPCM with a phase transition of 43°C, referred to hereafter as μPCM-43, was used in this investigation. The μPCM-43 is described as microscopic bi-component particles consisting of a core PCM and an outer shell, or capsule wall, and has a white, to slightly off-white color appearance in dry powder form, with particle sizes typically ranging between 0.014 to 0.024 mm. The PCM core consists of paraffin, while the capsule wall is a polymer. The capsule composition percentages are approximately 85% PCM and 15% polymer shell by mass. The capsule specific gravity is about 0.900, and the latent heat of fusion is between 220 and 230 J/g. Hence, μPCM-43 is used to regulate temperatures and heat storage in various applications, such

as the textile industry, electronics, and building materials. Based on TGA, the capsules are extremely stable, with less than 1% leakage when heated to 250ºC, and can be exposed to multiple thermal cycles without damage in the laboratory.

4.2.2 Unconventional asphalt binder and mixture testing

Dynamic shear rheometer testing

Although the μPCM particles exhibit good temperature stability, the mixing process took place just before specimen preparation. A control PG 64-22 binder was mixed with the μPCM-43 at 160°C using a mechanical agitator for 5 minutes. The rheological properties of μPCM-43 modified asphalt binders were characterized using recently explored DSR testing techniques. The unconventional DSR test protocol employed is based on the methods reported by Kakar et al. (2019b) and Kakar et al. (2019c). Accordingly, temperature sweep tests determined the μPCM-43 thermal effect on the modified asphalt binder's rheological response. The dynamic shear properties were measured using the parallel plate configuration of 2 mm thick specimens with 8 mm diameter. Temperature ramps from 60 to 20°C (and vice versa) were conducted while applying an oscillatory shear strain with a constant strain amplitude of 1.0% at a frequency of 10 rad/s. These testing inputs were selected to keep the rheological measurements within the linear viscoelastic range and equipment torque limits.

The control PG 64-22 was modified by total binder mass at six levels, 0, 5, 10, 20, 30 and 40%. In addition, the rheological testing was conducted at five different temperature ramps between 60 and 20°C, namely 3, 6, 9, 12, and 15 °C/h. For each binder-μPCM combination, a single specimen was examined. After loading the specimen in the DSR, the material was initially conditioned for 20 minutes at 60°C. Then, the rheological testing equipment was configured to run a cooling-heating cycle for each temperature rate. The DSR Peltier system decreased the temperature from 60 to 20°C within a specific time duration and increased the temperature from 20 to 60°C within the same time span. The temperature ramps were conducted successively from slowest to fastest, without interruptions. The set of temperature ramps used is comparable to the temperature change rates experienced by in-service asphalt pavements (Yavuzturk et al., 2005). The viscoelastic properties were measured at 30-second intervals, meaning that every 30 s, the DSR decreased a temperature step and reported the average results of the rheological

measurements continuously taken within the time step. Rheological measurements were accompanied by DSC tests conducted at 600 °C/h (or 10 °C/min).

Thermal cycling of asphalt mixtures

The thermal response of μPCM modified asphalt mixtures was also investigated. First, four asphalt mixtures gathered from three paving projects in Indiana were modified with PCM microcapsules at three levels, 0, 4, and 8%, by total mixture mass. Table 4.1 shows the characteristics of these mixtures. Mixture A was gathered from a paving project near Crawfordsville, IN, Mixture B from a pavement reconstruction section in Indianapolis, IN, and Mixtures C and D from a pavement overlay project near Fort Wayne, IN. Mixtures C and D have comparable aggregate blends, with the main difference being that Mixture C includes steel slag aggregate (Haddock et al., 2020).

Table 4.1. Asphalt mixtures used for thermal cycling preliminary assessment.

Mixture Name	Mixture A	Mixture B	Mixture C	Mixture D
Mixture Description	Surface Mainline	Base Mainline	Surface Mainline	Shoulder Mainline
Mixture Designation (mm)	9.5	19.0	9.5	9.5
Binder Type	PG 70-22	PG 64-22	PG 76-22	PG 64-22
Aggregate Material	9.5 mm Dolomite 4.75 mm Dolomite 2.36 mm Dolomite Sand 9.5 mm RAP Mineral Filler	19.0 mm Stone 9.5 mm Stone 4.75 mm Stone 2.36 mm Stone Sand 12.5 mm RAP 9.5 mm RAP Mineral Filler	9.5 mm Limestone 4.75 mm Limestone 9.5 mm Steel Slag 2.36 mm Manufactured Sand 9.5 mm RAP Mineral Filler	9.5 mm Limestone 4.75 mm Limestone 2.36 mm Natural Sand 2.36 mm Manufactured Sand 9.5 mm RAP Mineral Filler
Air Voids Content (%)	5.0	5.0	5.0	5.0
Voids in the Mineral Aggregate (%)	16.6	14.7	16.9	17.1
Voids Filled with Asphalt (%)	69.9	66.0	70.4	70.8
Asphalt Binder Content (%)	6.1	5.4	5.8	6.5
Effective Binder Content (%)	4.9	4.2	4.9	5.3
Virgin Binder (%)	4.6	4.6	4.7	5.6
Binder Replacement (%)	24.3	15.4	19.7	13.8
Dust-to-Binder Ratio	1.0	1.2	0.9	0.8
Number of Design Gyrations	50	50	50	50
SGC Pill Mass (g)	4825	4700	5140	4860

The plant-produced paving materials were heated in the laboratory at 135°C for two hours and then manually mixed with μPCM-43, as shown in Figure 4.1a, until all the particles exhibited a dark appearance (about 5 minutes). The μPCM-43 modified asphalt material was again placed in the oven for approximately 20 minutes to recuperate the 135°C established temperature for compaction. About 2700 g of mixture were compacted using the SGC to a specific height of 63.5 mm, or until a total of 50 SGC gyrations were reached. Little information is available in the literature regarding the compaction and fabrication of μPCM modified asphalt mixture specimens. Thus, a 63.5 mm height was specified to ensure that 50 mm tall specimens could be fabricated for thermal cycling experiments. However, during compaction, it was observed that all the specimens were compacted until the number of gyrations criterion was achieved, except the control specimen for Mixture C. The specimens modified with μPCM at 0, 4, and 8% by total mixture mass were compacted to an average height of 65.5, 68.6, and 76.2 mm, respectively. This increased in SGC pill height is primarily due to the low specific gravity of the μPCM particles, 0.900.

(a) (b)

Figure 4.1. (a) Mixing process of μPCM-43 and plant-produced asphalt mixture and (b) specimens prepared for thermal cycling, Mixture B.

Following compaction, the SGC pills were cut using a saw to fabricate 50 mm tall specimens. Subsequently, three type T thermocouples were placed on each specimen, one at the top surface (non-insulated circular face), one 25 mm from the top surface (mid-specimen), and one at the bottom surface. The mid-specimen temperature sensor was mounted at the center by drilling a hole to fit the thermocouple. Thermally conductive adhesive tape was applied to secure the thermocouples at the bottom and top surfaces. The specimens' bottom surface and outside diameter were then insulated using a 50-mm insulating board to produce a one-dimensional heat flow during thermal cycling testing (see Figure 4.1b). To further minimize heat loss, the gap between the specimen and insulating board, plus the incisions made in the board to place the thermocouples, were filled with an insulating foam sealant. After insulating and instrumenting the specimens, they were placed in an environmental chamber and exposed to a cooling-heating cycle. For the purpose of capturing the μPCM effect at about 43°C, the specimens were subjected to liquification and solidification transitions from 20 to 60°C and from 60 to 20°C, respectively.

Volumetric analysis was performed on the SGC pills before dimensioning the specimens to a height of 50 mm. Despite the changes in SGC specimen mass and reduction in mixture design compaction temperature, from the 150°C allowed by the Indiana Department of Transportation (INDOT) specifications to the 135°C used for this study, the air voids contents of the control mixtures' specimens fell within the permissible range. However, the air voids contents of the compacted μPCM-43 asphalt mixture specimens were out of the specification limits, between 3.6 and 6.4 percent. The air voids contents of the μPCM-43 modified asphalt mixtures' specimens were significantly below the lower specification limit. Not surprisingly, as more PCM microcapsules were included, the air voids contents departed even more from specifications. These volumetric results strengthen the argument that for the inclusion of μPCMs in asphalt mixtures, a portion of fine aggregate and mineral filler from the original mixture design should be replaced with μPCMs to satisfy the volumetric requirements (Refaa et al., 2018; Bueno et al., 2019). Some μPCM-43 modified specimens showed an air voids content even lower than one percent. To improve the feasibility of this technology, an appropriate mixture design procedure was anticipated by this dissertation.

4.2.3 Conventional asphalt binder and mixture testing

Design of μPCM-43 Mixtures

Table 4.2 illustrates how a Reference Mixture was re-designed to incorporate a significant portion of μPCM-43 at two different levels (about 2 and 4% by total mixture mass). The Reference Mixture had the same aggregate blend and volumetric properties of Mixture A (see Table 4.1), but it was prepared using a PG 64-22 asphalt binder. All the materials passing the 0.300- and 0.600 mm sieves were substituted with microcapsules for the 2%- and 4% μPCM-43 Mixtures, respectively. Considering that the capsules have a specific gravity of about 0.900, the replacement was estimated by volume and not by mass. Therefore, all the substituted fine aggregate and mineral filler material was assumed to have a specific gravity of 2.800.

Table 4.2. Batching for μPCM-43 re-designed asphalt mixtures.

	Component	Component Mass (g)		
		Reference Mixture	2% μPCM-43 Mixture	4% μPCM-43 Mixture
	PG 64-22 Asphalt Binder	325.4	325.4	325.4
Retained Sieve Size (mm)	12.5	0.0	0.0	0.0
	9.5	348.4	348.4	348.4
	4.75	2533.9	2533.9	2533.9
	2.36	1796.3	1796.3	1796.3
	1.18	1036.6	1036.6	1036.6
	0.600	587.9	587.9	587.9
	0.300	353.4	353.4	0.0
	0.150	179.1	0.0	0.0
	0.075	66.9	0.0	0.0
	Pan	172.1	0.0	0.0
	μPCM-43	0.0	134.4	248.0
	Total Mass	7400.0	6981.9	6876.5
Proportion of μPCM-43 by Total Mixture Mass (%)		0.0	1.9	3.6
μPCM-43 to Virgin Binder Ratio (%)		0.0	41.3	76.2
Maximum Specific Gravity		2.544	2.424	2.341
Retained materials at these sieves in the Reference Mixture were substituted with μPCM-43 for re-designed mixtures.				

First, the aggregate was batched as typically done for specimen fabrication. After batching, the aggregate was sieved to determine the mass of the material to be substituted. Then, the approximate volume of the material passing the critical sieve for each re-designed mixture was calculated by dividing its total mass by 2.800. The estimated volume was multiplied by 0.900 to

obtain the mass required to produce a similar volume replacement of μPCM-43. The mass of the virgin PG 64-22 asphalt binder was kept the same for the μPCM-43 re-designed mixtures. The retained material above the critical sieves and virgin binder were heated at 135°C for 2 hours and then mixed in the laboratory. Following mixing, the asphalt mixtures were short-term conditioned for mixture mechanical property testing at 135°C, in accordance with AASHTO R 30. After conditioning, the μPCM-43 particles were added and manually mixed to the laboratory-prepared mixture until all the μPCM-43 particles looked coated with asphalt binder (about 5 minutes). The μPCM-43 modified asphalt mixtures were again placed in the oven for approximately 20 minutes to re-gain the 135°C required temperature for compaction. The modification is reported by the masses of raw material needed to prepare SGC specimens that were 180 mm in height (see Figure 4.2a), from which specimens with air voids content of 5.0 ±0.5% could be extracted for mechanical testing. The same batching and mixing procedures were performed to prepare the required amount of material to determine each mixture's G_{mm}, according to AASHTO T 209.

(a) (b)

Figure 4.2. (a) 4% μPCM-43 Mixture, 180 mm in height SGC specimen and (b) dynamic modulus testing setup of small μPCM-43 Mixture specimen.

A wide variety of CPCM and μPCM dosages have been investigated in experimental and numerical studies. The proportions of μPCM-43 by total mixture mass evaluated in this study are in good agreement with recent investigations and comparable to the CPCM and μPCM amounts reported in the literature (Jin et al., 2017; Kakar et al., 2019b; Kakar et al., 2019c; Wei et al., 2019b, Ma et al., 2019; Bueno et al., 2019). Perhaps the most interesting aspect of this study is the alteration of aggregate components to allow for μPCM incorporation. Few studies have attempted to entirely re-designed an asphalt mixture using μPCMs. Instead, most investigations have added the μPCMs directly to an existing asphalt mixture design without performing variations to the aggregate blend or just replaced the mineral filler (Bueno et al., 2019). As indicated by the G_{mm} values of the Reference and μPCM-43 Mixtures, a significant G_{mm} reduction is observed when μPCM is used instead for fine aggregates. Simultaneously, a lower amount of material is required to fabricate a desirable SGC specimen for the μPCM-43 Mixtures relative to the Reference Mixture. Although replacing fine aggregate and mineral filler with μPCM-43 seems straightforward, such a change will cause a difference in volumetric properties and, consequently, mechanical performance.

Mechanical performance of μPCM-43 Mixtures

To better understand the mechanical behavior of the μPCM-43 Mixtures, the dynamic modulus for the re-designed asphalt mixtures was determined using two specimen geometries, namely 100 mm diameter by 150 mm tall (large specimen) and 38 mm diameter by 110 mm tall (small specimen). The stress-strain ratio under vibratory conditions of large specimens was defined according to AASHTO T 378, while small specimen dynamic modulus testing was conducted according to AASHTO TP 132 (see Figure 4.2b). Additionally, small specimens' damage characteristic curve and fatigue analysis parameters were estimated via the direct tension cyclic fatigue test, as specified by AASHTO TP 133. The big specimens were also measured for Flow Number to examine the resistance of the Reference and μPCM-43 Mixtures to permanent deformation. Finally, the fracture resistance of asphalt mixtures at low temperatures was characterized by means of the AASHTO T 394 test method, Semi-Circular Bend (SCB) geometry testing. Specimens with a 150 mm diameter and 25 mm thickness were utilized to fabricate semicircular specimens for SCB testing. Table 4.3 summarizes the asphalt mixture mechanical testing for this study. A PG 64-22 binder was used for all tests.

Table 4.3. Asphalt mixture mechanical testing.

Test Method	Reference Mixture	2% μPCM-43 Mixture	4% μPCM-43 Mixture
Dynamic Modulus Small Specimens, AASHTO TP 132	PG 64-22	PG 64-22	PG 64-22
Dynamic Modulus Big Specimens, AASHTO T 378	PG 64-22	PG 64-22	PG 64-22
Flow Number, AASHTO T 378	PG 64-22	PG 64-22	PG 64-22
Cyclic Fatigue Test, AASHTO TP 133	PG 64-22	PG 64-22	PG 64-22
Semi Circular Bend, AASHTO T 394	PG 64-22	PG 64-22	PG 64-22

In addition, the thermal response of μPCM-43 Mixture specimens was investigated. The specimens were 100 mm in diameter and 50 mm thick and were instrumented with thermocouples and insulated, as shown in Figure 4.3. The changes in temperature of a Reference Mixture specimen with 5% air voids content, 2% μPCM-43 Mixture specimen having a 5% air voids content, and 4% μPCM-43 Mixture specimens with 4, 5, and 6% air voids content under controlled environmental conditions (same thermal cycle used for Mixtures A-D).

(a) (b)

Figure 4.3. (a) 4% μPCM-43 Mixture, 180 mm in height SGC specimen and (b) dynamic modulus testing setup of small μPCM-43 Mixture specimen.

Rheological performance of μPCM-43 modified binders

The mechanical characterization of μPCM-43 Mixtures is supplemented with rheological performance tests of μPCM-43 modified binders. As shown in Table 4.4, the properties of interest are the elastic response in an asphalt binder under shear creep and recovery, resistance to fatigue damage through cyclic loading, low-temperature relaxation, and the G* Change Rate (determined at 12 °C/h). The G* Change Rate is a parameter developed by this study, and it is introduced in the following section. The testing matrix included three original binders, PG 64-22, PG 70-22, and PG 76-22. The PG 64-22 is the same used for asphalt mixture testing. Initially, the μPCM-43 dosages of interest were 40 and 80% by binder mass because these percentages reflect the ratios of μPCM-43 to virgin binder in the μPCM-43 Mixtures. However, the 80% μPCM dosage was not workable with stiff binders, making it impossible to prepare reliable binder specimens. Consequently, the dosages selected for μPCM-43 binder modification were 20 and 40% by binder mass, but data at an 80% μPCM-43 dosage was still gathered using PG 64-22 and DSR tests. All the tests were completed on original binder conditions; no Rolling Thin-Film Oven (RTFO) or Pressure Aging Vessel (PAV) aging protocols were performed.

Table 4.4. Testing matrix for asphalt binders with and without μPCM-43.

Test Method	μPCM Dosage (by binder mass)		
	0%	20%	40%
Multiple Stress Creep Recovery, AASHTO T 350	PG 64-22	PG 64-22	PG 64-22
	PG 70-22	PG 70-22	PG 70-22
	PG 76-22	PG 76-22	PG 76-22
Linear Amplitude Sweep, AASHTO T 101-14	PG 64-22	PG 64-22	PG 64-22
	PG 70-22	PG 70-22	PG 70-22
	PG 76-22	PG 76-22	PG 76-22
Delta Tc Parameter, ASTM D7643	PG 64-22	PG 64-22	PG 64-22
	PG 70-22	PG 70-22	PG 70-22
	PG 76-22	PG 76-22	PG 76-22
G* Change Rate	PG 64-22	PG 64-22	PG 64-22
	PG 70-22	PG 70-22	PG 70-22
	PG 76-22	PG 76-22	PG 76-22

4.3 Results and Discussion

4.3.1 Complex shear modulus change rate

Studies into the viscoelastic behavior of asphalt binders have received increased interest from various researchers since the early 1990s, following the Strategic Highway Research Program (SHRP) (Anderson et al., 1994; Yusoff et al., 2011). The SHRP research effort reported that over most of the range of interest in asphalt binder applications, the rate of change of Complex Shear Modulus (G*) with respect to temperature ranges from 15 to 25 percent per degree Celsius (Anderson et al., 1994), which means that asphalt binders should exhibit a relatively constant G* Change Rate when subjected to a continuous temperature gradient. Such a concept has not been thoroughly investigated over the years, in significant part because of equipment limitations. Many of the commercial rheological testing devices available in the early 1990s were designed primarily for use with polymers, foodstuffs such as cheese, and other materials, many of which exhibit low-temperature dependency compared to asphalt binder (Anderson et al., 1994). In such a situation, most rheological testing devices provided just enough temperature control accuracy for maintaining suitable repeatability of test data. Consequently, as per specifications, asphalt binder tests are typically performed under steady-state temperature conditions. However, today, rheological testing devices can perform temperature fluctuations and ramps with a great deal of accuracy. Some rheological testing devices can guarantee a homogeneous convection temperature distribution and, thus, accurate and stable temperature control for various testing protocols.

Figure 4.4 confirms that an asphalt binder subjected to a constant temperature increase (from 20 to 60°C) will show a relatively stable G* Change Rate. This calculation will vary depending on the temperature ramp applied and the interval at which rheological measurements are taken. For this study, the measurements were taken at 30-second intervals. This time step is used to calculate the G* Change Rate, as shown in Equation 4.1.

$$G^{*}Change\ Rate = \frac{G_i^*}{G_{i-1}^*} \qquad \text{(Eq. 4.1)}$$

where:

G_i^* = G^* at a given temperature, and

G_{i-1}^* = G^* obtained at the previous time step for the predetermined temperature change rate during the solidification or liquification transition.

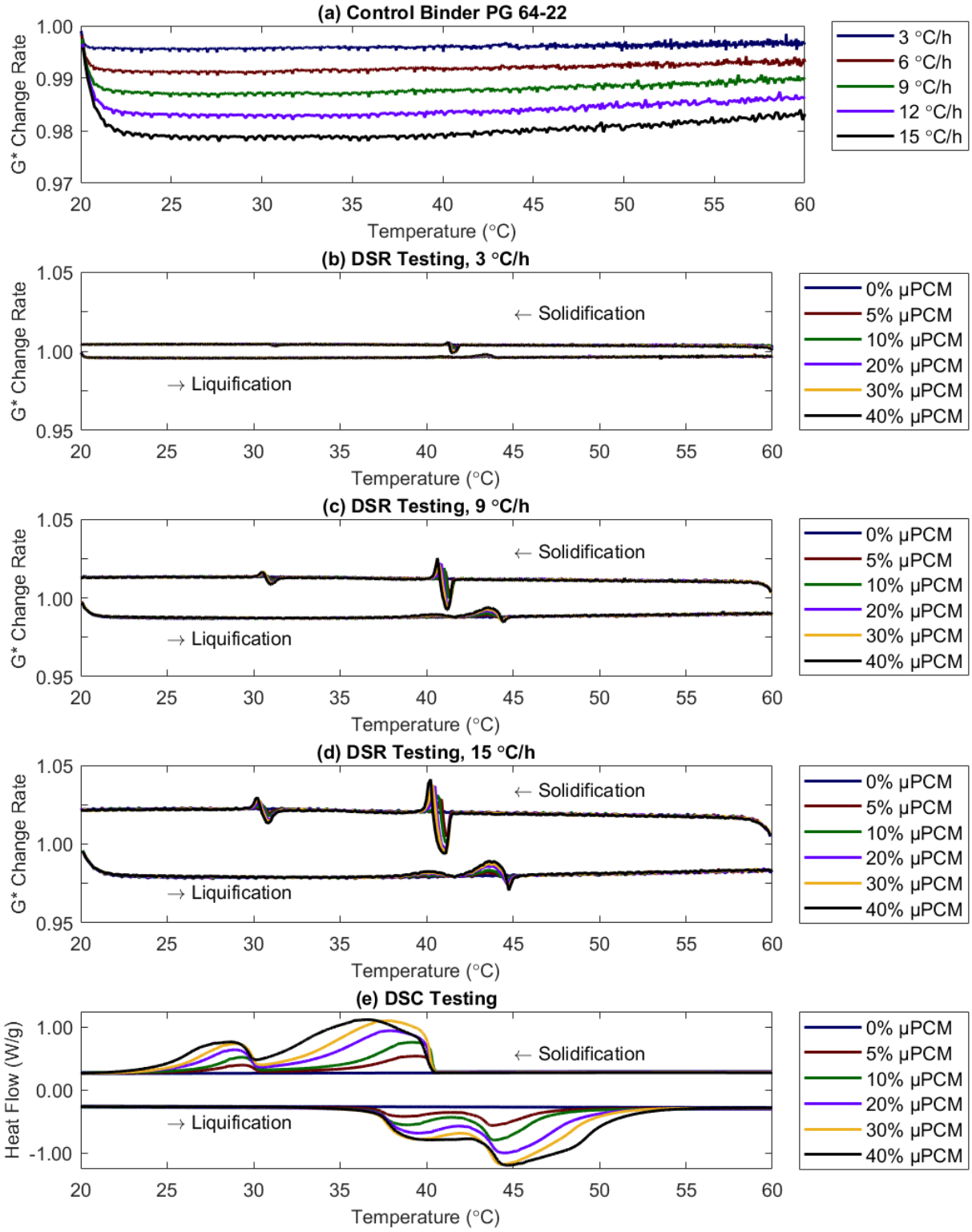

Figure 4.4. Asphalt binder experiments using Dynamic Shear Rheometer and Differential Scanning Calorimeter.

Data from several studies have demonstrated that the temperature can be shifted or reduced by incorporating μPCMs into asphalt binders (Refaa et al., 2018; Kakar et al., 2019b; Kakar et al., 2019c; Wei et al., 2019b). Although previous studies have encouraged the use of DSR measurements, a method to fully understand the μPCM effect in asphalt binders using rheological data was not identified. For example, Kakar et al. (2019c) modified control asphalt binders with a μPCM having a phase transition temperature close to 6°C, at three different levels, 0, 1, and 3% by total binder mass. In Kakar et al. (2019c), the rheological measurements were taken by performing temperature ramps between 20 and -10°C, using a rate of about 26 °C/h for cooling and heating transitions. The constant strain amplitude and frequency applied to run the tests were 0.1% and 6.3 rad/s, respectively. The rheological measuring system had a diameter of 8 mm and specimen thickness of 2 mm. To interpret the results, master curve, complex shear modulus versus temperature, and phase angle versus temperature plots were generated by Kakar et al. (2019c). After analyzing the data, Kakar et al. (2019c) suggested that during cooling ramps, no thermal effect due to μPCM incorporation is noticed on the rheological response of modified asphalt binders, and concluded that perhaps at higher μPCM concentrations, the effect could be detectable. The work presented herein differs from previous research regarding the idea that a μPCM effect cannot be captured by performing rheological measurements. If the data is normalized utilizing the G* Change Rate, the μPCM effect is noticeable during solidification and liquification transitions regardless of μPCM dosage and through temperature fluctuations comparable to those experienced by asphalt pavements in the field.

Figure 4.4 shows that the rate of change concept can help quantify the μPCM effect in asphalt materials. This rheological data analysis is in good agreement with the results obtained from DSC measurements, as can be inferred from Figure 4.4e. The evidence is murky because DSC measurements were performed at a cooling-heating rate of 600 °C/h (or 10 °C/min), which is a typical testing parameter for this thermal procedure. This cooling-heating rate is inconceivable for the rheological analysis of asphalt binders. Although DSC measurements were performed at a significantly higher cooling-heating rate, the μPCM effect peaks observed are connected to the rheological results obtained at cooling and heating rates between 3 and 15 °C/h. When the μPCM-43 releases heat (solidification phase), a G* Change Rate reduction is observed, primarily due to a thermal lag in the asphalt binder specimen. The specimen is no longer transitioning at a constant temperature rate because of the μPCM-43. In contrast, when the μPCM-43 absorbs heat

(liquification phase) from the system, an increase is noticed in the G* Change Rate, meaning the DSR must apply a higher torque (or activation energy) to generate the predetermined strain amplitude of 1.0% in the asphalt binder specimen. In both phases, a countereffect is observed in the rheological measurement after the μPCM-43 effect is completed, as compared to DSC results. A possible explanation for this might be that the binder experiences an accelerated temperature transition. Due to the thermal lag, there might be a significant temperature gradient between the DSR plates and μPCM-43 modified binder, causing a sudden temperature shift in the specimen. Additionally, in the DSR testing setup used for this study, the asphalt binder was susceptible to heat losses as opposed to DSC testing, where the specimen was enclosed in a thermal chamber. More research is necessary to understand the cause of this countereffect and its potential ramifications.

The rheological results are consistent with the present evidence suggesting that the latent heat peak's intensity depends on the cooling-heating rate applied because thermal gradients are built up differently in the PCM. A study on the phase change process and latent heat of PCM impregnated LWA concluded that DSC tests with higher cooling and heating rates intensify the verticality of the curve at the peak temperature (Kheradmand et al., 2015). Likewise, the rheological results of this study demonstrate that as the cooling-heating rate increases, the G* Change Rate peak intensifies, as shown in Figures 4.4b-d. It should be noted that regardless of the cooling-heating rate used in DSC testing, the amount of latent heat absorbed and released by the μPCM-43 is constant. This fundamental concept can be demonstrated by calculating the integral under the DSC peak above the baseline (Kheradmand et al., 2015). The analogous DSR and DSC plots suggest that a similar analysis might be applicable for the rheological results. Although the rheological findings should be treated with a degree of caution, the results are interesting because they identify an approach for capturing the μPCM effect in asphalt binders. This analysis warrants further investigations to correlate the G* Change Rate to the latent heat capacity of the μPCM-43 modified asphalt binders and quantify their potential relaxation benefits. Table 4.5 reports the latent heat characteristics of μPCM-43 modified asphalt binders according to the DSC measurements.

Table 4.5. Differential Scanning Calorimeter results for μPCM-43 modified asphalt binders.

μPCM-43 Content by Binder Mass (%)	Solidification Phase		Liquification Phase	
	Temperature Range (°C)	Latent Heat (J/g)	Temperature Range (°C)	Latent Heat (J/g)
5	29.3 – 39.5	8.3	38.5 – 43.8	8.8
10	29.3 – 39.1	16.4	38.8 – 44.0	16.8
20	28.9 – 37.9	31.1	39.3 – 44.5	31.6
30	28.9 – 37.7	42.7	39.4 – 42.4	42.8
40	28.6 – 36.7	50.7	39.5 – 44.5	50.7

4.3.2 Thermal cycling of μPCM-43 modified asphalt mixtures

Figure 4.5 shows the thermal response of asphalt specimens with and without μPCM-43. The control asphalt mixture is a 9.5-mm plant-produced mixture gathered in-situ through plate sampling on the road, namely Mixture A. The specimens were exposed to a temperature cycle between 20 and 60°C to capture the μPCM effect at about 43°C. When the μPCM particles liquify, the μPCM-43 product delays the modified asphalt specimens from reaching a threshold temperature of 45°C and creates a thermal lag in the specimens. As a result, the temperature of the μPCM modified asphalt specimens dwells at about 43°C for a longer time than if the μPCM was not present. Likewise, during solidification, the μPCM effect provides additional relaxation time to the asphalt specimen during the temperature transition from 60 to 20°C, at approximately 43°C. A closer examination reveals a second thermal lag experienced at about 30°C when the μPCM-43 is cooling. This observation is more evident for the specimen modified with 8% μPCM-43 by total mixture mass. Overall, the thermal responses of the μPCM-43 modified asphalt specimens mimic the rheological analysis found for the asphalt binders, as presented in the previous section. As the μPCM-43 solidifies, two sharp peaks are detectable for the G* Change Rate, at about 43 and 30°C. Conversely, when the μPCM-43 is transitioning to a liquid, the DSR, DSC, and thermal cycling measurements agree that the μPCM effect occurs more uniformly between 35 and 45°C. Similar observations can be made for the other three asphalt mixtures tested, Mixtures B, C, and D.

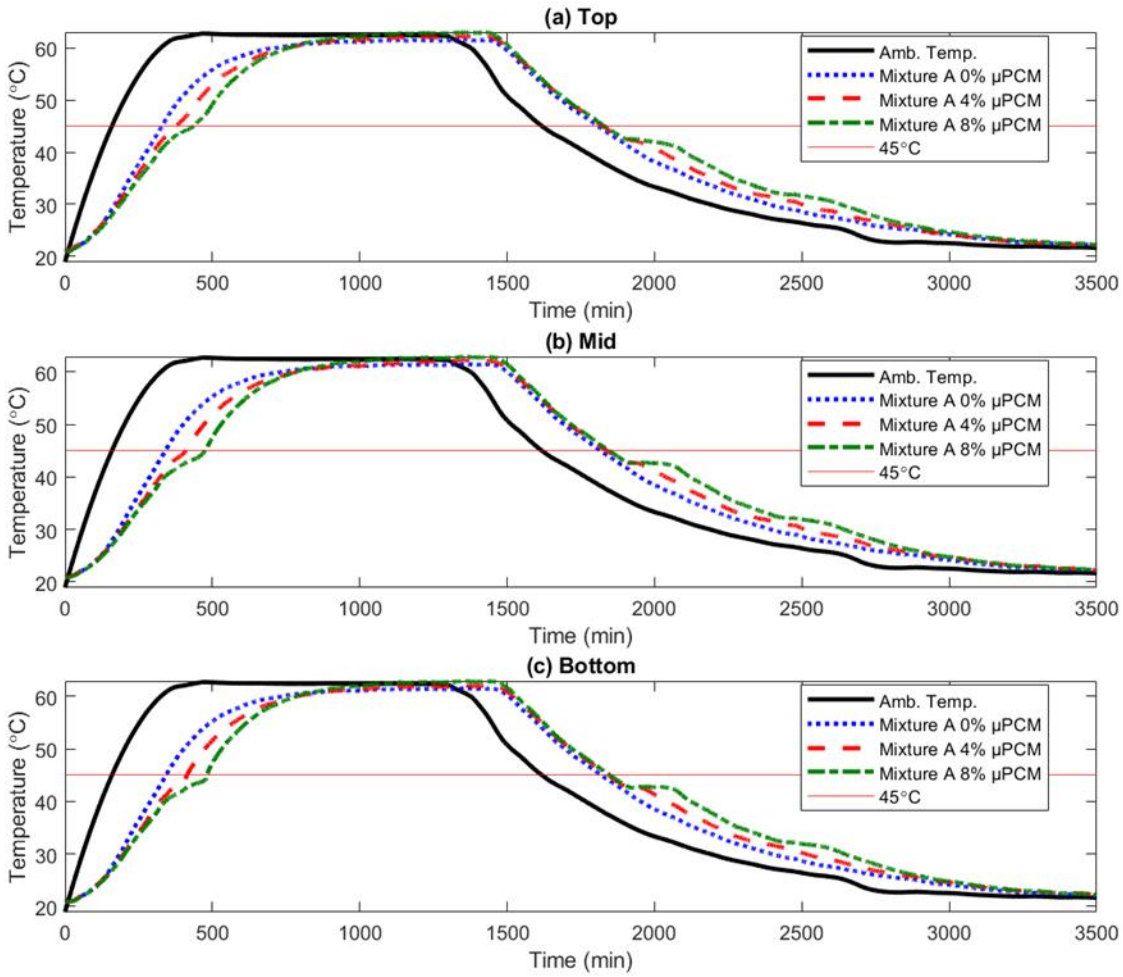

Figure 4.5. Mixture A thermal response of asphalt specimens, with and without µPCM-43, at different depths from the top surface.

Table 4.6 reports the differences in temperature obtained at different depths from the top surface for the specimens with µPCM-43 relative to the control specimens. The liquification (from 20 to 60°C) and solidification (from 60 to 20°C) µPCM-43 transitions demonstrate disparities in the absolute temperature differences observed. During PCM solidification, the temperature differences are consistently lower for all mixture types. Thus, the µPCM-43 appears to be more beneficial when liquifying, meaning that the µPCM-43 does a better job delaying the appearance of temperatures higher than 43°C in comparison to hindering temperatures lower than 43°C. This outcome is contingent on the type of µPCM and ambient temperature profile, along with other factors. Still, at first glance, the µPCM-43 effect seems promising in delaying temperatures above 45°C. The µPCM impact is more meaningful as the depth from the top surface increases. Another

important observation of this study is that the thermal cycling tests included mixtures composed of a wide variety of raw materials. The A, B, C, and D mixtures were gathered as part of a research project on implementing asphalt mixture design changes in Indiana (Haddock et al., 2020). As a result, the mixtures used in the experiments come from various areas of the state. Consequently, the thermal cycling results suggest the μPCM effect is applicable for a broad array of asphalt mixture materials.

Table 4.6. Absolute maximum temperature difference between control and μPCM-43 modified mixture specimens.

Control Mixture	μPCM-43 Content by Total Mixture Mass (%)	Phase Transition	Absolute Maximum Temperature Difference (°C)		
			Depth from Top Surface (mm)		
			0 (Top Surface)	25 (Mid-Specimen)	50 (Bottom Surface)
Mixture A	4	Liquification	4.64	5.68	6.16
		Solidification	2.61	2.81	2.92
	8	Liquification	7.93	9.48	10.13
		Solidification	4.56	5.22	5.43
Mixture B	4	Liquification	4.70	5.27	6.25
		Solidification	2.70	3.04	3.32
	8	Liquification	6.10	8.46	9.30
		Solidification	3.53	4.66	4.99
Mixture C	4	Liquification	4.72	5.62	6.29
		Solidification	2.47	2.85	3.19
	8	Liquification	7.53	9.06	10.32
		Solidification	4.10	4.74	5.46
Mixture D	4	Liquification	3.74	5.65	6.34
		Solidification	1.91	2.89	3.15
	8	Liquification	7.23	8.83	9.64
		Solidification	3.75	4.39	4.64

4.3.3 Mechanical performance of μPCM-43 modified asphalt materials

Dynamic modulus μPCM-43 Mixtures

As shown in Figure 5.3, a comparison of small specimens' dynamic modulus master curves reveals that the Reference Mixture has a higher stiffness than the μPCM-43 Mixtures, especially at the intermediate test temperatures (i.e., loading frequencies between 0.1 and 100 Hz). Previous studies have not discussed the reduction in dynamic modulus due to the presence of μPCM-43 particles (Refaa et al., 2018; Kakar et al., 2019b; Kakar et al., 2019c; Wei et al., 2019b*;* Bueno et al., 2019; Tian et al., 2019). Several investigations have implied that the transient decrease in temperature

due to the thermal lag effect of μPCMs translates directly to a higher asphalt mixture or binder stiffness without acknowledging the mechanical impact of the μPCM-43 particles and substitution of traditional mineral fillers. For conventional asphalt mixtures, some rules of thumb have been validated and can be used for quantifying the improvement of performance in asphalt mixtures due to temperature reduction (Si et al., 2015), where a slight shift in asphalt pavement temperature could lead to a significant increase in stiffness, or relaxation, and enhance pavement life-cycle performance. For example, a 5°C reduction in temperature can delay the risk of cracking for about three years (Si et al., 2015). However, the results presented herein suggest that these relationships may not directly apply to μPCM modified asphalt mixtures. The reduction in dynamic modulus may be associated with the stiffness, surface area properties, and interfacial adhesion of the μPCM particles. These factors should be further investigated through experimental testing and thermomechanical modeling, along with the thermal relaxation benefits that μPCM might provide due to the transient reductions of temperature.

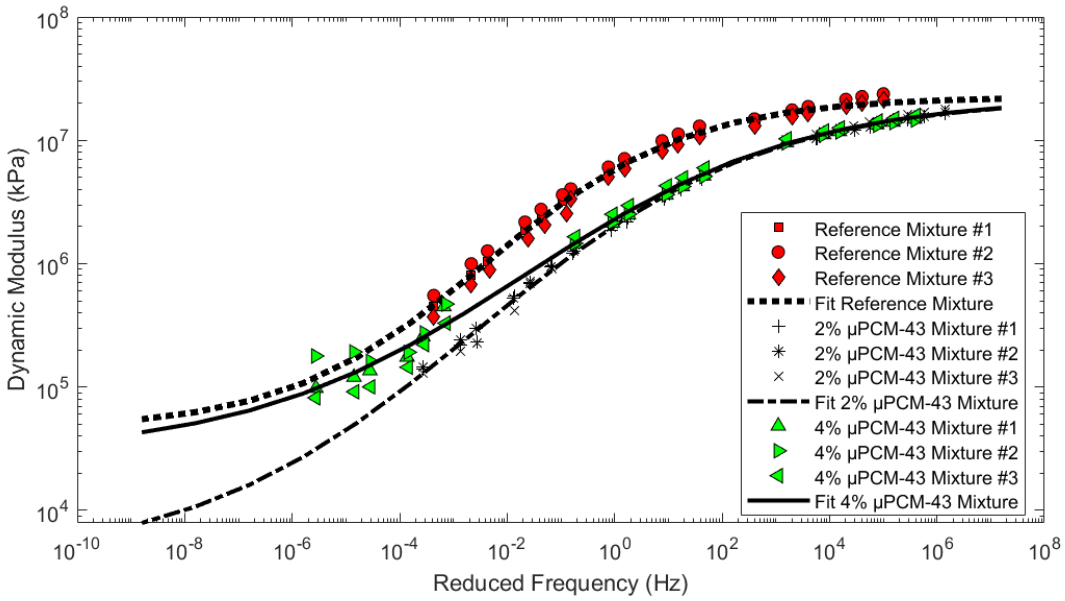

Figure 4.6. Dynamic modulus of Reference and μPCM-43 Mixtures, small specimens.

The data suggest issues related to the repeatability and reproducibility of the test methods for the μPCM-43 Mixtures at high temperatures. These results are consistent with laboratory observations. The dynamic modulus testing was conducted at three temperatures, 4, 20, and 40°C. During temperature conditioning and testing, a waxy appearance was noticed in the μPCM-43

Mixture specimens at 40°C. Presumably, some of the capsules did not survive the mixing and specimen fabrication process, leading to paraffin leakage. As demonstrated by the DSC measurements, at temperatures below 38°C, the core material of the μPCM-43, paraffin, is solid. But, at temperatures above 38°C, it transforms into a liquid. Comparable observations can be derived for big specimens. Overall, despite all the current limitations of the technology, the stiffness of μPCM-43 Mixtures is not too dissimilar to a conventional asphalt mixture's behavior, as illustrated by the master curve analysis.

Permanent deformation of μPCM-43 modified asphalt materials

The test methods applied to evaluate the permanent deformation resistance of μPCM-43 modified asphalt binders and mixtures were the Multiple Stress Creep Recovery (MSCR) and Flow Number procedures. First, the MSCR results are presented in Table 4.7. The MSCR test has shown to be satisfactory for discriminating in identifying the rutting potential of both modified and neat binders. Lower non-recoverable creep compliance of asphalt binder correlates to a better rutting performance. However, these data must be interpreted with caution because the measurements were performed on original binders. The MSCR method is intended for use with residue from the RTFO procedure. The results obtained suggest that the μPCM-43 particles act as a filler that stiffens the binder. The reduction in the non-recoverable creep compliance parameters is consistent across the three binder types examined, and it depends on the amount of μPCM included in the asphalt binder specimens. The percentage differences with base binder and relative variability of the results are coherent, indicating a good affinity between the μPCM-43 particles and base asphalt binders. The average non-recoverable creep compliance reported for each experimental combination corresponds to the results obtained from three replicates. The stiffening effect of the μPCM-43 on the asphalt binders was also observed by the high-temperature parameter ($G^*/\sin\delta$) used for binder grading.

Table 4.7. Multiple Stress Creep Recovery results for binders with and without μPCM-43.

Base Binder	Non-Recoverable Creep Compliance at 3.2 kPa, $Jnr_{3.2}$							
	μPCM Dosage (by binder mass)							
	0%		20%			40%		
	Average (kPa^{-1})	CV (%)	Average (kPa^{-1})	CV (%)	Percentage difference with base binder (%)	Average (kPa^{-1})	CV (%)	Percentage difference with base binder (%)
PG 64-22	6.5	1.0	3.7	0.4	43.0	2.0	0.8	69.7
PG 70-22	5.6	0.5	2.5	0.6	56.0	1.8	0.6	68.1
PG 76-22	11.7	0.0	6.1	1.4	47.7	3.1	1.2	73.5

Flow Number test results contrast with the MSCR results. Figure 4.7 shows that the Flow Number testing was conducted under unconfined testing conditions for the Reference Mixture and unconfined and confined environments for the 4% μPCM-43 Mixture. Confining pressure was used for the μPCM-43 Mixtures because under unconfined testing conditions, the specimens will have failed immediately after a few cycles (permanent strain higher than 10%), as demonstrated by the 4% μPCM-43 Mixture specimen tested unconfined. This outcome corroborated the suspicions that some PCM liquid might be leaking at high temperatures. The testing temperature for Flow Number evaluations was 53°C, a typical test parameter used for this method in Indiana. The permanent deformation results for the Reference Mixture specimens suggested an average Flow Number of 562 by fitting the experimental data to the Francken model. This average Flow Number satisfies the minimum criteria in AASHTO T 378 for a traffic level between 10 and 30 million Equivalent Single Axle Loads (ESALs). The Francken model approach also indicated that the Flow Number for the 4% μPCM-43 Mixture specimens under a confining pressure of 50, 100, and 200 kPa was 2076, 4517, and 7281, respectively. What emerges from the results reported in this section is that the μPCM-43 Mixtures are susceptible to permanent deformation. Presumably, the loss of resistance to deformation under load is because PCM leaking due to shell breakage during mixing and compaction, leading to a detrimental interaction between the PCM, asphalt binder, and aggregate materials, especially at temperatures above 40°C.

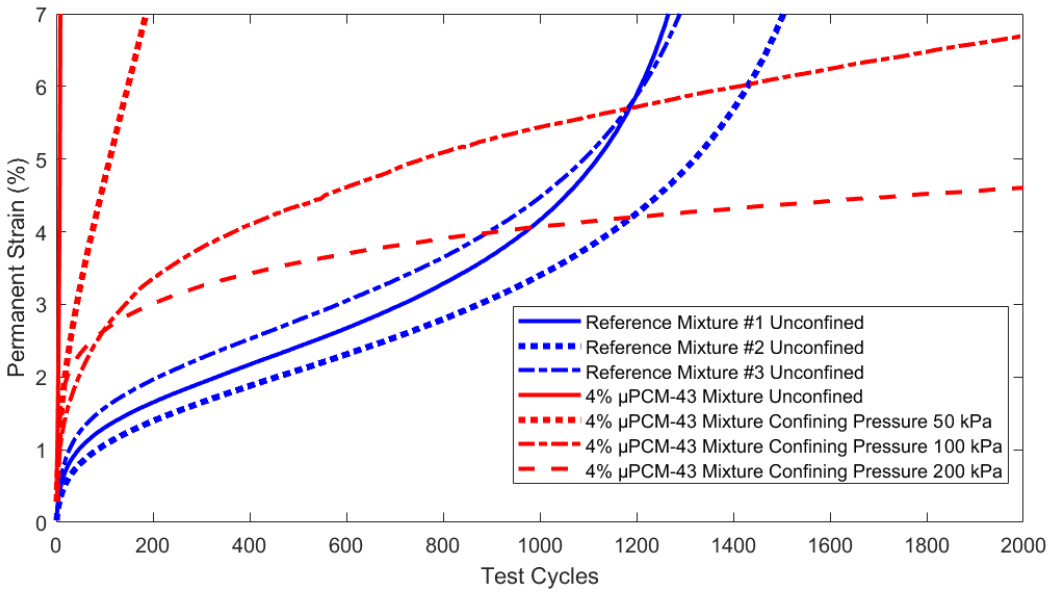

Figure 4.7. Flow number test results.

Fatigue characteristics of µPCM-43 modified asphalt materials

The fatigue characteristics of base and µPCM-43 modified binders were characterized using the Linear Amplitude Sweep (LAS) test method described in AASHTO TP 101-14. The LAS tests were performed at temperature levels that could correlate with asphalt mixture testing (or the average of high and low PG temperatures minus 3°C), precisely 18°C for PG 64-22, 21°C for PG 70-22, and 24°C for PG 76-22. Table 4.8 reports the allowable binder fatigue life for 2.5 and 5.0% strain amplitudes, as determined by the asphalt binder fatigue model. The 5% strain amplitude used to predict the binder fatigue performance corresponds to a mixture strain of approximately 1,000µε, which is typically considered a high strain level in pavements (Johnson, 2010). A lower strain amplitude of 2.5% is also reported in this portion of the study, as this strain level is typically used in similar investigations (Roque et al., 2020). The fatigue life analysis suggests that lower resistance to cyclic loading should be expected for µPCM-43 modified asphalt binders compared to non-µPCM modified binders. This decrement in fatigue resistance seems proportional to the amount of µPCM-43 modification and type of base binder.

Relatively speaking, the PG 76-22 specimens with and without µPCM-43 outperformed the PG 64-22 and PG 70-22 specimens at all µPCM dosages. Additionally, the percentages differences because of µPCM-43 modification are lower for PG 76-22 binders than PG 64-22 and

PG 70-22 binders. This outcome implies that a shortage in fatigue performance due to μPCM-43 incorporation could be balanced using a base binder that better withstands damage accumulation caused by repetitive traffic loading. It should be noticed that the PG 76-22 showed the highest susceptibility to permanent deformation at all μPCM dosages when compared to PG 64-22 and PG 70-22.

Table 4.8. Fatigue life of binders with and without μPCM-43.

Base Binder	Fatigue Performance Parameter at 2.5% Applied Strain, N_f							
	μPCM Dosage (by binder mass)							
	0%		20%			40%		
	Average N_f	CV (%)	Average N_f	CV (%)	Percentage difference with base binder (%)	Average N_f	CV (%)	Percentage difference with base binder (%)
PG 64-22	5636	5.9	5069	3.2	10.1	3103	16.8	44.9
PG 70-22	4386	5.2	3587	17.3	18.2	1730	5.4	60.6
PG 76-22	18762	4.0	16682	2.3	11.1	14198	5.8	24.3
Base Binder	Fatigue Performance Parameter at 5.0% Applied Strain, N_f							
	μPCM Dosage (by binder mass)							
	0%		20%			40%		
	Average N_f	CV (%)	Average N_f	CV (%)	Percentage difference with base binder (%)	Average N_f	CV (%)	Percentage difference with base binder (%)
PG 64-22	807	4.9	661	5.1	18.1	425	15.0	47.4
PG 70-22	655	4.5	483	14.6	26.2	234	7.4	64.3
PG 76-22	2867	1.5	2622	2.4	8.6	2328	6.9	18.8

Figure 4.8 illustrates the newly developed Cyclic Fatigue Index Parameter (S_{app}) for the mixtures investigated for this research, Reference and μPCM-43 Mixtures, and for a Mineral Filler Mixture. The Mineral Filler Mixture contained a significant volume of fine particles, equivalent to the volume of μPCM particles in the 4% μPCM-43 Mixture. In the Mineral Filler Mixture, all the material passing the 0.600 mm sieve in the Reference Mixture was substituted with baghouse fines. This type of mixture was prepared to understand further the fatigue resistance of asphalt mixtures having a significant portion of fine particles. Three replicates are reported for each type of mixture. All the fatigue performance testing for this study was conducted at 18°C. The average S_{app} results for the Reference Mixture, 2% μPCM-43 Mixture, 4% μPCM-43 Mixture and Mineral Filler Mixture are 20.2, 22.5, 23.5, and 22.3, respectively. Considering that the S_{app} can distinguish the fatigue resistance of asphalt mixtures with various properties (including aggregate gradation), the results demonstrate that the modifications performed to produce the μPCM-43 Mixtures are not a

concern for their fatigue performance. The µPCM-43 modified mixtures and Mineral Filler Mixture provided slightly higher average S_{app} results compared to the Reference Mixture. The S_{app} accounts for the effects of a material's modulus and toughness on its fatigue resistance and is a measure of the amount of fatigue damage the material can tolerate under loading. Higher S_{app} values indicate better fatigue resistance of the mixture (Wang et al., 2020). Additionally, the S_{app} results of the µPCM-43 modified mixtures are similar to the values obtained for the Mineral Filler Mixture, suggesting that the microcapsules act as a conventional filler at an intermediate temperature. The µPCM-43 particles inherently impact the fatigue resistance of the modified asphalt mixtures due to their characteristics, but no adverse effects are observed.

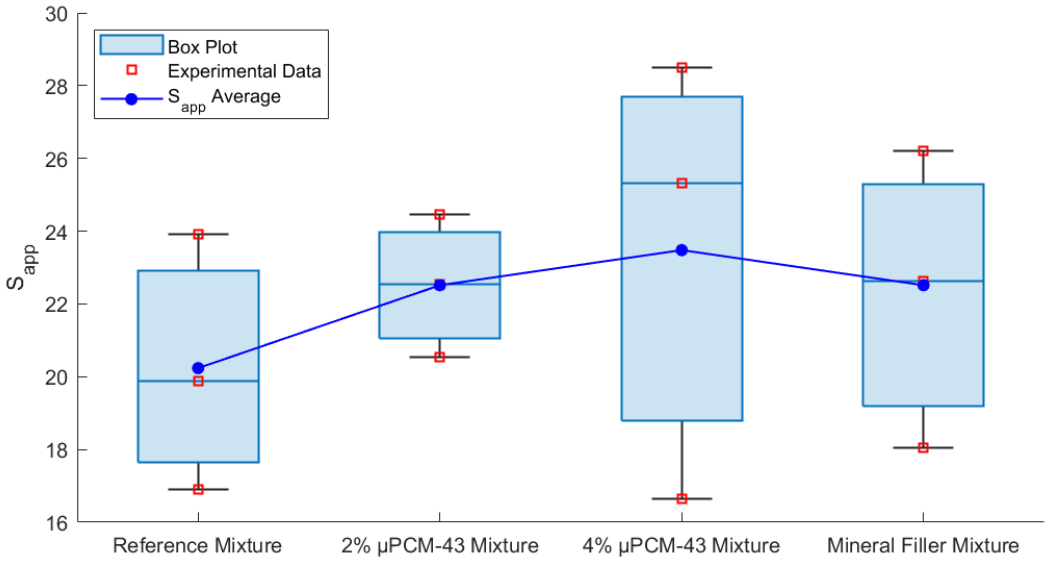

Figure 4.8. Cycling fatigue test results.

Low-temperature performance of µPCM-43 modified asphalt materials

Table 4.9 reports the low-temperature characteristics of asphalt binders with and without µPCM-43 estimated using the Bending Beam Rheometer (BBR) test method (AASHTO T 313) at a testing temperature equal to -16°C and loading time of 60 s. The most striking observation from the data comparison is the dramatic increase in stiffness when the base binders are modified with µPCM-43. When the base asphalts are adjusted by 40% of total binder mass with µPCM-43, the stiffness can be doubled, raising concerns about the brittleness of µPCM-43 modified binders at low

temperatures. This matter could be mitigated by a proper selection of base binder and μPCM-43 dosage. For instance, the control PG 70-22 binder's estimated stiffness is higher than PG 64-22 and PG 76-22 with a 20% μPCM-43 dosage. The relaxation properties of the base binders seem not to be as substantially influenced by the μPCM particles as the stiffness parameter. This behavior is in good agreement with the mechanical response of binders modified with any other filler having a comparable particle size distribution. Previous work suggests that although the stiffness increases due to the addition of fine particles in a binder matrix, the filler effect does not seriously hamper the ability of the system to dissipate energy by relaxation (Little and Petersen, 2005). These findings are confirmed by the Delta Tc parameter (ΔT_c) results, which suggest that the unaged binders with and without μPCM-43 are stiffness-controlled. All the ΔT_c values are between 0.5 and 2.2. To calculate the ΔT_c parameter, three replicates were tested at -10, -16, -22, and -28°C using the BBR for each binder combination.

Table 4.9. Low-temperature performance of binders with and without μPCM-43.

Base Binder	Estimated Stiffness at -16°C and 60 s, S							
	μPCM Dosage (by binder mass)							
	0%		20%			40%		
	Average S (MPa)	CV (%)	Average S (MPa)	CV (%)	Percentage difference with base binder (%)	Average S (MPa)	CV (%)	Percentage difference with base binder (%)
PG 64-22	175.9	1.9	251.8	0.6	43.1	350.1	6.6	99.0
PG 70-22	275.5	7.6	385.1	3.6	39.8	493.1	7.2	79.0
PG 76-22	188.4	3.1	263.8	5.4	40.0	413.0	5.0	119.2
Base Binder	m-value at -16°C and 60 s							
	μPCM Dosage (by binder mass)							
	0%		20%			40%		
	Average m-value	CV (%)	Average m-value	CV (%)	Percentage difference with base binder (%)	Average m-value	CV (%)	Percentage difference with base binder (%)
PG 64-22	0.372	1.0	0.347	1.2	6.6	0.302	3.5	18.6
PG 70-22	0.323	3.4	0.302	0.3	6.5	0.273	2.9	15.6
PG 76-22	0.366	1.1	0.323	0.3	11.7	0.287	0.2	21.4
Base Binder	Delta Tc Parameter, ΔT_c							
	μPCM Dosage (by binder mass)							
	0%		20%			40%		
	Average ΔT_c	CV (%)	Average ΔT_c	CV (%)	Percentage difference with base binder (%)	Average ΔT_c	CV (%)	Percentage difference with base binder (%)
PG 64-22	1.5	15.9	1.6	12.4	8.1	1.3	22.4	12.2
PG 70-22	1.3	5.7	1.7	7.5	29.6	2.2	5.5	74.5
PG 76-22	1.2	10.6	0.5	70.1	56.5	1.3	13.2	13.2

Figure 4.9 shows the stiffness results calculated from semicircular asphalt mixture testing, according to AASHTO T 394. The stiffness is relatable to the elastic modulus of asphalt mixtures at low temperatures and is calculated as the slope of the linear part of the ascending load-average line displacement ($P - u$) curve. The unit measure for this stiffness parameter is kN/mm. The asphalt mixtures' low-temperature responses were determined at two levels, -12 and -24°C. As expected, an increased asphalt mixture stiffness was observed at a lower testing temperature. The average stiffness parameters measured at -12°C for the Reference, 2% μPCM-43 and 4% μPCM-43 Mixtures are 9.5, 6.3, and 6.4 kN/mm, respectively. Whereas the average stiffness parameters achieved at -24°C for the Reference, 2% μPCM-43 and 4% μPCM-43 Mixtures are 15.2, 8.6, and 9.0 kN/mm, correspondingly. In addition, much more variability was observed in the stiffness results obtained at -24°C than at -12°C. However, the μPCM-43 effect found at both temperatures is the same. A sharp reduction in stiffness is observed when the μPCM-43 particles are incorporated into the asphalt mixtures at both aggregate replacement quantities, 2 and 4% by total mixture mass. The causes and implications of this finding need further research. But two interesting aspects can be derived from the SCB data. First, the fracture resistance of asphalt mixtures at low temperatures is altered with the inclusion of μPCM-43. Second, the stiffness parameter might be limited to discriminate among different levels of μPCM-43 modification, or a similar low-temperature response is obtained regardless of the amount of μPCM-43.

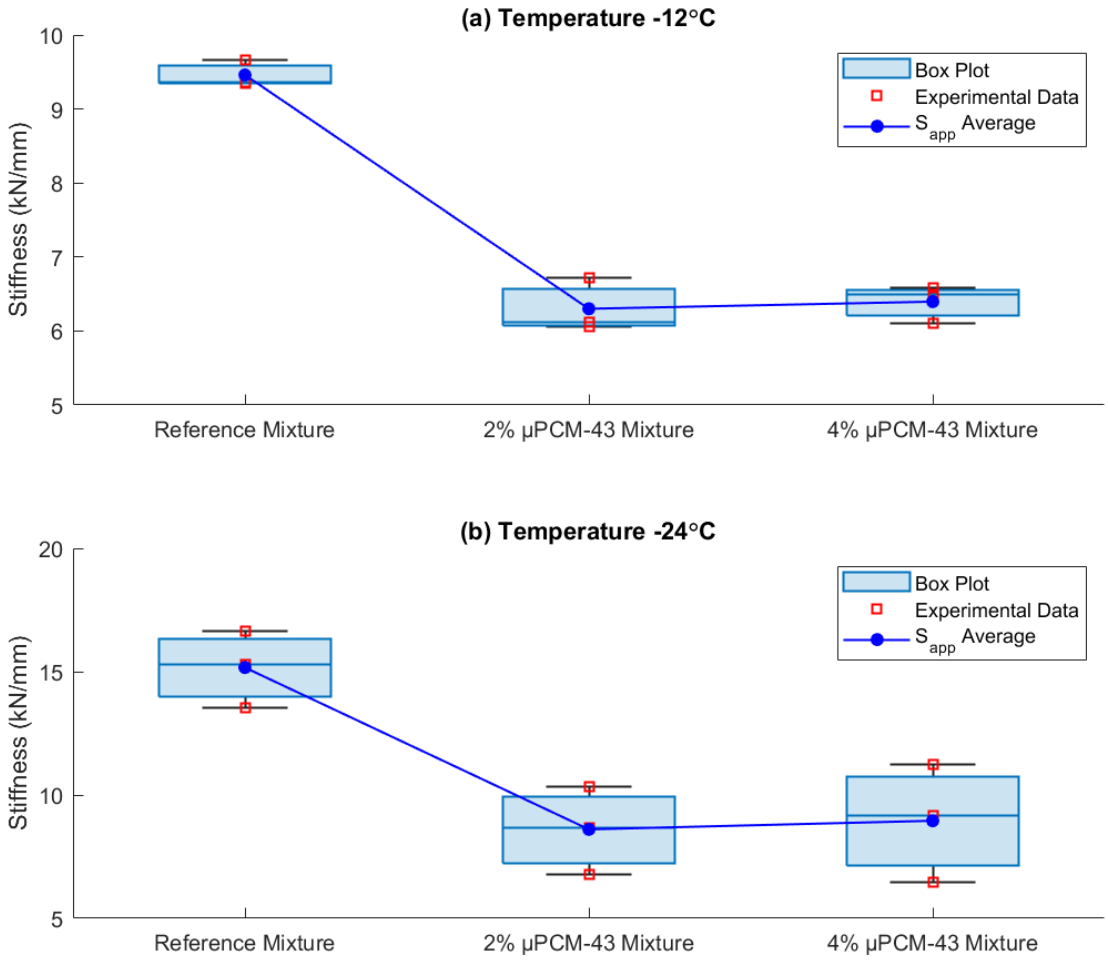

Figure 4.9. Stiffness results from semicircular asphalt mixture testing.

4.3.4 Thermal response of µPCM-43 Mixtures

Figure 4.10 shows the thermal responses of the Reference Mixture, without µPCM, and the 4% µPCM-43 Mixture with different air voids contents. The results resemble the thermal behavior of the µPCM-43 modified asphalt mixtures previously discussed, Mixtures A-D (see Figure 4.5), but the 4% µPCM-43 Mixture has air voids contents within the acceptable air voids content range. The mixture was purposely re-designed to incorporate the µPCM without including an excessive amount of fine particles (combination of fine aggregate, mineral filler, and µPCM).

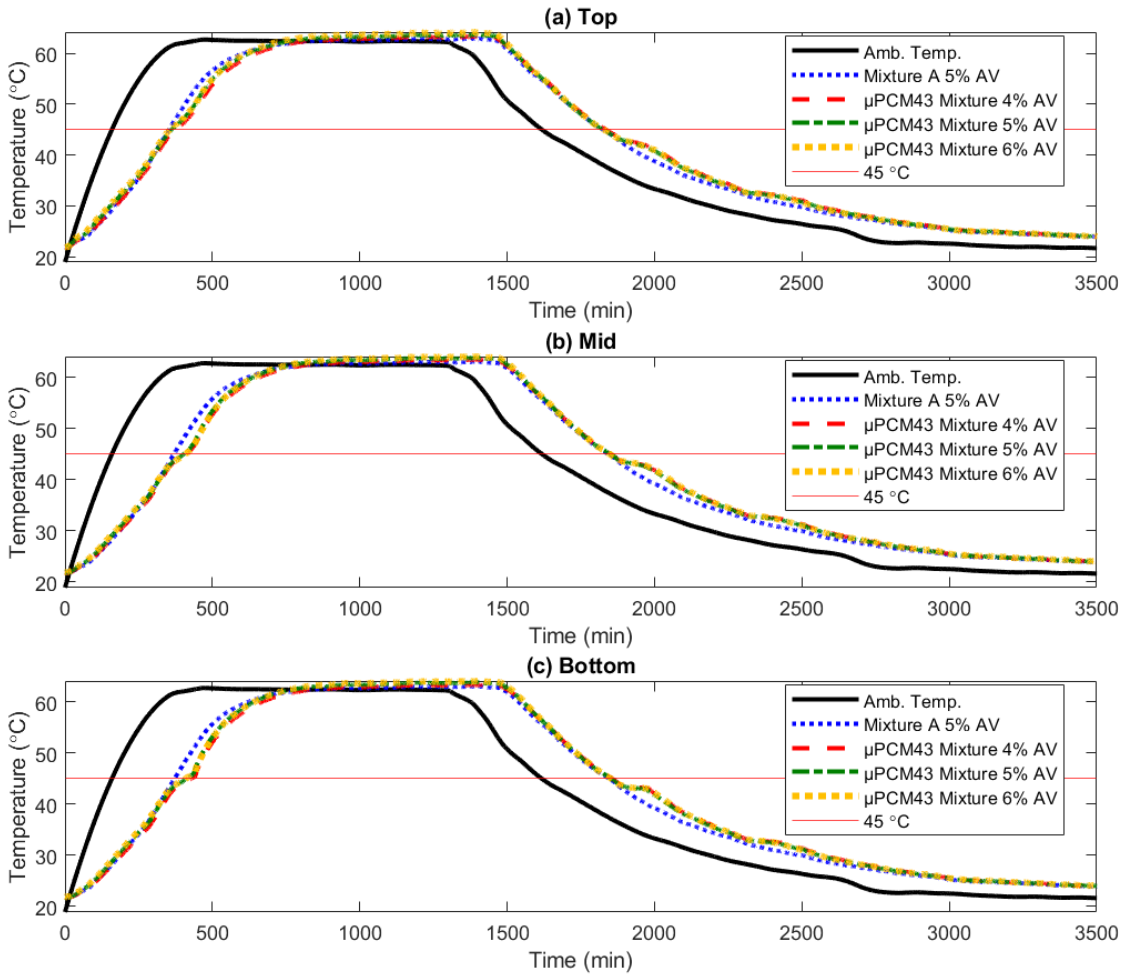

Figure 4.10. Thermal response of 4% μPCM-43 Mixture specimens with various air voids contents at different depths from the top surface.

Table 4.10 summarizes the results for both μPCM-43 Mixtures and highlights the air voids content's importance to the temperature profile and heat flow within the μPCM-43 Mixture specimens. More μPCM-43 particles in the mixture yield a higher temperature shift between the mixture with and without μPCM. Furthermore, as the air voids content increases, the μPCM-43 effect seems to decrease, as demonstrated by the absolute maximum temperature difference between Reference Mixture and μPCM-43 Mixture specimens. The average absolute temperature difference observed at the surface for all the μPCM-43 Mixture specimens under liquification, and solidification transitions is 2.65°C. This outcome agrees with the work reported in Refaa et al. (2018), which through numerical analysis, determined that replacing similar portions of fine aggregate and mineral filler with μPCMs could reduce the surface temperature by about 2.70°C.

Table 4.10. Absolute maximum temperature difference between Reference Mixture and μPCM-43 Mixture specimens.

Mixture Type	Air Voids Content (%)	Phase Transition	Absolute Maximum Temperature Difference (°C)		
			Depth from Top Surface (mm)		
			0 (Top Surface)	25 (Mid-Specimen)	50 (Bottom Surface)
4% μPCM-43 Mixture	4.0	Liquification	4.16	4.66	5.89
		Solidification	2.49	2.73	3.28
	5.0	Liquification	3.12	4.43	5.22
		Solidification	2.28	2.81	3.29
	6.0	Liquification	3.06	4.02	4.92
		Solidification	2.09	2.51	2.90
2% μPCM-43 Mixture	5.0	Liquification	2.49	3.06	3.92
		Solidification	1.48	1.72	2.01

It should be emphasized that all temperature differences are relative to the control Reference Mixture specimen, which has an air voids content of 5.0 percent. However, the tendency is undeniable and corroborates previous research studying the effect of air voids content on thermal properties of asphalt mixtures. Hassn et al. (2016) determined that asphalt mixtures with high air voids contents have lower thermal conductivity and specific heat capacity than those with lower air voids contents. Consequently, asphalt mixtures with high air voids contents are more suitable to alleviate the urban heat island effect. In contrast, asphalt mixtures with low air voids are recommended for harvesting solar energy from the environment. Given the results obtained for the 4% μPCM-43 Mixture, it is plausible that slightly lower air voids contents might be more beneficial to maximize the μPCM effect.

4.3.5 Link between binder and mixture performance

As explained earlier, an attempt was made to identify the association between the binder and mixture results for μPCM modified asphalt materials. By modifying a PG 64-22 asphalt binder with μPCM-43 at 40 and 80% by binder mass (percentages that reflect the ratios of μPCM-43 to virgin binder in the μPCM-43 Mixtures), the possible correlation between asphalt binder and mixture results was investigated. As has already been noted, the mechanical asphalt binder and mixture experiments provided compelling information about the behavior of μPCM modified asphalt materials. However, the experimental data gathered was insufficient to establish a correlation between the mechanical behavior of μPCM modified asphalt binder and mixtures; the μPCM particles influenced their mechanical responses in an ambivalent manner. Nevertheless, a

groundbreaking connection was found between the rheological response of μPCM-43 modified asphalt binders and the thermal response of μPCM-43 Mixtures, which is illustrated in Figure 4.11.

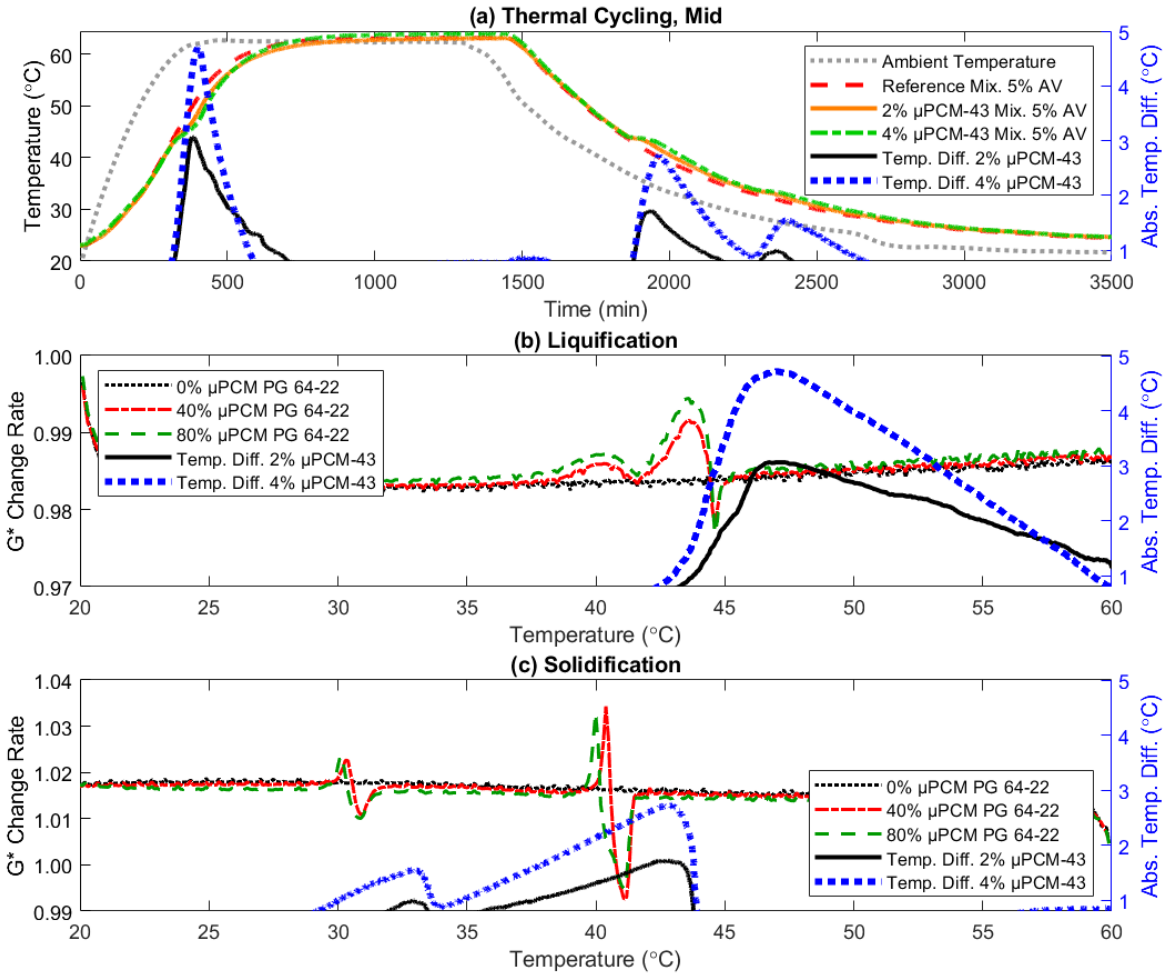

Figure 4.11. Relationship between rheological measurements and thermal cycling experiments.

The absolute temperature difference plots delineate the gaps in temperature between the Reference Mixture and μPCM-43 Mixture specimens with 5% air voids content. The disparities in temperature caused by the presence of μPCM have been the subject of investigation of previous studies (Si et al., 2015; Ma et al., 2019). Based on the fundamental theory of latent heat, Ma et al. (2019) proposed quantifying the accumulation of temperature difference between a μPCM asphalt mixture and a non-μPCM modified asphalt mixture in a time range as a measurement of the μPCM modification effectiveness. The parameter's theoretical background suggests estimating the accumulated temperature difference (or area below the curve) as soon as a discrepancy is observed.

Thus, Ma et al. (2019) failed to account for inherent temperature differences because of different material properties and proportions or thermocouple measurement errors. As shown in Figure 4.11, the differences in temperature below 1°C could be ignored as these disparities are not necessarily because of the latent heat effect of μPCMs.

To further assess the capability of the G* Change Rate, the rheological results reported in this section correspond to PG 64-22 asphalt binder specimens modified with μPCM at 0, 40, and 80% by total binder mass. These asphalt binder to μPCM ratios are in good agreement with the raw quantities of material included in the μPCM-43 Mixtures (see Table 4.2). The G* Change Rate was determined by conducting DSR tests at 12 °C/h. The number, shape, and intensity of the G* Change Rate peaks are analogous to the temperature difference curves observed between the Reference Mixture and μPCM-43 Mixture specimens. As previously reported, the thermal peak in the PCM liquification transition is more uniform, generating a higher temperature difference than the solidification transition. When the paraffin material inside the μPCM-43 is crystallizing, the latent heat effect is divided into two parts, as confirmed in Figure 4.11c. It should be highlighted that as more μPCM-43 particles are included in the DSR testing, the G* Change Rate slightly drifts from the baseline, or the G* Change Rate reported by the control PG 64-22 binder specimen. However, the concept is still applicable. Similar observations can be made for PG 70-22 and PG 76-22 asphalt binders modified with μPCM-43.

4.4 Summary and Conclusions

This chapter attempts to understand the environmental tuning of asphalt pavement materials using μPCMs. In general, the work presented herein advances the modification of asphalt pavements with μPCMs by developing a rheological measurement, framing a mixture design approach for μPCM incorporation, and linking the thermal responses of μPCM modified asphalt binders and mixtures. Additionally, the mechanical performance of asphalt binders and mixtures enhanced with μPCM was carefully examined at high, intermediate, and low temperatures. The mechanical and thermal results presented will contribute to optimum dosages of μPCM in asphalt paving materials. The tuning of asphalt materials to their anticipated environment is expected to improve asphalt mixture performance and extend asphalt pavement service life, leading to more sustainable paving technologies.

The evidence from this chapter suggests that rheological measurements by means of the DSR equipment can help identify the latent heat effect of μPCM particles in asphalt binders. This study's findings propose using the G* Change Rate parameter to determine the temperatures at which the μPCM effect occurs. This approach can also provide insights into the intensity of the μPCM thermal impact on asphalt mixtures. Moreover, the experimental results confirm that μPCM modified asphalt mixture specimens can experience temperature differences between 1.8 and 10.3°C, as compared to non-μPCM modified asphalt mixture specimens subjected to the same ambient temperatures. In practice, this suggests that μPCMs can delay the appearance of undesirable temperatures in asphalt pavements. However, this outcome depends on the amount and characteristics of μPCM, asphalt mixture materials, ambient temperature, phase change transition (solidification or liquification), depth from the pavement surface, and density of the compacted asphalt mixture.

The current data highlights the importance of the temperature dependency of asphalt materials. DSR and DSC results confirm that asphalt binder viscoelastic flow is a thermally activated process. The rate at which asphalt binder stiffness changes is conditional on the temperature fluctuations experienced by the material. The G* Change Rate analysis found a countereffect in the viscoelastic flow of μPCM modified, which should warrant further investigations. Therefore, a natural progression of this work is to determine the causes and possible implications of this finding.

Finally, the asphalt binder and mixture mechanical test results suggest ambivalent performance outcomes caused by the incorporation of μPCMs in asphalt paving materials. Overall, the mechanical analysis indicates that the μPCM particles could behave like a conventional mineral filler if they suffer no damage during mixing and compaction. Future work is needed to evaluate the survivability of μPCMs during the production, placement, and compaction of asphalt mixtures. In addition, the long-term performance of μPCMs under repetitive vehicle loading and temperature fluctuations must be assessed.

5. INCREASING ASPHALT PAVEMENT DENSITY THROUGH MIXTURE DESIGN: A FIELD PROJECT[c]

[c]This Chapter is reproduced from the paper "Increasing Asphalt Pavement Density Through Mixture Design: A Field Project" published in Asphalt Paving Technology on 2018 (DOI: 10.12783/aapt2018/33800)

5.1 Introduction

This dissertation has focused on incorporating PCMs into asphalt pavement materials, which is the main line of research for this study. Several aspects of the potential benefits, design, and challenges of the environmental tuning of asphalt pavements with PCMs have been revealed. Within the findings presented so far, critical elements about asphalt pavement technology have been part of the discussion, such as the air voids content of asphalt mixtures, survivability of PCM formulations through asphalt mixture production, and smooth placement of PCM modified asphalt layers, either for PCMs contained in embedded pipes or asphalt mixtures doped with μPCMs. Implementing environmentally tuned asphalt pavements with PCMs depends on the formulation of thermoregulating agents and paving methods that required minimal or no additional accommodations in relation to traditional and current asphalt pavement technology practices. Although paving techniques have evolved over the years, the paving fundamentals have remained about the same since the first asphalt road projects were documented in the 19th century (Brown, 2009; Mansell, 2021). This chapter presents a case study reported in 2018 that exemplifies how modifications in asphalt mixture design could substantially benefit asphalt pavements' construction and long-term performance. Additionally, the chapter contains information associated with asphalt pavement construction best practices. This chapter intends to bridge further the available knowledge about general asphalt pavement technology and PCM formulation and implementation.

5.1.1 Scope

For decades, asphalt mixture design methods have specified that optimum asphalt binder content for a given gradation be selected at 4% air voids content. On average, such design methods have typically resulted in asphalt mixtures with in-place densities between 92 to 93 percent (Brown, 2009). The in-place density acceptance criterion is regarded as one of the most important controls

used to ensure the quality of an asphalt pavement because density is a good indicator of future pavement performance (Smith and Diefenderfer, 2008). However, recent developments in asphalt pavement construction and service life performance specifications indicate the need for increasing pavement density. Data from several studies suggest that a slight in-place density increase can lead to a significant increase in asphalt pavement service life (Tran et al., 2016).

In an attempt to increase in-place asphalt pavement densities and thereby improve pavement durability, previous research has shown that if appropriately designed, asphalt mixtures can be field compacted to 95% density without the need for compaction effort additional to that used for standard Superpave-designed mixtures. According to Hekmatfar et al. (2015), this can be accomplished by designing asphalt mixtures with optimum asphalt binder content selected at 5% air voids using a lower laboratory compaction level than the current specified by the Superpave mixture design method. An extensive investigation suggested that mixtures designed at 5% air voids content and placed at 95% of G_{mm} could outperform mixtures designed at 4% air voids content and placed at the typical 92-93% G_{mm}, in terms of mechanical properties (Hekmatfar, 2016).

Although a modified mixture design procedure had been successfully developed and two closely controlled field trials were completed prior to this research effort was performed, additional field data was required to support the original findings and proceed with a state-wide implementation, specifically, a less controlled field trial. In the two previous field trials, the modified mixture designs were carefully performed, and the mechanical properties of the resulting mixtures were tested in the research laboratory before field placement (Hekmatfar, 2016). Additionally, the research team assisted with the mixture Quality Control (QC) during construction. This chapter reports on a third paving demonstration project carried out on US 40 near Richmond, Indiana. For this project, the contractor completed the modified mixture design and production QC with no input from the research team, nor did the research team test the modified mixture before its placement. The project's objectives were to appraise the INDOT preliminary modified mixture design method in an uncontrolled experiment and determine if 95% density could be achieved in the resulting pavement during construction.

To achieve the objectives of the project, the contractor designed and placed both control and test mixtures. Optimum binder content was chosen at 4% air voids content for the control mixture according to the conventional Superpave volumetric mixture design method, AASHTO

M 323. Conversely, the test mixture was prepared according to INDOT's proposed modified mixture design method, with the Number of Design Gyrations (N_{des}) lowered to 50 from 100 and optimum binder content selected at 5% air voids content (Hekmatfar et al., 2015). During construction (Figure 5.1), asphalt mixture gradation, asphalt binder content, and volumetric properties were controlled by the contractor to achieve the desirable in-place density results. Laboratory measurements of plate and core samples were used to assess if the modified mixture design improved the density of the as-constructed asphalt pavement layer. Additional probabilistic and analytical studies of QC and construction acceptance data from Quality Assurance (QA) were conducted to evaluate the effectiveness of each mixture in achieving the targets for in-place density, laboratory air voids content, from now on referred to as V_a, Asphalt Binder Content (P_b), and VMA. Comparisons between the two mixtures using new construction performance metrics were made from a user perspective. Throughout this chapter, the term QC is used to describe sampling and testing performed by the contractor, and the term QA refers to data gathered by INDOT for construction acceptance.

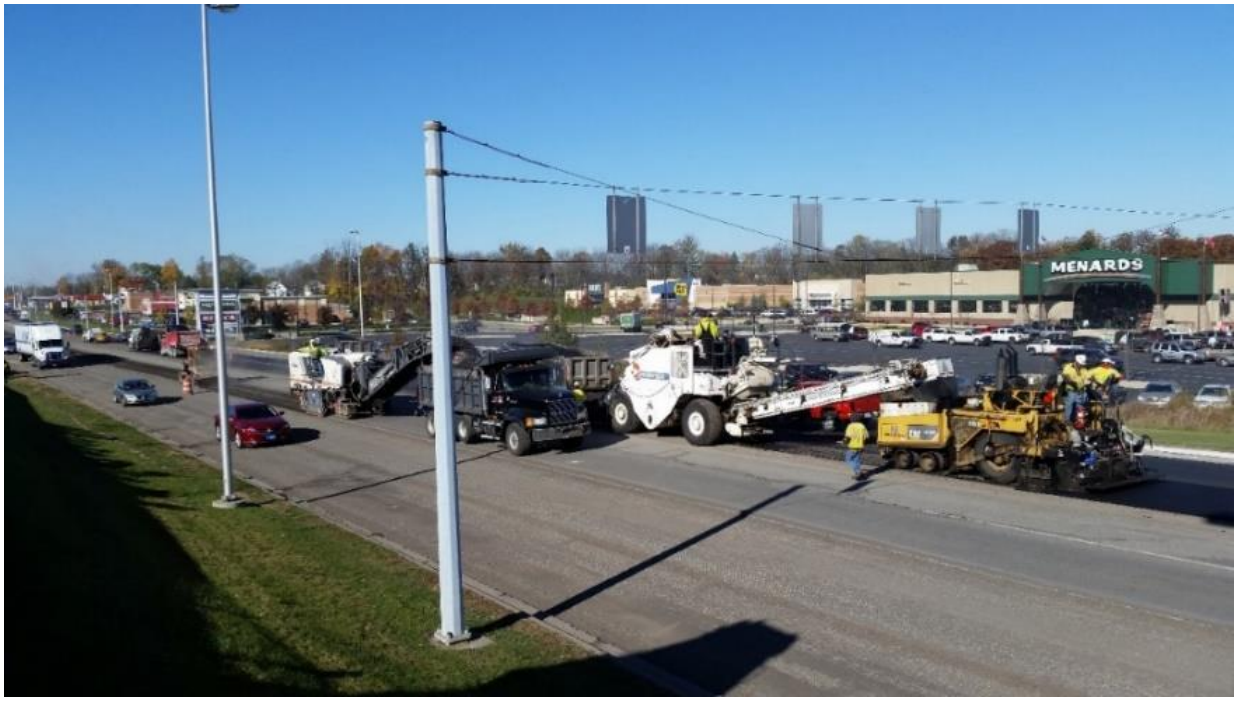

Figure 5.1. Milling and paving operations on US 40 in Richmond, Indiana.

5.2 Field Construction

5.2.1 Project background

In early 2016 the INDOT awarded a contract for paving repairs to US 40 in Richmond, Indiana. The project was described as an asphalt resurface intended to extend the pavement's service life and enhance highway safety and consisted of milling approximately 25 mm of the existing pavement and overlaying the milled surface with 25 mm of new asphalt mixture. Such projects are intended to improve serviceability or to provide additional strength (INDOT, 2013a). The intended design life of the new asphalt mixture overlay is approximately ten years. In November 2016, the US 40 project was executed as part of the Federal Highway Administration's (FHWA) increased in-place density initiative (Aschenbrener et al., 2017).

US 40 starts in Atlantic City, New Jersey, and extends across twelve states, terminating in Silver Summit, Utah. It passes through Richmond, Indiana, located in east-central Indiana and bordering Ohio, serving as Richmond's "Main Street." Placement of the new asphalt mixture extended from 22nd Street to Sycamore Drive, covering a length of approximately 1.8 miles. The current traffic characteristics for this pavement section are estimated at 17,790 Average Annual Daily Traffic (AADT) with 5% trucks.

Prior to milling, the existing asphalt pavement surface was moderately deteriorated, with raveling, weathering, and moderate to severe cracking, rutting, and friction loss. Overall, the structural capacity of the existing pavement, a near 125 mm asphalt layer over Portland cement concrete, had been sufficient to sustain the prevailing loads. Therefore, the existing pavement structure was considered appropriate for the projected future traffic and more than adequate to support construction procedures. The support of the underlying layers plays a critical role in achieving optimal in-place densities and evaluating the gain in long-term performance (Tran et al., 2016).

5.2.2 Project quantities and schedule

The total amount of new asphalt mixture was estimated at 5,300 tons to overlay approximately 9 lane-miles of pavement. As shown in Figure 5.2, these 9 lane miles consisted of 1.8 centerline miles of two eastbound, two westbound, and one center turn lane of the roadway on US 40. For performance comparison purposes, one lane in each direction was paved with the control mixture

while the other was paved with the test mixture. One-half of the turn lane length was paved with the control mixture, while the other half was completed with the test mixture.

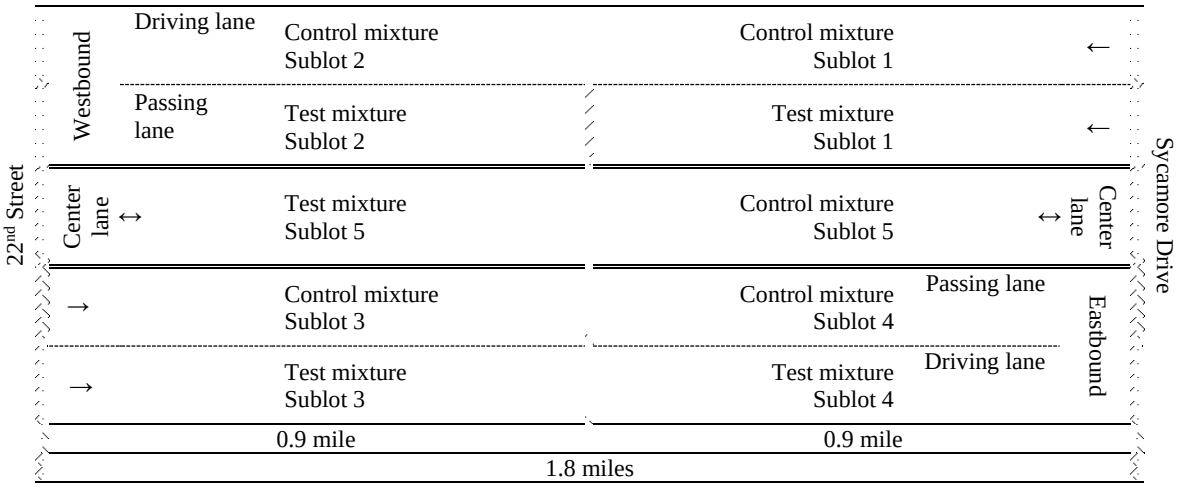

Figure 5.2. Control and test mixture sublots diagram.

Each of the two mixtures was considered one lot for the project and further subdivided into sublots for testing purposes. Each sublot consisted of approximately 530 tons of mixture. Asphalt mixture placement began on 9 November 2016, along the westbound driving lane. Table 5.1 shows the construction schedule, including the prevailing climatic conditions for each workday. The construction work window was between 8 am and 5 pm each day.

Table 5.1. Project schedule and climatic data.

Date (mm/dd/yy)	Lane	Mixture Type	Ambient Temperature Range (°C)	Relative Humidity Range (%)	Prevalent Condition
11-09-16	Westbound Driving Lane	Control	6.1 – 11.1	58 – 93	Mostly Cloudy
11-10-16	Westbound Passing Lane	Test	5.0 – 15.0	36 – 93	Partly Cloudy
11-11-16	Eastbound Driving Lane	Test	6.1 – 12.2	50 – 100	Scattered Clouds
11-12-16	Eastbound Passing Lane	Control	2.8 – 8.9	43 – 87	Clear
11-14-16	Center Lane	Test and Control	3.9 – 13.9	38 – 81	Clear

5.2.3 Mixture designs

The standard INDOT specifications (INDOT, 2013b) called for a 9.5-mm, Category 3 surface mixture for the project. In 2016, the acceptance criteria for such mixtures were based on in-place density, laboratory V_a at N_{des}, P_b, and VMA at N_{des}. Category 3 indicates expected traffic of 3 to less than 10 million ESALs over the pavement design life. A polymer modified PG 70-22 was selected as the correct binder type.

Optimum binder content for the control mixture was selected at 4% V_a using the conventional Superpave volumetric mixture design method (AASHTO M 323). Conversely, the test mixture was designed by selecting optimum binder content at 5% V_a according to the modified mixture design proposed by Hekmatfar et al. (2015), colloquially referred to as the "Superpave 5" asphalt mixture design method (Aschenbrener et al., 2017). It should also be noted that the control mixture and test mixture were compacted in the laboratory at 100 and 50 SGC gyrations, respectively. The volumetric targets for each asphalt mixture are presented in Table 5.2.

Table 5.2. Asphalt mixture design targets.

Property	Control Mixture	Test Mixture
In-place Density (%)	94.0	95.0
Air Voids Content (%)	4.0	5.0
Asphalt Binder Content (%)	6.7	7.1
Voids in the Mineral Aggregate (%)	15.6	16.7
Effective Asphalt Binder Content (%)	5.2	5.2
Number of Design Gyrations	100	50

5.2.4 Aggregate properties, blends, and gradations

Table 5.3 shows the project's aggregate materials and their properties, bulk specific gravity (G_{sb}), and water absorption. The RAP had a binder content of 5.9%, while the Reclaimed Asphalt Shingles (RAS) had a binder content of 22.9 percent. As shown in Table 5.4, the same aggregates at different proportions were used for both aggregate blends. The test mixture blend and gradation were designed using the Bailey method to achieve 5% V_a at a lower gyration level with the same Effective Asphalt Binder Content (P_{be}) as the 4% V_a mixture (Vavrik et al., 2002). The P_{be} for both mixtures was 5.2 percent. Table 5.5 presents the mixtures' aggregate gradations.

Table 5.3. Aggregate materials.

Aggregate	Bulk Specific Gravity	Water Absorption (%)
9.5 mm Stone	2.592	2.09
4.75 mm Stone	2.541	3.20
2.36 mm Stone Sand	2.589	2.54
RAP	2.640	1.00
RAS	2.500	1.00
Baghouse	2.800	1.00

Table 5.4. Aggregate blends.

Aggregate	Control Mixture				Test Mixture			
	Percent of Total Aggregate (%)				Percent of Total Aggregate (%)			
	Mixture Design	Sublot			Mixture Design	Sublot		
		1 and 2	3 and 4	5		1 and 2	3 and 4	5
9.5 mm Dolomite	49.0	33.0	33.0	33.0	46.5	43.5	44.0	44.0
4.75 mm Dolomite	10.0	31.0	27.0	25.0	8.0	18.0	15.0	14.0
2.36 mm Dolomite Sand	22.0	18.5	21.5	21.5	27.0	20.0	22.5	22.5
RAP	14.5	13.0	14.0	16.0	14.1	14.1	14.1	15.1
RAS	3.0	3.0	3.0	3.0	2.9	2.9	2.9	2.9
Baghouse	1.5	1.5	1.5	1.5	1.5	1.5	1.5	1.5
Blend Bulk Specific Gravity	2.593	2.582	2.584	2.586	2.594	2.589	2.590	2.591

Table 5.5. Mixture aggregate gradations.

Sieve Size (mm)	Specification	Control Mixture		Test Mixture	
		Percent Passing (%)		Percent Passing (%)	
		Mixture Design	Lot Average	Mixture Design	Lot Average
12.5	100.0	100.0	100.0	100.0	100.0
9.5	90.0-100.0	94.1	94.9	94.4	93.3
4.75	<90.0	59.3	64.3	63.9	60.2
2.36	32.0-67.0	34.4	33.2	38.7	34.6
1.18		21.7	20.6	24.1	21.3
0.600		13.3	13.2	14.4	13.6
0.300		8.1	8.5	8.6	8.7
0.150		6.1	6.2	6.5	6.3
0.075	2.0-10.0	4.9	4.8	5.3	4.9

5.2.5 Asphalt mixture production and transportation

The asphalt mixtures were produced in a drum mix facility located at the intersection of New Paris Pike and Porterfield Road, approximately three miles from the paving location (Figure 5.3). Before beginning production, the asphalt plant was calibrated to properly proportion, blend and heat

aggregates and asphalt to produce high-quality mixtures. The mixing temperature for both the control and test mixtures was 157 ±15°C.

Figure 5.3. Hot-mix asphalt plant used to produce the control and test mixtures.

The plant production rate was approximately 210 tons/h for each mixture; both mixtures were uniform and workable. No substantial problems were observed during production and transport. Tri-axle end dumps trucks were used to transport the mixtures from the plant to the construction site with haul distances ranging between 2.4 and 4.0 miles and haul times between 10 and 25 minutes, depending on which end of the project was being paved. The trucks' loading, weighing, ticketing, and sampling were uninterrupted, with no delays in delivering mixture to the job site. Each loaded truck carried roughly 20 tons of asphalt mixture. As shown in Figure 5.4, the trucks were tarped to prevent excessive cooling and crust formation on the asphalt mixture surface.

Figure 5.4. Haul truck at the mixing facility.

5.2.6 Asphalt mixture placement and compaction

Figure 5.5 shows the asphalt mixture placement. A joint adhesive was placed between adjacent mats to provide a waterproof seal at the longitudinal joint, where required. Before the overlay placement, an emulsified asphalt tack coat was applied as per INDOT specifications to ensure a bond between the existing milled pavement surface and the new asphalt mixture. The haul trucks delivered each mixture to a materials transfer vehicle that kept it warm and re-mixed it slightly before delivering it to the paving machine. The mixture temperature from the trucks was approximately 143 ±15°C.

Figure 5.5. Asphalt mixture placement.

Mixture compaction for both the control and test mixtures was accomplished with three tandem vibratory rollers, as shown in Figure 5.6. Immediately behind the paver, two breakdown rollers ran in echelon to cover the full lane-width, typically 12 ±2 ft. The breakdown rollers had an operating weight of 11898 kg and a compaction width of 2000 mm, and the overlap between rollers was within 50 to 75 mm. Each breakdown roller applied five vibratory and two static passes, a pass being defined as one movement away from or towards the paver. The finish roller (10804 kg) followed the breakdown rollers, carefully working the longitudinal joint and mat width; the finish roller applied two static coverages. A coverage is defined as the compaction of one full lane-width by one roller. All the compaction was performed according to INDOT specifications (INDOT, 2013b). The compaction temperature for both the control and test mixtures was approximately 127 ±15°C. Table 5.6 summarizes the compaction.

Figure 5.6. Mixture compaction.

Table 5.6. Compaction operating characteristics.

	Breakdown	Finish
Number of Rollers	2	1
Vibratory Passes	5	0
Static Passes	2	5
Operating Weight (kg)	11898	10804
Drum Width (mm)	2000	1700
Static Linear Load (kg/mm)	3.0	3.2

5.2.7 Mixture sampling

Plate and core samples were randomly obtained from the pavement mats such that all of the mat had an equal chance of being sampled, so there was no sampling bias. Plate samples are obtained by placing a metal plate on the milled surface, allowing the paver to place asphalt mixture over the milled surface, including covering the plate and then removing the plate before compaction, as shown in Figure 5.7. A total of six plate samples were obtained from each sublot for laboratory quality testing. The contractor's representative who obtained the sample and the INDOT representative who witnessed the sample being taken properly identified the samples for each plate sample. Plate samples were used to measure the laboratory V_a at N_{des}, P_b, and VMA. For further data analysis, the contractor and INDOT each provided one P_b, and two V_a at N_{des} and VMA measurements per sublot.

Figure 5.7. Asphalt mixture plate sampling.

Figure 5.8 shows photographs taken during core extraction; the contractor, under the supervision of INDOT personnel, core sampled the same day as paving. One hundred fifty-mm diameter core samples were extracted and used to determine in-place densities. Two different locations in each sublot were randomly selected as locations to extract two core samples. For each sampling location, one core sample was evaluated by the contractor and the other by INDOT. A total of twenty core samples were examined for each mixture. The samples were carefully removed from the pavement to ensure no core sample damage.

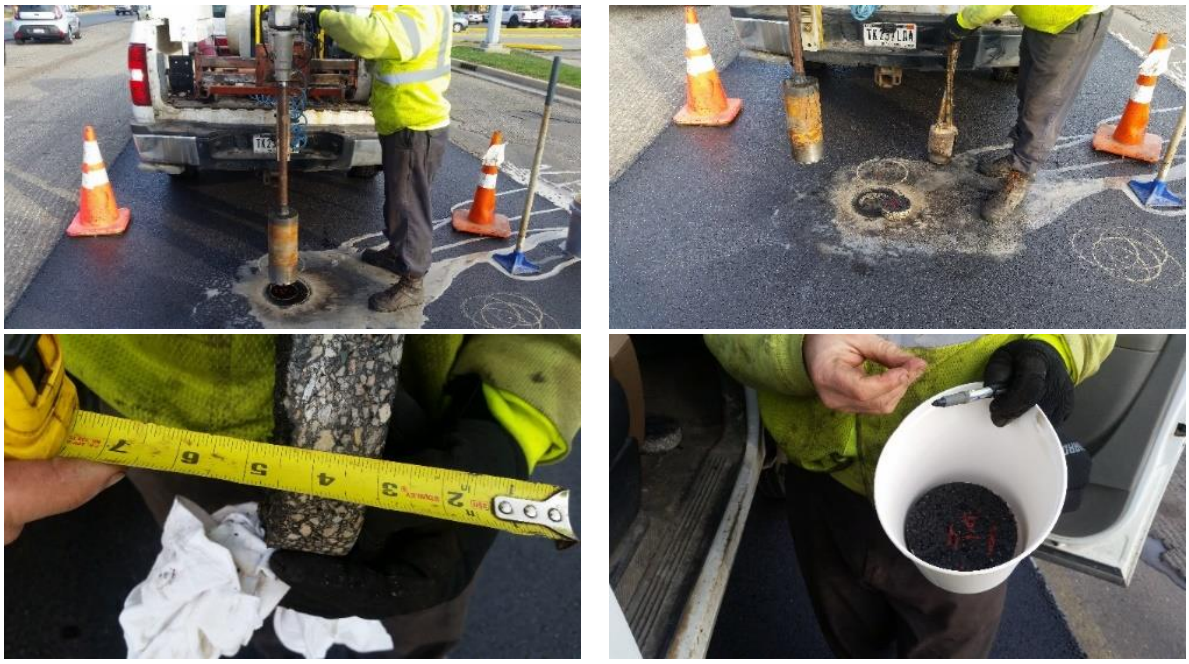

Figure 5.8. Core sample extraction.

5.3 Data Analysis

QC data from the contractor and QA acceptance data from INDOT were analyzed to evaluate if each mixture had achieved the volumetric targets. Figure 5.9 summarizes the in-place density data obtained from the core samples. Preliminary statistical analysis involved an unrelated t-test between QC and QA data in determining whether there was a statistically significant difference between the contractor and INDOT sample means for in-place density, V_a at N_{des}, P_b, and VMA. No mean differences were observed for any of the four properties. Therefore, the QC and QA data were combined to establish comparisons between the control and test mixtures. Descriptive statistics (i.e. sample mean, standard deviation) were generated for the combined QC and QA datasets.

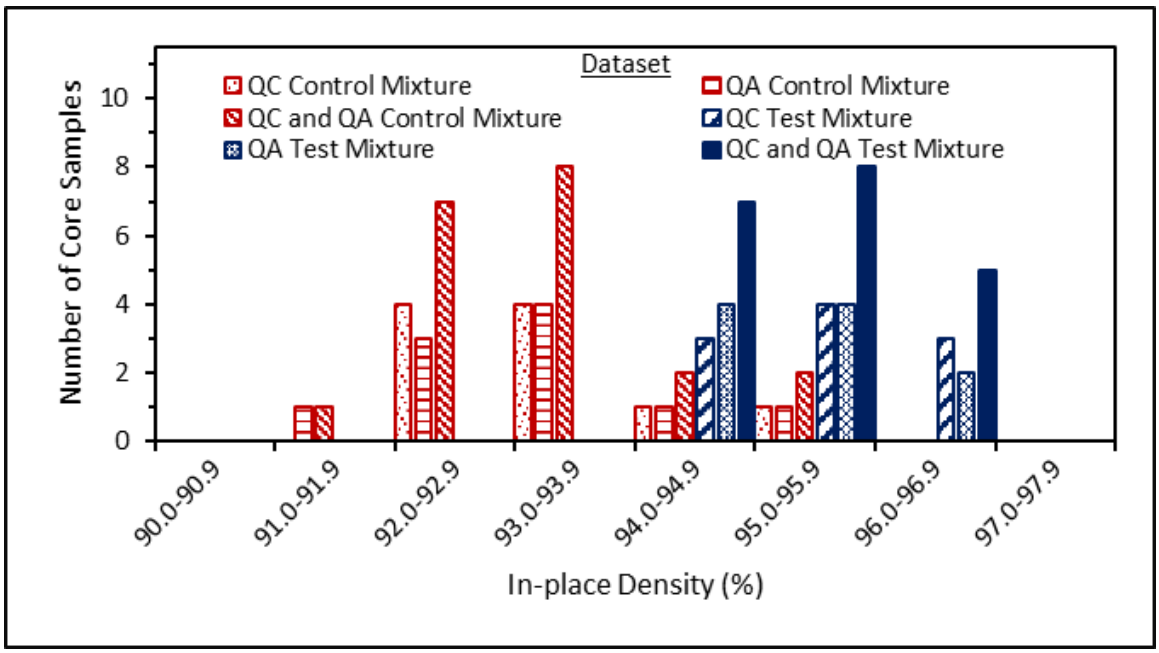

Figure 5.9. In-place density data.

To determine the effectiveness of each mixture in meeting the targeted volumetric properties, which is also referred to in this chapter as construction performance, one-sample t-statistics were computed using Equation 5.1. The higher the absolute value of the t-statistic, the more significant the difference between the targeted values and the as-constructed asphalt mixture volumetric properties. Based on the t-statistics, the probability of the control and test mixture volumetric properties being off-target (≠ TRG) was estimated (P(Volumetric Property ≠ TRG)). Additionally, the statistical significance of the differences between sample means and targets was analyzed using two-tailed t-tests. Significance levels were set at the one percent level.

$$t_{(x)} = \left| \frac{\bar{x} - \mu}{s/\sqrt{n}} \right| \qquad \text{(Eq. 5.1)}$$

where:

$t_{(x)}$ = t-statistic of volumetric property,

$\bar{x}$ = sample mean of volumetric property,

μ = target of volumetric property,

s = sample standard deviation, and

n = sample size.

Since t-tests are dependent upon the sample size (LaVassar et al., 2009), an Absolute Percentage Error (APE) was estimated to corroborate the probability results. An APE estimation is a helpful tool for determining the accuracy of an experimental procedure achieving a theoretical value (Tofallis, 2015). A percentage close to zero implies a slight difference between the experimental and targeted values. The APE for each volumetric property is determined using Equation 5.2.

$$APE_{(x)} = \left|\frac{\bar{x} - \mu}{\mu}\right| \times 100\% \quad \text{(Eq. 5.2)}$$

where:

$APE_{(x)}$= absolute percentage error of volumetric property,

$\bar{x}$ = sample mean of volumetric property, and

μ = target of volumetric property.

INDOT's construction acceptance criterion for in-place density is a percent-within-limits, which had a specification with a lower threshold limit of 91% of G_{mm} (before 2019). This lower limit was based on historical data and experience with prior construction methodologies (INDOT, 2013b; Tran et al., 2016). However, Figure 5.9 shows that no in-place density value below 91% was obtained for both mixtures. A percent-within-limits specification is an ideal quality measure to prevent the contractor from increasing the production variability, and therefore promotes the consistency of field-produced materials (Akkinepally and Attoh-Okine, 2006). However, a percent-within-limits specification is not entirely adequate to capture the effectiveness of a mixture in meeting its optimal volumetric properties in the field.

As the industry moves toward using laboratory performance tests for mixture design and construction acceptance (National Center for Asphalt Technology [NCAT], 2017), achieving optimal volumetric properties in the field is expected to become even more critical. Therefore, two new asphalt pavement construction metrics were used to compare the control and test mixtures for this study. The first is the "Probability of Volumetric Discrepancy (PVD)," and is arithmetically defined in Equation 5.3. The probabilities of the volumetric properties being off-target are considered statistically independent events, and thus the likelihood of all four volumetric properties being off-target is estimated using a probability multiplication rule (Ang and Tang, 2007). The PVD metric is analogous to the probability of failure of a parallel system, which fails if all its components fail (Hohenbichler and Rackwitz, 1982). In this study, the likelihood of each

asphalt mixture component failing is denoted by the probability of each volumetric property being off-target. Therefore, the overall asphalt mixture failure in achieving optimal volumetric properties is calculated using PVD. The higher the PVD, the higher the likelihood of a difference between the volumetric properties of the mixture design and the as-constructed asphalt pavement mat.

$$PVD = P(Density \neq TRG) \times P(V_a \; at \; N_{des} \neq TRG) \times P(P_b \neq TRG) \times P(VMA \neq TRG) \times 100\% \quad \text{(Eq. 5.3)}$$

where:

PVD = probability of volumetric discrepancy (%),

$P(Density \neq TRG)$ = probability of in-place density being off-target,

$P(V_a \; at \; N_{des} \neq TRG)$ = probability of air voids at N_{des} being off-target,

$P(P_b \neq TRG)$ = probability of asphalt binder content being off-target, and

$P(VMA \neq TRG)$ = probability of voids in the mineral aggregate being off-target.

The second metric is the "Mean Absolute Percentage Error (MAPE)" and one of the most widely used measures of accuracy in business organizations (Tofallis, 2015). In assessing the accuracy of multiple components, calculating the arithmetic mean of the APE estimates aggregates the results, as shown in Equation 5.4. Low MAPE are good indicators that an asphalt mixture has achieved targeted values during construction. Although these new parameters seem arbitrary at first glance, data analyses indicate the metrics are highly correlated to an asphalt mixture being constructed as designed. PVD and MAPE could serve to identify discrepancies from volumetric targets within asphalt mixtures and establish comparisons across projects and new construction techniques and paving resources, including PCM modified asphalt pavement materials.

$$MAPE = \frac{APE_{(Density)} + APE_{(V_a \; at \; N_{des})} + APE_{(P_b)} + APE_{(VMA)}}{4} \quad \text{(Eq. 5.4)}$$

where:

$MAPE$ = mean absolute percentage error,

$APE_{(Density)}$ = absolute percentage error in-place density,

$APE_{(V_a \; at \; N_{des})}$ = absolute percentage error air voids at N_{des} content,

$APE_{(P_b)}$ = absolute percentage error asphalt binder content, and

$APE_{(VMA)}$ = absolute percentage error voids in the mineral aggregate.

5.4 Results and Discussion

5.4.1 In-place density

The data in Table 5.7 indicate that asphalt mixtures designed in the laboratory to have optimum asphalt binder content at 5% V_a can be compacted to 95% G_{mm} in the field. As can be seen in the table, the in-place density sample means for the control and test mixtures were 93.3 and 95.3%, respectively. The unrelated one-tailed t-test between the control and test mixtures data was performed to determine if the 2% in-place density increase was statistically significant. At a one percent significance level, the analysis indicated that the sample mean difference between the control and test mixtures was different. Therefore, this field project result demonstrates that comprehensive asphalt mixture design modifications can be a genuine alternative for providing increased in-place asphalt mat densities without augmenting the amount of compaction energy used to achieve density. According to past studies, a 2% increase in in-place density could extend the service life of an asphalt pavement by approximately 20% (Tran et al., 2016).

Table 5.7. Comparison of in-place density experimental results.

Parameter	Control Mixture	Test Mixture
In-place density target (%)	94.0	95.0
Sample mean (%)	93.3	95.3
Sample size (n)	20	20
Standard deviation	1.0	0.8
$t - statistic_{(Density)}$	3.4	1.9
$P(Density \neq TRG)$ (%)	99.7	92.6
Difference between sample mean and target	Significant	Not Significant
Sample mean difference between control and test mixture	Significant	
$APE_{(Density)}$	0.8	0.4

The difference between the sample mean and the test mixture's target of 95% in-place density is statistically insignificant. Thus, there is not sufficient evidence to suggest the test mixture in-place density sample mean and construction target are dissimilar. Conversely, the difference between the sample mean and the target of 94% in-place density for the control mixture is statistically significant, indicating the two values are different. The APE values confirm that the experimental and in-place density difference is higher for the control mixture than for the test mixture.

5.4.2 Laboratory air voids content at N_{des}

Table 5.8 shows the comparisons of laboratory air voids for both the control and test asphalt mixtures. The test mixture exhibited no statistically significant difference between the sample mean and the target of 5% V_a at N_{des}. Additionally, the test mixture compacted at 50 SGC gyrations in the laboratory better correlated to field compaction than the control mixture compacted at 100 SGC gyrations, as shown in Figure 5.10. The test mixture relationship between V_a at N_{des} and in-place density compares favorably. In contrast, the control mixture shows significant deviations from the 4% V_a at N_{des} target. Hence, lowering the compaction effort in the laboratory appears to be a reliable technique for delivering lower in-place air voids. As explained later in the binder section, the observed departures from the 5% air voids target for the test mixture are mainly due to inconsistent P_b in the test mixture.

Table 5.8. Comparison of air voids results.

Parameter	Control Mixture	Test Mixture
Air voids content at N_{des} target (%)	4.0	5.0
Sample mean (%)	4.7	5.6
Sample size (n)	20	20
Standard deviation	1.1	1.0
$t - statistic_{(V_a \, at \, N_{des})}$	3.0	2.7
$P(V_a \, at \, N_{des} \neq TRG)$ (%)	99.2	98.5
Difference between sample mean and target	Significant	Not Significant
$APE_{(V_a \, at \, N_{des})}$	17.7	12.2

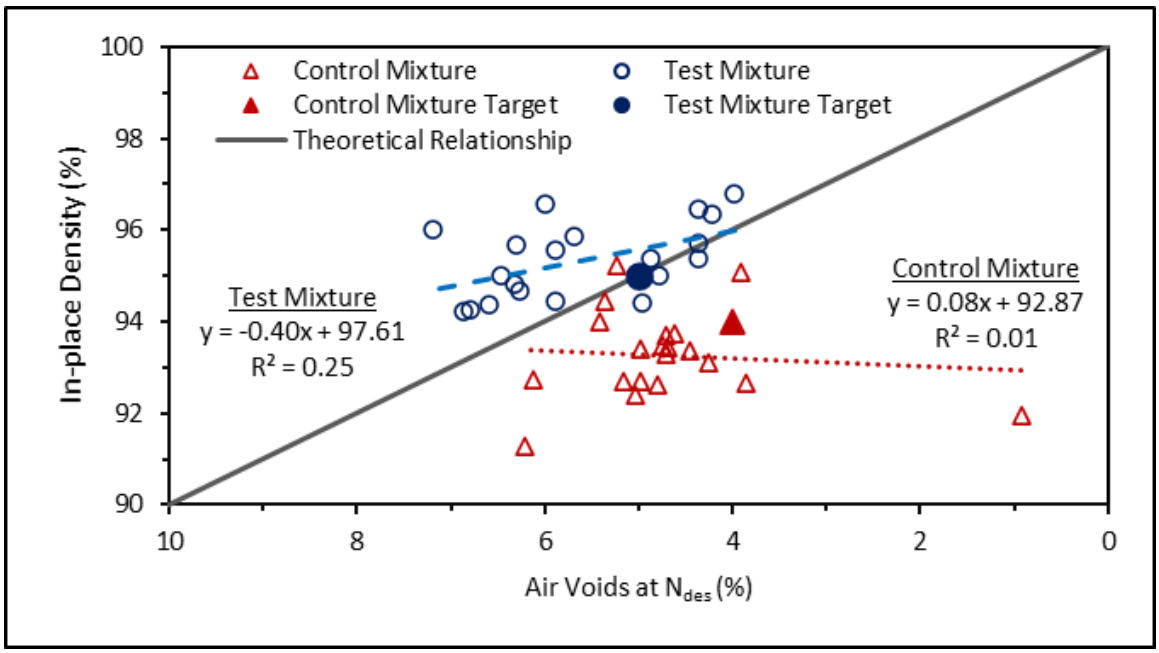

Figure 5.10. In-place density as a function of air voids content at N_{des}.

5.4.3 Asphalt binder content

The P_b results obtained from the plate samples are summarized in Table 5.9. Although the test mixture difference between sample mean and binder content target was found to be statistically insignificant, Figure 5.11 shows the asphalt binder was added in a less consistent fashion to the test mixture than it was to the control mixture. The APE analysis corroborates that the departure from the P_b target was higher for the test mixture than for the control mixture. RAP and RAS materials were used in both the control and test mixtures, so the inconsistent asphalt binder content in the test mixture is likely, not due to the addition of RAP and RAS.

Table 5.9. Comparison of asphalt binder content results.

Parameter	Control Mixture	Test Mixture
Asphalt binder content target (%)	6.7	7.1
Sample mean (%)	6.5	6.7
Sample size (n)	10	10
Standard deviation	0.1	0.4
$t - statistic_{(P_b)}$	6.6	3.2
$P(P_b \neq TRG)$ (%)	100.0	98.9
Difference between sample mean and target	Significant	Not Significant
$APE_{(P_b)}$	3.2	5.8

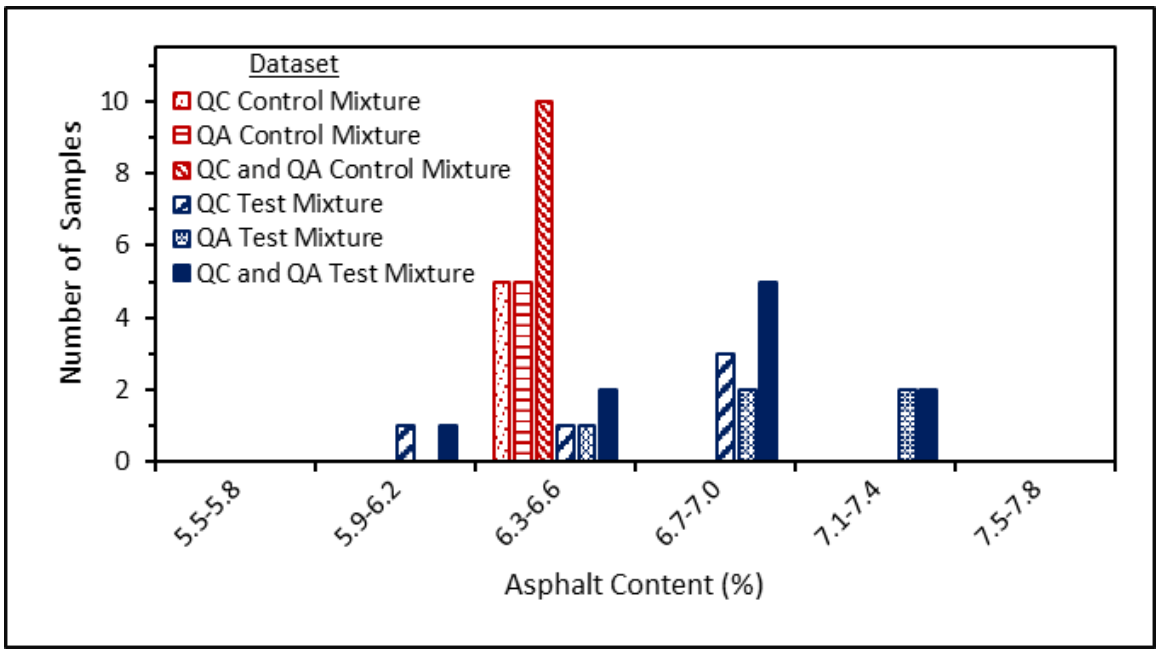

Figure 5.11. Asphalt binder content data.

Table 5.9 shows that the average P_b for both mixtures was slightly reduced during mixture production at the plant. P_b adjustments at the plant have long been used to help meet construction acceptance specifications based on historical data and experience. Hence, the P_b is slightly increased or decreased within specification limits, whenever required, to achieve asphalt mixture volumetric properties and maximize construction performance incentives (Buddhavarapu et al., 2016). In contrast to traditionally designed asphalt mixtures, a Superpave 5 mixture is intended to pack better. The data would seem to indicate that such mixtures are less sensitive to P_b fluctuations. As can be seen in Figure 5.12, for the test mixture, no in-place densities below 94% were observed due to the mixture's compaction attributes. However, though the test mixture may be less sensitive to binder content fluctuations than the control mixture, Figure 5.12 also shows that air voids are correlated to the binder content.

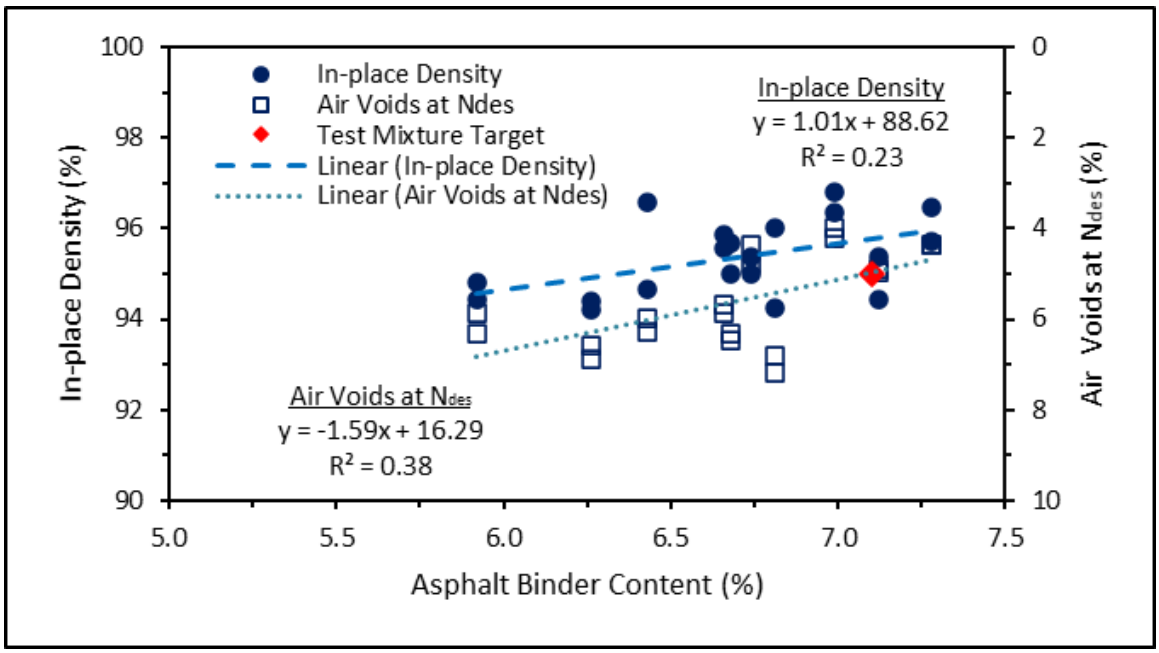

Figure 5.12. Test mixture in-place density and laboratory air voids as a function of asphalt binder content.

To deliver pavements with optimal in-place densities and laboratory air voids, optimum amounts of binder should be incorporated in the mixture. Asphalt mixture designs are a starting point for selecting an optimum P_b, but it is typical to make adjustments during mixture production. However, P_b adjustments should only be made to correct significant differences between laboratory-mixed and field-produced materials (i.e., aggregate moisture content and stockpile variability). Care should be taken when making such adjustments as they can significantly impact the packing and performance of asphalt mixtures (Aschenbrener et al., 2017).

5.4.4 Voids in the mineral aggregate

As shown in Table 5.10, both asphalt mixtures show insignificant differences between sample means and target VMA values. The mixture design VMA targets for the control mixture and test mixture were 15.6 and 16.7%, respectively. However, Figure 5.13 shows that some VMA values fall below the control mixture's Superpave design minimum VMA requirement of 15 percent. Similarly, the test mixture data have values below the required minimum of 16 percent (raising the design air voids by one percent requires increasing the VMA requirement by one percent). However, when the test mixture P_b is close to the target of 7.1%, the VMA values required are

typically met. Additionally, the use of the modified mixture design reduces by approximately 20 percentage points the probability of VMA measurements being off-target, in comparison to the conventional Superpave volumetric mixture design (63.6% rather than 83.4%).

Table 5.10. Comparison of voids in the mineral aggregate results.

Parameter	Control Mixture	Test Mixture
Voids in the mineral aggregate target (%)	15.6	16.7
Sample mean (%)	15.3	16.6
Sample size (n)	20	20
Standard deviation	1.0	0.5
$t - statistic_{(VMA)}$	1.4	0.9
$P(VMA \neq TRG)$ (%)	83.4	63.6
Difference between sample mean and target	Not significant	Not Significant
$APE_{(VMA)}$	2.1	0.6

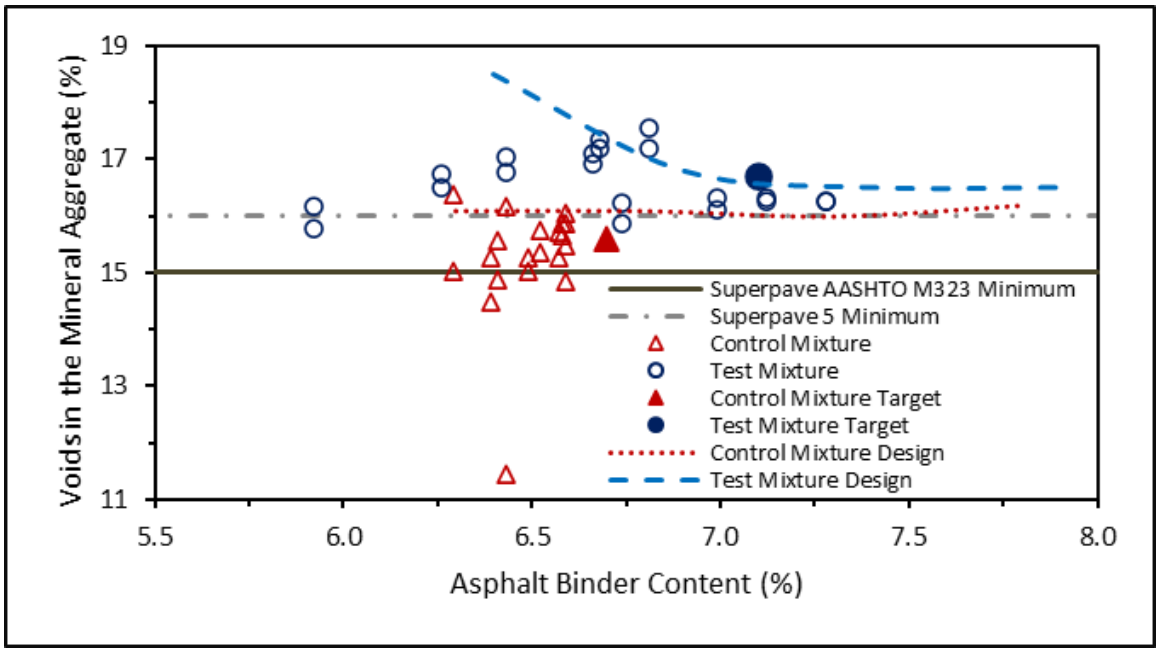

Figure 5.13. Relationships between asphalt binder content and voids in the mineral aggregate.

It should be highlighted that improvements to in-place density cannot overcome performance issues due to asphalt mixtures constructed with unacceptable volumetric properties (Aschenbrener et al., 2017). In particular, a minimum VMA is used in the Superpave mixture design specifications to eradicate potentially poor-performing mixtures. The VMA parameter is regarded as one of the most important asphalt mixture volumetric properties, if not the most

(Prowell et al., 2005). As shown in Figure 5.13, the modified mixture design enhances the design relationship between VMA and P_b by using the Bailey method to provide an optimal VMA for good durability. This improvement allows identifying an adequate amount of asphalt binder to ensure the asphalt mixture has proper stability and a minimum volume of air voids (Vavrik et al., 2002). As previously shown in Figure 5.10, no V_a at N_{des} below 4% was observed for the test mixture, despite the higher amount of asphalt binder added to the mixture. However, the control mixture exhibited V_a at N_{des} as low as 1% (VMA = 11.5%). Lowering the V_a at N_{des} and VMA to increase pavement densities may significantly compromise asphalt mixture rutting performance.

5.4.5 New statistics for asphalt mixture construction analysis

Considering that increased in-place densities cannot overcome performance issues due to asphalt mixtures constructed with unacceptable volumetric properties, the probability of achieving increased densities without sacrificing optimal volumetric properties should be analyzed. Probabilistic approaches are considered appropriate when a deterministic quantification is not possible because of a prohibitive reason for sampling a total population and measurement errors (Popescu et al., 2005).

Figure 5.14 compares the construction performance of the mixtures in achieving each volumetric target using the off-target probabilities and percentage errors. For both mixtures, a lower discrepancy from target was observed for VMA than for P_b. The variability associated with the aggregate properties, such as bulk specific gravity, is typically considered the primary source of variation and error related to asphalt mixtures (NCAT, 2017). However, this field study demonstrates that in practice, more considerable variations and errors from the targets can be obtained for P_b than for VMA. If significant asphalt plant variations occur, it becomes difficult if not impossible to achieve the targeted in-place density and laboratory air voids values.

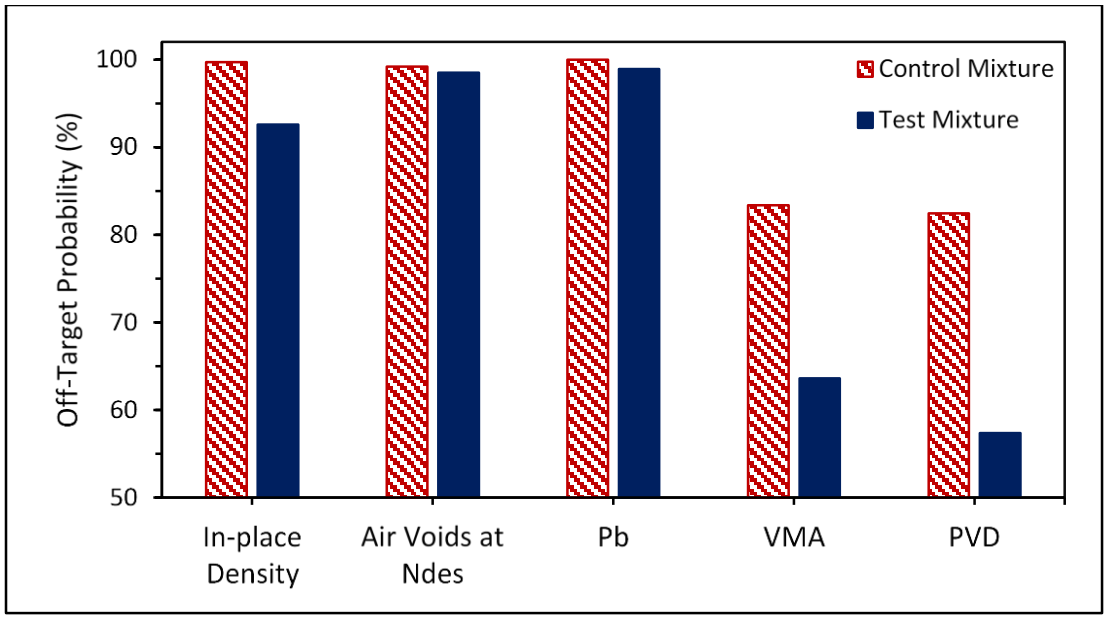

(a)

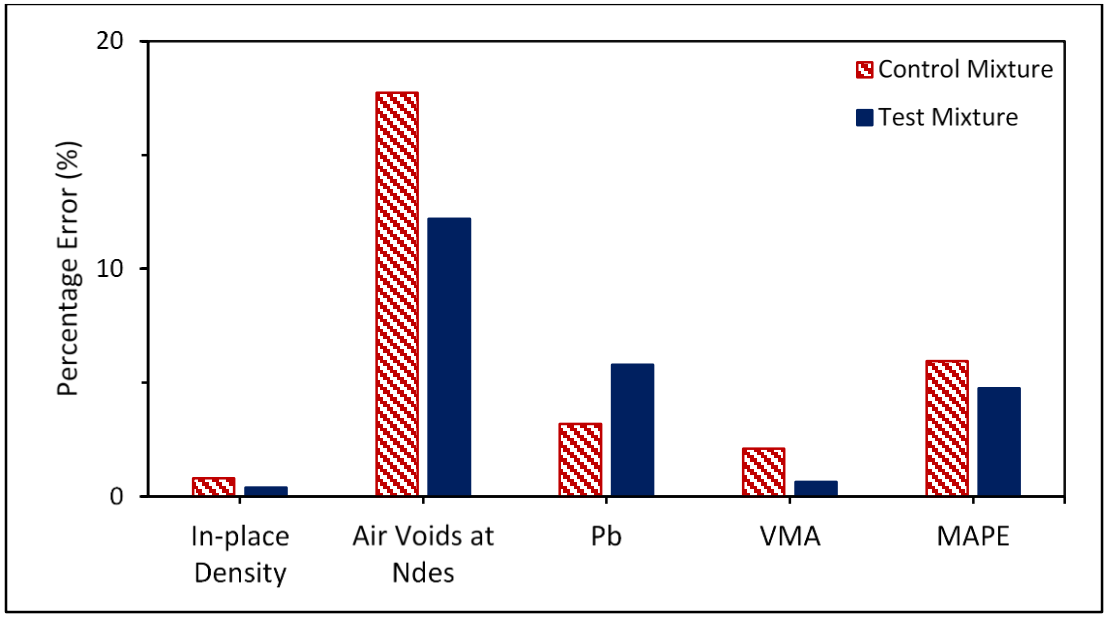

(b)

Figure 5.14. Control and test mixtures: (a) Off-target probabilities and probabilities of volumetric discrepancy, and (b) Absolute percentage errors and mean absolute percentage errors.

Figure 5.14 also provides the overall construction performance of the mixtures in terms of PVD and MAPE. As previously explained, lower PVD and MAPE values indicate a lower likelihood of all four volumetric properties being off-target. Although the asphalt binder was added to the test mixture less consistently than the control mixture, the test mixture outperforms the

control mixture in terms of PVD and MAPE. In general, these results indicate that one is more likely to construct an asphalt pavement as desired using the Superpave 5 modified mixture design. By choosing optimum P_b at 5% V_a and using lower laboratory compaction levels, the error between a semi-static pressure laboratory compaction method (i.e., SGC) and dynamic and static field compaction (rollers) is decreased. The experimental results suggest that the test mixture designed in the laboratory to have 5% V_a was compacted to 95% G_{mm} in the field. As a result, this modified mixture design noticeably reduces the variance and error associated with transferring a mixture design from the laboratory to field production.

PVD can be defined as a simplistic probabilistic approach but yet effective method to estimate the probability of randomly choosing any spot on an asphalt pavement mat and determining that all four volumetric properties are off-target. The sources of variation for a specific volumetric property to be off-target can significantly vary from asphalt mixture design to QC or QA testing procedure. Other sources of error are inconsistencies during plant production, problems with construction equipment and processes, plate and core sampling, etc. However, the mixture design is the first step in reducing the most defective area in an asphalt pavement mat in which all four volumetric properties are may be off-target. As shown in Figure 5.14a, using a modified mixture design, the PVD was reduced by approximately 25 percentage points compared to the control mixture. The MAPE validates this probability result; a reduction in the total error associated with field construction is observed for the test mixture in Figure 5.14b. Hence, using a modified mixture design increases pavement densities and enhances correlation between laboratory and field volumetric properties.

An inconsistent P_b in this field project set hindered the potential benefits of using a modified mixture design. However, data analysis at the sublot level was performed for the test mixture to exclude or at least control the variation somewhat. Figure 5.15 compares the departures from volumetric targets within the test mixture. It should be noted that PVD and MAPE decreased as the demonstration project progressed from sublots 1 to 5. This is mainly attributed to the contractor's gain in experience and knowledge in implementing the Superpave 5 asphalt mixture. When new methods are put into practice, an initial margin of variance and error should be expected to satisfactorily introduce new pavement construction procedures. It should also be noted that at a sublot level a consistent and inherent VMA variability and error was observed, despite the P_b

adjustments. However, as previously shown, no significant departure from the VMA target was observed when the test mixture asphalt binder contents were close to the target.

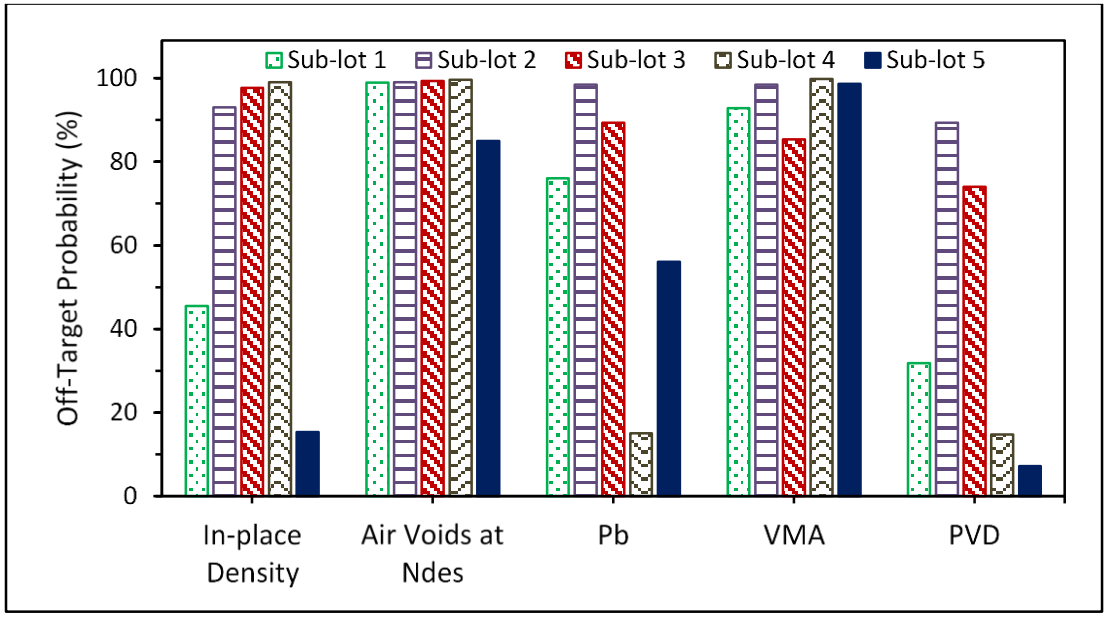

(a)

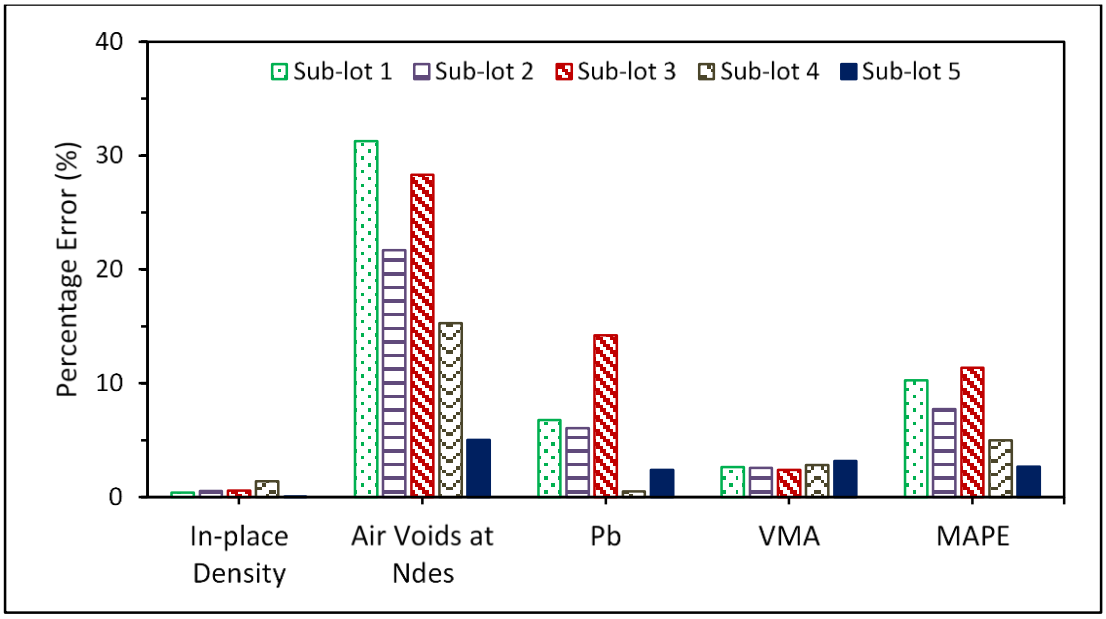

(b)

Figure 5.15. Test mixture sublot level data analysis: (a) Off-target probabilities and probabilities of volumetric discrepancy, and (b) Absolute percentage errors and mean absolute percentage errors.

Data analysis for the test mixture revealed that sublot 5 showed the lowest PVD and MAPE values. As can be seen in Figure 5.15, the discrepancies between field and theoretical volumetric targets are insignificant for this sublot. Sublot 5 reported the closest to target P_b and G_{mm} values. Therefore, it can be presumed that for sublot 5 the P_{be} (5.2%) was held constant in the field. For sublot 5, the probability of all four volumetric properties being off-target (PVD) was reduced to 7%, and the likelihood of in-place density being off-target was decreased to 15 percent. These experimental results indicate that to effectively construct asphalt mixtures, it is essential to achieve volumetric targets in a consistent fashion. This outcome can be accomplished by using mixture design methods that positively correlate to field construction. Designing asphalt mixtures with optimum P_b at 5% V_a and lowering the laboratory compaction effort appear to be sound mixture design modifications to optimize the relationship between laboratory and field volumetric targets and construct asphalt mixtures as designed.

5.5 Summary and Conclusions

The primary objective of the demonstration project presented herein was to determine if a modified asphalt mixture design method could be used to increase asphalt pavement mat densities in an uncontrolled experiment. The findings from this field study showed that designing asphalt mixtures by choosing optimum asphalt content at 5% air voids, rather than 4%, and lowering the laboratory compaction effort can indeed lead to increased pavement densities. The asphalt mixture prepared using the modified mixture design method showed an enhanced correlation between laboratory and field volumetric properties.

This work also provides a new framework to identify variance and error from volumetric targets and thus quantify the benefits of using a modified asphalt mixture design, or any other new method that improves asphalt pavement construction. The new probabilistic and analytical metrics could serve as a decision-making tool to implement technologies that help ensure asphalt mixtures are placed in the field with optimal volumetric properties. As a result, increased pavement densities can be more easily accomplished and replicated under various field conditions. Future work should explore the use of sophisticated probabilistic approaches to quantify the fluctuations of asphalt pavements more precisely around their targeted volumetric properties.

This research shows that implementing new methodologies that reduce the margin of error between laboratory and field mixture volumetric properties is still required. From a construction

and service life performance perspective, volumetric properties are the fundamentals of flexible pavements. If asphalt mixtures are not adequately designed to meet specific volumetric requirements, any effort to achieve optimal in-place densities in an effective manner and replicate similar pavement characteristics will be futile. In contrast, this study has shown, using rigorous metrics, that asphalt mixtures designed in the laboratory at 5% air voids can be compacted to an optimal 95% in-place density in the field. Thus, asphalt pavements could be constructed as design, and their service life performance can be optimized as desired. Finally, this study serves also as a blueprint to implement innovative modified asphalt pavements, such as environmentally tuned asphalt pavements with PCMs.

6. ESTIMATING ASPHALT MIXTURE VOLUMETRIC PROPERTIES USING SEEMINGLY UNRELATED REGRESSION EQUATIONS APPROACHES[d]

[d]This Chapter is reproduced from the paper "Estimating Asphalt Mixture Volumetric Properties Using Seemingly Unrelated Regression Equations Approaches" published in Construction and Building Materials on 2019 (DOI: 10.1016/j.conbuildmat.2019.07.266).

6.1 Introduction

Although the design of asphalt mixtures is advancing toward a performance-based methodology, the volumetric properties are still essential characteristics of asphalt mixtures. As demonstrated in previous chapters of this dissertation, volumetric properties play a vital role in the permeability of PCM modified slabs, the thermal response of μPCM Mixtures, and ultimate pavement performance. Furthermore, as the asphalt pavement industry seeks to manufacture multifunctional products with low variability, advances in modeling approaches that help optimize asphalt materials are lagging behind. Typically, well-controlled paving projects provide asphalt mixture volumetric properties with low variability, while poorly controlled projects result in higher variability in asphalt mixture volumetric properties. On many occasions, the management of all the factors influencing asphalt mixture production and construction is inadequate. The work described in this chapter demonstrates that Seemingly Unrelated Regression Equations (SURE) approaches can be used to estimate asphalt mixture volumetric properties using mixture design, material properties, and testing inputs. SURE approaches can help evaluate asphalt mixture production and placement by accounting for the deficiencies and limitations in QA data. Moreover, SURE approaches analyze asphalt mixtures in a concise, yet robust, manner. The findings of this chapter could be extended to simultaneously predict the volumetric, mechanical, and thermal properties of PCM modified asphalt materials and, therefore, help tune paving products.

6.1.1 Scope

The work described in this chapter attempts to contribute to a better understanding of how to achieve desirable asphalt mixture volumetric properties in order to improve asphalt mixture performance, and thereby asphalt pavement performance. The study's primary objective is to

demonstrate that SURE approaches can estimate asphalt mixture volumetric properties and analyze asphalt pavement QA data. Using QA data obtained from a demonstration project, this paper compares the gain in efficiency of the model parameter estimates under three modeling approaches, Ordinary Least Squares (OLS) single equation model, SURE model with serially independent disturbances, and SURE model with first-order serially correlated disturbances. Then, the effects of mixture design, laboratory variability, asphalt binder content, and aggregate proportions and gradation on asphalt mixture volumetric properties are analyzed.

SURE approaches are typically used to explain economic, financial, sociological, and transportation-related phenomena (Wang, 2010; Gkritza et al., 2011). Based on the literature, SURE approaches have been applied to study the performance of asphalt pavements (Prozzi and Hong, 2008; Anastasopoulos et al., 2012). Prozzi and Hong (2008) introduced a SURE approach to model multiple pavement-performance indicators, such as roughness and rutting. Structural components, material properties, design approaches, environmental factors, and maintenance conditions were used as explanatory variables. Anastasopoulus et al. (2012) developed a SURE approach to study the effects of traffic loading, weather conditions, the soil type beneath a pavement, condition of the drainage system, and the characteristics of rehabilitation treatments on the international roughness index, rut depth, pavement condition rating, and falling weight deflectometer-measured pavement deflection of recently rehabilitated asphalt pavement roads. Although previous research supports the use of SURE approaches to explain asphalt pavement-related phenomena, to the author's knowledge, SURE approaches have not been implemented to evaluate the construction phase of asphalt paving projects. Hence, this paper seeks to assess the applicability of SURE approaches to estimate asphalt mixture volumetric properties.

6.2 Methodology

6.2.1 Data description

The QA data used for this study was obtained from an asphalt pavement demonstration project carried out on US 40 near Richmond, Indiana, as part of the FHWA increased in-place density initiative (Aschenbrener et al., 2017). The project's QA data gathering process, asphalt mixture design, and field construction aspects have been previously reported by Montoya et al. (2018). The project's scope was to corroborate the potential benefits of using a modified mixture design method

to construct asphalt pavements with increased densities. In reviewing data from the project, Montoya et al. (2018) concluded the need for the use of robust modeling approaches to more precisely quantify asphalt mixture variations around their targeted volumetric properties.

Accordingly, this research effort involves the estimation of asphalt mixture volumetric properties using SURE approaches. SURE models are a generalization of a linear regression model that consists of several regression equations, each having its own dependent variable and potentially different sets of exogenous explanatory variables (Washington et al., 2011). As shown in Table 6.1, the dependent variables for this study are in-place density, V_a, and VMA. In-place density is used to determine the effectiveness of field compaction. Thus, it is a vital asphalt mixture volumetric property because it is a good indicator of future pavement performance (Aschenbrener et al., 2017). In-place density is typically expressed as a percentage of the G_{mm}, which is the combined specific gravity of the asphalt binder and aggregate excluding air voids (Tran et al., 2016).

Table 6.1. Quality assurance data descriptive statistics.

Description	Mean (Standard deviation)	Minimum/ Maximum	Number of observations
Dependent variables:			
In-place density (%)	94.31 (1.37)	91.28 / 96.80	40
Laboratory air voids content, V_a (%)	5.16 (1.13)	0.93 / 7.20	40
Voids in the mineral aggregate, VMA (%)	15.71 (1.09)	11.21 / 17.39	40
Independent variables:			
Mixture type (control = 0, and test = 1)	0.5 (0.5)	0.00 / 1.00	40
Data source (Agency= 0, and Contractor = 1)	0.5 (0.5)	0.00 / 1.00	40
Asphalt binder content, P_b (%)	6.59 (0.30)	5.92 / 7.28	40
Aggregate blend specific gravity, G_{sb}	2.587 (0.003)	2.582 / 2.591	40
Aggregate blend proportions			
9.5 mm Stone (%)	38.40 (5.47)	33.00 / 44.00	40
4.75 mm Stone (%)	22.10 (6.52)	14.00 / 31.00	40
2.36 mm Stone Sand (%)	20.90 (1.50)	18.50 / 22.50	40
Reclaimed asphalt pavement, RAP (%)	14.15 (0.85)	13.00 / 16.00	40
Recycled asphalt shingles, RAS (%)	2.95 (0.05)	2.90 / 3.00	40
Aggregate gradation percent passing			
9.5 mm sieve (%)	94.07 (1.58)	92.00 / 96.10	40
4.75 mm sieve (%)	62.22 (3.29)	57.60 / 68.40	40
2.36 mm sieve (%)	33.90 (1.57)	31.30 / 36.00	40
1.18 mm sieve (%)	20.95 (0.88)	19.00 / 22.10	40
0.600 mm sieve (%)	13.37 (0.57)	12.10 / 14.10	40
0.300 mm sieve (%)	8.57 (0.35)	7.70 / 8.90	40
0.150 mm sieve (%)	6.21 (0.27)	5.50 / 6.50	40
0.075 mm sieve (%)	4.84 (0.21)	4.30 / 5.00	40

The V_a refers to the total volume of small pockets of air between the coated aggregate particles throughout a laboratory compacted asphalt mixture, and it is expressed as a percent of the total volume of the sample. The VMA parameter is defined as the volume of intergranular void space between the aggregate particles of a laboratory compacted asphalt mixture that includes the V_a and P_{be}, expressed as a percent of the total sample volume. Asphalt mixture design specifications use the V_a and VMA properties to eliminate poor-performing mixtures (Brown, 2009).

The independent variables included in this study are an indicator variable for mixture type and data source, plus P_b, aggregate blend Bulk Specific Gravity (G_{sb}), and aggregate blend proportions and gradation. Control and test mixtures were used to complete the demonstration project and evaluate the effect of mixture design modifications on the volumetric properties. The control mixture was designed at 4% V_a using the conventional Superpave volumetric mixture design method, AASHTO M 323. In contrast, the test mixture was prepared at 5% V_a using the modified laboratory mixture design proposed by Hekmatfar et al. (2015) or Superpave 5 (Aschenbrener et al., 2017).

The data for this study was gathered from the owner agency and project contractor. The agency provided the data used for acceptance, which is the process whereby all factors used by the agency (i.e., sampling, testing, and inspection) are evaluated to determine the degree of compliance. The contractor provided the quality control, the data used by a contractor to monitor, assess, and adjust its production or placement processes. Considering that QA is the summation of various elements, such as quality control, independent assurance, acceptance, and dispute resolution, the database used in this paper is referred to as QA data, as specified by AASHTO R 10.

The agency and contractor provided 20 measurements for in-place density and laboratory V_a and VMA, and 10 computations for P_b per asphalt mixture type. Additionally, the contractor supplied the aggregate blend proportions used to produce the asphalt mixture at the production plant, including the amounts of RAP and RAS. Based on the aggregate blend proportions, the G_{sb} were calculated. The contractor also gathered samples from the haul trucks at the asphalt plant to control the asphalt mixture gradation during production. The QA data was assembled to generate an entire dataset of 40 observations for further statistical analysis.

6.2.2 Modeling approaches

The effect of the independent variables on the asphalt mixture volumetric properties was estimated using OLS single equation and SURE approaches. Table 6.2 shows the correlation coefficients among volumetric properties for the entire dataset. As expected, the magnitudes of the correlation coefficients imply that in-place density, V_a, and VMA are correlated (or at least somehow interrelated). The interactions between the dependent variables suggest that the asphalt mixture volumetric properties are influenced by similar characteristics and share unobserved factors or missing information (Washington et al., 2011). Therefore, there is a likelihood that similar unobserved factors may be determinants of the variability in the volumetric properties. Variability in asphalt pavement mixtures is largely determined by the proportion of its main constituents: (1) asphalt binder and (2) aggregates. However, asphalt mixture variations also depend on many more factors, such as equipment used for production and construction, sampling and testing, as well as other less controllable factors (i.e., climatic conditions and human operation) (Brown, 2009).

Table 6.2. Correlation coefficients for the volumetric properties.

Volumetric Property	In-place density	V_a	VMA
In-place density	1.00		
V_a	0.21	1.00	
VMA	0.58	0.84	1.00

Accounting for the correlation among the volumetric properties is a primary concern in selecting an appropriate modeling approach. A contemporaneous (or cross-equation) disturbance correlation occurs when a group of dependent variables are correlated (Washington et al., 2011). As a result, treating the model as a collection of separate relationships will be suboptimal when drawing inferences about the model's parameter estimates. SURE models are typically used to account for the contemporaneous correlation among the disturbance terms in each seemingly unrelated regression equation. SURE models introduce additional information over and above that available when the individual equations are considered separately (Srivastava and Giles, 1987; Washington et al., 2011). For such a reason, the SURE approach was deemed to be appropriate for this study.

SURE models generalize OLS single equation models and are specified as a set of *M* seemingly unrelated regression equations, each with p_i independent variables and *T* observations. Equation 6.1 shows how the *i*th equation is specified in SURE models (Zellner, 1962).

$$y_i = X_i \cdot \beta_i + \varepsilon_i \, , i = 1, \dots, M \qquad \text{(Eq. 6.1)}$$

where:

y_i = a $T \times 1$ vector of observed values on the *i*th dependent variable,

X_i = a $T \times p_i$ matrix with rank p_i of observations on p_i independent variables,

β_i = a $p_i \times 1$ vector of unknown regression parameters, and

ε_i = a $T \times 1$ vector of disturbance terms.

It is assumed that $\varepsilon = \varepsilon_1, \varepsilon_2, \dots, \varepsilon_M$ has a multivariate normal density with mean $E(\varepsilon) = 0$ and covariance $E(\varepsilon\varepsilon') = \sum \otimes I_T = V$, where $\sum = \sigma_{ij}$ is a positive symmetric matrix and I_T is a $T \times T$ identity matrix and $\otimes$ is the Kronecker product. The SURE model equation can be written similarly to an OLS single equation model, as shown in Equation 6.2.

$$Y = X\beta + \varepsilon \qquad \text{(Eq. 6.2)}$$

where:

$Y = y_1 \; y_1, y_2, \dots, y_M$,

$\beta = \beta_1, \beta_2, \dots, \beta_M$, and

$X = I_T \otimes X_i$.

Using generalized least squares, a best linear unbiased estimator is obtained (Pindyck and Rubinfeld, 1998; Washington et al., 2011), as presented in Equation 6.3.

$$\hat{\beta} = \left[X' \left(\sum \emptyset I_T\right)^{-1} \cdot X\right]^{-1} \cdot X' \left(\sum \emptyset I_T\right)^{-1} \cdot Y \qquad \text{(Eq. 6.3)}$$

Equation 6.4 shows the First-Order Autoregressive, AR(1), process used in this study to allow for serial correlation. The ρ parameter in Equation 6.4 is defined as the first-order serial correlation coefficient (Srivastava and Giles, 1987; Greene, 2003). Accordingly, Equation 6.1 represents a SURE model with serially independent disturbances, and Equation 6.4 specifies the extension required to develop a SURE model with first-order serially correlated disturbances, from now on referred to as SURE without AR(1) and SURE with AR(1), respectively.

$$\varepsilon_{it} = \rho_i \cdot \varepsilon_{i,t-1} + u_{it}, i = 1, \dots, M; t = 1, \dots, T \quad \text{(Eq. 6.4)}$$

where:

$|\rho_i| < 1$= a constant, and

u_{it} = a stochastic variable, which properties are shown in Equation 6.5.

$$E(u_{it}) = 0 \qquad for\ all\ t\ and\ i$$
$$E(u_{it}u_{js}) = \begin{cases} \sigma_{ij} & for\ all\ t\ and\ i \\ 0 & for\ t \neq s\ and\ all\ i\ and\ j \end{cases} \quad \text{(Eq. 6.5)}$$

Serially correlated disturbances can result when observations are dependent across individuals, time, space, or any given serial unit (Washington et al., 2011). In asphalt pavement construction, QA data typically derives from a number of serial units referred to as sublots. When the disturbances associated with observations in one sublot are dependent on disturbances from prior sublots a serial correlation issue may be raised. Asphalt mixtures are likely adjusted during production to make the volumetric properties satisfy specification requirements (Aschenbrener et al., 2017). These field adjustments are typically based on the information available from prior sublots. Thus, it is reasonable to assume that the equation disturbances follow trends. According to Equation 6.4, the expectation of the disturbance terms is ρ times the value of the previous disturbance. Although serial correlation does not affect the unbiasedness or consistency of regression parameter estimates, it does affect their efficiency (Srivastava and Giles, 1987; Washington et al., 2011).

This work compares the gain in efficiency of the model parameter estimates under three modeling approaches: (1) OLS single equation, (2) SURE without AR(1), and (3) SURE with AR(1). Efficiency is a relative parameter estimate property in that an estimator is efficient relative to another, which means that an estimator has a smaller standard error than an alternative estimator (Washington et al., 2011). Thus, the performance of each modeling approach was assessed by observing the standard errors of the parameter estimates. For this study, the feasible generalized least squares estimation technique is used to determine the ρ parameters required for serial correlation correction. The methodological approach was conducted using a commercial econometric and statistical software package.

6.2.3 Model selection

In developing the models, the first step was to explore the correlation between the independent variables. While most paired variables exhibited no correlation among the independent variables, several pairs exhibited high correlations with values between approximately 0.60 and 0.80. For example, the mixture indicator variable showed correlations with the 9.5- and 4.75 mm sieves, and G_{sb}. To avoid potential multicollinearity issues, the pairs of variables with high correlations (above 0.50) were not included concurrently in any equation.

The best-fit SURE models were selected using the Durbin-Watson (DW) statistic and adjusted R^2 measurements. The DW test statistic was used to assess the model potential for serial correlation. When no serially correlated disturbances are present, the DW statistic will yield a value of 2. As the statistic gets farther away from 2, there is less confidence that no serial correlation exists in the model. Additionally, details of this statistic are provided in Durbin and Watson (1951). The adjusted R^2 measurement was used to evaluate the overall goodness-of-fit of the SURE models. Adjusted R^2 measures are used to identify potentially insignificant variables added to the model and estimate the model's contribution to understanding the phenomenon under investigation (Washington et al., 2011). A model with a DW statistics closer to 2 and higher adjusted R^2 values was preferred between competing models. The DW statistics and adjusted R^2 values were automatically computed by the econometric and statistical software package used for this study.

Additionally, Quantile-Quantile (QQ) plots were prepared to test for normality and detect the presence of any outlying observations. Following the model selection specifications previously mentioned, statistical models were developed using four different datasets. The first dataset consists of the entire demonstration project QA data (40 observations). Since an outlying observation was detected in the SURE models developed using the entire dataset, a second dataset was prepared using a reduced number of observations. The reduced dataset contains 39 observations. Then, in an effort to examine separately the influence of the independent variables on the control mixture and test mixture volumetric properties, SURE models for each mixture type were developed. The control mixture and test mixture datasets consist of 19 and 20 observations, respectively.

6.3 Results and Discussion

6.3.1 Assessment of modeling approaches

Table 6.3 shows the results of the models developed using the entire dataset. The results include the parameter estimates for OLS single equations, SURE without AR(1), and SURE with AR(1). Lower standard errors were obtained for the SURE models' parameter estimates compared to the parameter estimates in the OLS single equations. Parameter estimates with smaller standard errors are more efficient. Hence, a gain in efficiency of the SURE parameter estimates over the OLS single equation coefficients is revealed. Additionally, some independent variables used to predict a certain volumetric property in the SURE models were found insignificant when estimating the same volumetric property in an OLS single equation model.

Table 6.3. Estimation results using the entire dataset.

Description	Parameter estimate (Standard error)		
	OLS Single Equation	SURE without AR(1)	SURE with AR(1)
Eq. (1). Dependent variable: In-place density (%)			
Constant	85.68 (3.91)[a]	85.52 (3.61)[a]	85.09 (3.34)[a]
Mixture type (Indicator)	1.74 (0.26)[a]	1.73 (0.24)[a]	1.71 (0.22)[a]
Data source (Indicator)	0.41 (0.23)[c]	0.41 (0.21)[c]	0.41 (0.21)[b]
P_b (%)	1.00 (0.43)[b]	1.00 (0.39)[b]	0.98 (0.37)[a]
RAP (%)	-0.41 (0.14)[b]	-0.40 (0.13)[a]	-0.37 (0.12)[a]
2.36 mm sieve (%)	0.20 (0.08)[b]	0.20 (0.08)[a]	0.21 (0.07)[a]
Eq. (2). Dependent variable: V_a (%)			
Constant	24.08 (5.04)[a]	19.61 (0.93)[a]	19.64 (0.91)[a]
Mixture type (Indicator)	1.50 (0.33)[a]	1.38 (0.28)[a]	1.36 (0.27)[a]
Data source (Indicator)	-0.49 (0.30)	-0.49 (0.05)[a]	-0.48 (0.05)[a]
P_b (%)	-1.35 (0.55)	-1.61 (0.10)[a]	-1.61 (0.10)[a]
RAP (%)	-0.33 (0.18)[c]	-0.07 (0.03)[b]	-0.07 (0.03)[b]
2.36 mm sieve (%)	-0.17 (0.11)	-0.10 (0.02)[a]	-0.10 (0.02)[a]
Eq. (3). Dependent variable: VMA (%)			
Constant	14.96 (0.18)[a]	14.96 (0.17)[a]	14.97 (0.17)[a]
Mixture type (Indicator)	1.49 (0.25)[a]	1.49 (0.25)[a]	1.47 (0.24)[a]
Number of observations	40	40	40
DW statistic – Eq. (1)	2.185	2.192	2.043
DW statistic – Eq. (2)	2.060	2.009	1.953
DW statistic – Eq. (3)	2.086	2.086	2.006
ρ used for AR(1) – Eq. (1)	-	-	-0.09
ρ used for AR(1) – Eq. (2)	-	-	-0.03
ρ used for AR(1) – Eq. (3)	-	-	-0.04
Adjusted R^2 – Eq. (1)	0.73	0.73	0.74
Adjusted R^2 – Eq. (2)	0.35	0.31	0.31
Adjusted R^2 – Eq. (3)	0.46	0.46	0.47

[a] Variables significant at the 99% confidence interval.
[b] Variables significant at the 95% confidence interval.
[c] Variables significant at the 90% confidence interval.

In general, a better fit is observed for the SURE models in contrast to comparable OLS single equation models. Similar observations can be made for all the datasets used in this study. Furthermore, the SURE approach was found to perform better with correction for serial correlation. The results show that the standard errors of the parameter estimates obtained for the SURE with AR(1) are typically lower than that of the SURE without AR(1). As a result, the SURE with AR(1) reveals slight improvements in the DW statistics and adjusted R^2 values. The serial correlation seems not to be an issue for the entire dataset based on the DW statistics. This dataset includes the control mixture and test mixture observations, which are not necessarily dependent across sublots. The disturbances appear not to be associated because asphalt mixture variability and field adjustments are typically mixture-specific. Thus, the DW statistics are relatively close to 2, meaning that there is acceptable confidence that no serial correlation is present in the models. However, when the control mixture and test mixture datasets are used to develop the models, the DW statistics depart away from 2 (as shown in section 6.3.4). Taken together, the results of this study suggest that SURE with AR(1) seems the most reliable approach for modeling asphalt mixture QA data when compared to OLS single equation and SURE without AR(1). The decision criteria to include any variable in the SURE with AR(1) was selected as a two-tailed t-test with a 95% confidence interval.

6.3.2 Removal of outlying observation

Despite the robustness and acceptability of the SURE models developed using the entire dataset, the adjusted R^2 values suggest that more variability is explained under field conditions rather than under laboratory conditions. Adjusted R^2 values are a useful goodness-of-fit statistic for providing feedback on the extent of knowledge about the uncertainty involved with the phenomenon of interest (Washington et al., 2011). In theory, more uncertainties are related to field compaction than laboratory compaction (Brown, 2009). Thus, more variability should be explained by the models for laboratory V_a and VMA than for in-place density.

In the laboratory, the compaction energy applied is consistent and can be calculated. In contrast, the amount of compaction energy put into field asphalt material cannot be readily determined with traditional equipment due to several factors, such as confinement and asphalt mixture temperature. The same independent variables were found significant in the SURE model equations for in-place density and V_a. However, according to the adjusted R^2 values, the variability

associated with in-place density and Va described by the models are approximately 74 and 31%, respectively (see Table 6.3). Hence, the percentage of variance accounted by the SURE models is more significant for in-place density than for V_a.

Since the adjusted R^2 measurement might not be a sufficient measure to judge the quality of the models (Washington et al., 2011), QQ plots were generated to test for normality and detect the presence of any outlying observations. Figure 6.1 shows the QQ plots prepared for each volumetric property using the results obtained for the SURE with AR(1) in Table 3. Although out-of-sample data is not used to validate the SURE with AR (1), the results can be considered satisfactory. For in-place density, the actual versus predicted values are relatively close to the 45° line without significant outliers. However, for V_a and VMA, the actual versus predicted values show a normal relationship except for an outlying observation. Interestingly, this outlying observation is the same for both QQ plots (Figures 6.1b and -c), and it is part of the control mixture QA data.

This outlying observation is likely the result of significant variations in asphalt mixture constituents, malfunctioning equipment, or other errors that might have occurred during QA data collection. Typically, normally distributed observations are within 3 standard deviations of the sample mean (Russo et al., 2018). However, this outlying observation is over 4 standard deviations of the V_a and VMA sample means, respectively. Also, based on the interquartile range method, this observation was identified as an outlier. A safe rule is to discard an outlier only if direct evidence represents an error in recording, a miscalculation, or a similar type of circumstance. Outliers could cause a misleading fit if the outlying observation resulted from a mistake or other extraneous cause. On the other hand, outliers may convey important information, as an outlier occurs because of an interaction with another predictor variable omitted from the model (Kutner, 2013).

Asphalt pavement construction QA data is assumed to be well distributed and without deviations from normality (Brown, 2009). However, non-normal variations may occur in response to difficult-to-control factors such as the materials' nature, specific construction and testing techniques, and technical errors (Al-Khayat et al., 2020). As a result, a recent study suggests the use of filtering criteria to identify potential anomalous QA data points before developing models to predict asphalt mixture volumetric properties (Russo et al., 2018). Regardless of the legitimate reason for the appearance of the outlying observation, this data point influences the amount of

variability explained by the model under laboratory conditions. Therefore, to demonstrate the full capability of SURE models using normally distributed data, this outlying observation was removed from the entire dataset. Consequently, the three datasets used for further data analysis are reduced (39 observations), control mixture (19 observations), and test mixture (20 observations).

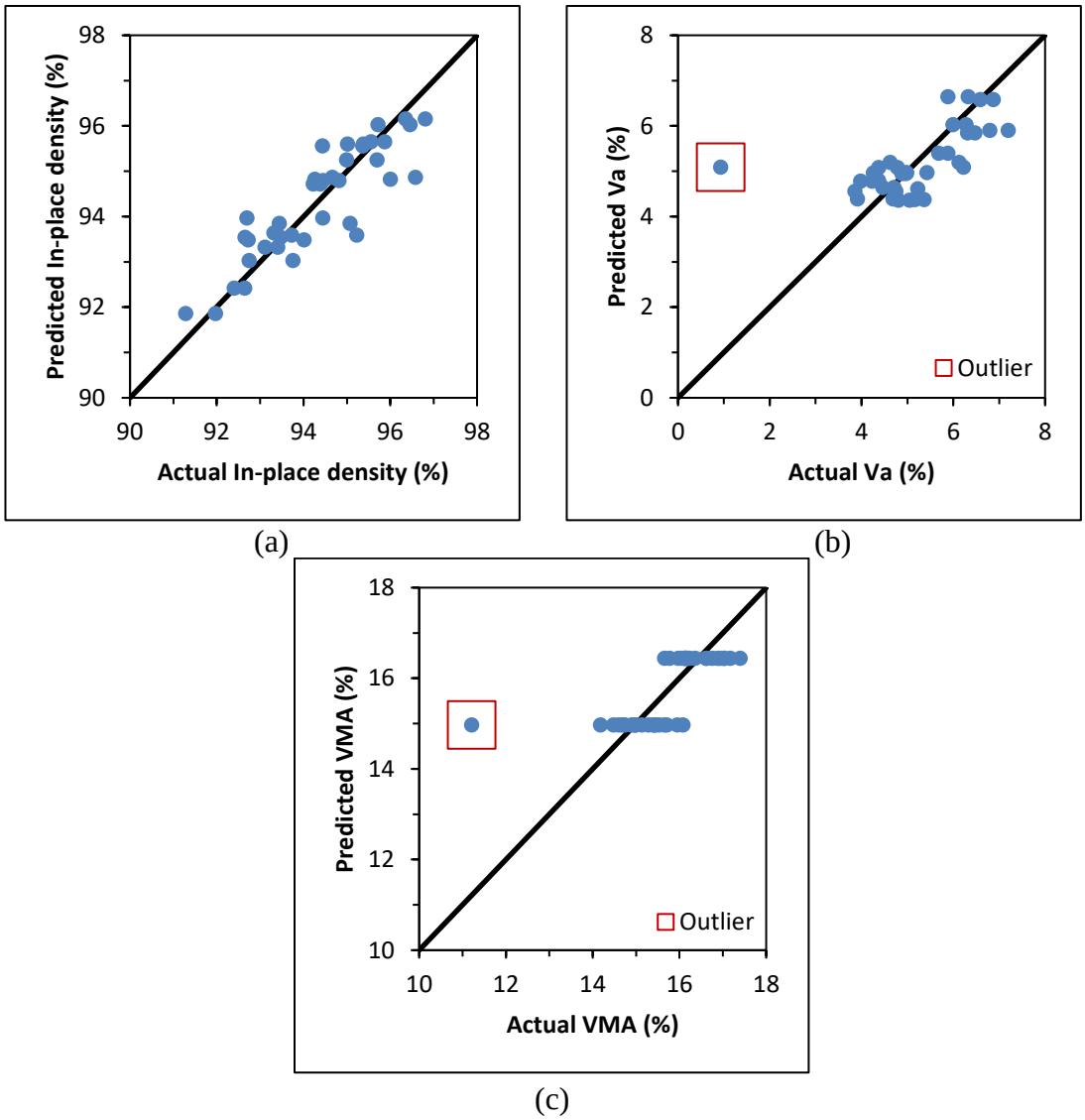

Figure 6.1. QQ plots, actual vs. predicted, SURE with AR(1) developed using entire dataset: (a) In-place density, (b) Laboratory air voids content, V_a, and (c) Voids in the mineral aggregate, VMA.

6.3.3 SURE with AR(1) using reduced dataset

Table 6.4 presents the SURE with AR(1) developed using a reduced dataset. The removal of the outlying observation provided valuable improvements to the estimated results of the model. For example, more independent variables were found significant to estimate VMA. Thus, the SURE with AR(1) developed using the reduced dataset is more informative than the SURE with AR(1) developed using the entire dataset, as shown in Figure 6.2. Also, the model results are sound with DW statistics close to 2 and adjusted R^2 values higher than 0.69. These arguments support the interpretation of the parameter estimates and statistical measures.

Table 6.4. Estimation results for SURE with AR(1)-reduced dataset.

Description	Parameter estimate (Standard error)	t-statistic (p-value)	95% Confidence interval
Eq. (1). Dependent variable: In-place density (%)			
Constant	85.72 (3.15)	27.18 (0.00)	79.54, 91.90
Mixture type (Indicator)	1.73 (0.21)	8.28 (0.00)	1.32, 2.15
RAP (%)	-0.44 (0.11)	-3.81 (0.00)	-0.66, -0.21
2.36 mm sieve (%)	0.21 (0.07)	3.07 (0.00)	0.08, 0.35
P_b (%)	0.98 (0.35)	2.78 (0.01)	0.29, 1.67
Data source (Indicator)	0.41 (0.21)	1.97 (0.05)	0.00, 0.83
Eq. (2). Dependent variable: V_a (%)			
Constant	24.38 (2.25)	10.81 (0.00)	19.96, 28.80
P_b (%)	-1.60 (0.11)	-14.64 (0.00)	-1.82, -1.39
Mixture type (Indicator)	1.26 (0.21)	6.04 (0.00)	0.85, 1.67
Data source (Indicator)	-0.79 (0.15)	-5.41 (0.00)	-1.07, -0.50
2.36 mm sieve (%)	-0.26 (0.07)	-3.95 (0.00)	-0.39, -0.13
Eq. (3). Dependent variable: VMA (%)			
Constant	20.02 (1.86)	10.77 (0.00)	16.37, 23.66
Mixture type (Indicator)	1.41 (0.17)	8.11 (0.00)	1.07, 1.76
2.36 mm sieve (%)	-0.14 (0.06)	-2.53 (0.01)	-0.25, -0.03
Data source (Indicator)	-0.27 (0.13)	-2.03 (0.04)	-0.52, -0.01
Number of observations		39	
DW statistic – Eq. (1)		1.992	
DW statistic – Eq. (2)		2.085	
DW statistic – Eq. (3)		2.062	
ρ used for AR(1) – Eq. (1)		-0.15	
ρ used for AR(1) – Eq. (2)		0.24	
ρ used for AR(1) – Eq. (3)		0.18	
Adjusted R^2 – Eq. (1)		0.72	
Adjusted R^2 – Eq. (2)		0.69	
Adjusted R^2 – Eq. (3)		0.70	

All variables are significant at the 95% confidence interval.

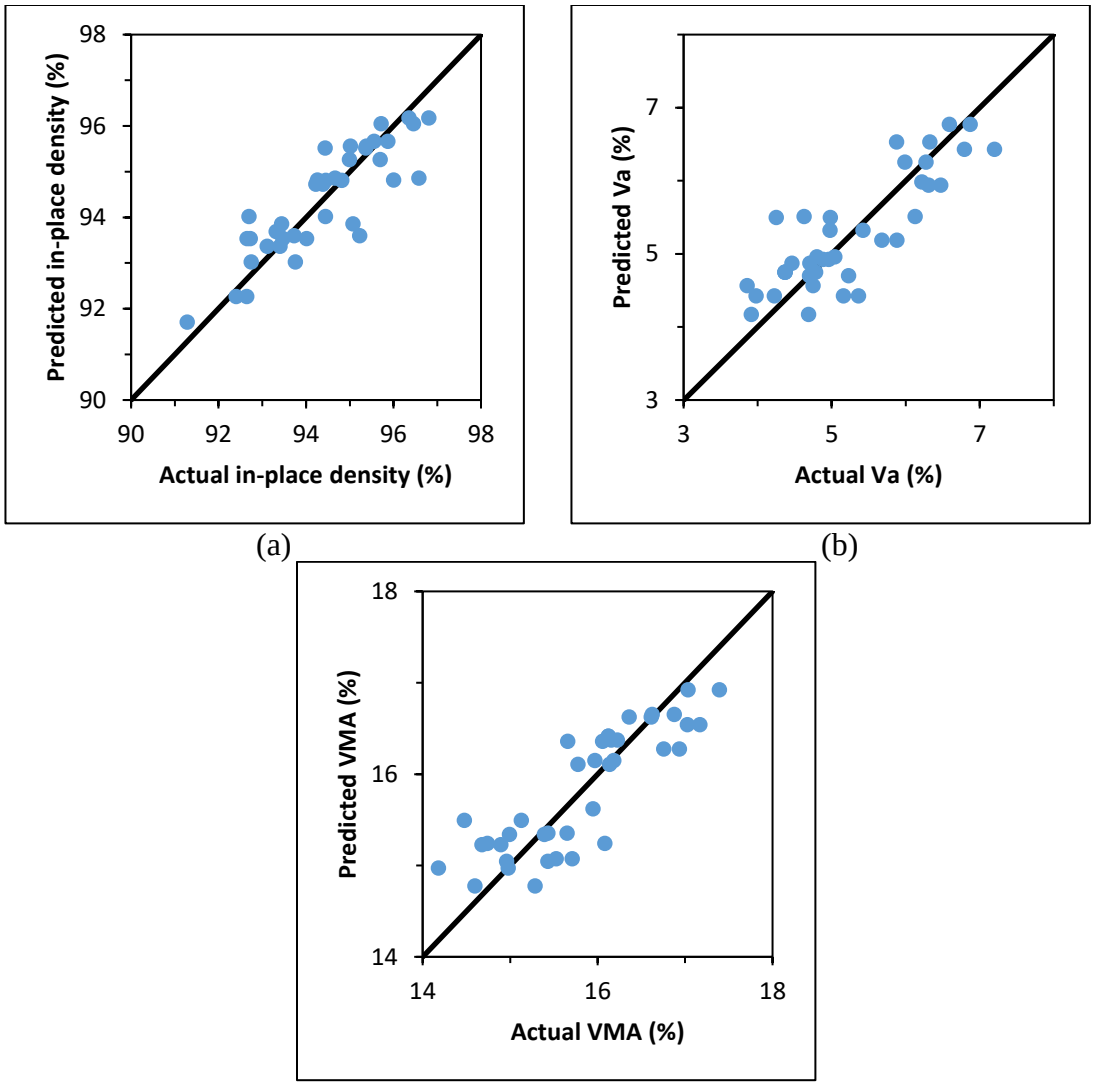

Figure 6.2. QQ plots, actual vs. predicted, SURE with AR(1) developed using reduced dataset: (a) In-place density, (b) Laboratory air voids content, V_a, and (c) Voids in the mineral aggregate, VMA.

In each equation of the model, the independent variables are arranged in descending order based on their t-statistic value (or level of significance). Accordingly, the most significant independent variable to predict in-place density and VMA for this dataset seems to be mixture type. The model implies that an increase of about 1.73% in field density can be obtained by using the modified mixture design proposed by Hekmatfar et al. (2015). Furthermore, the model indicates that by using a modified mixture design the V_a and VMA are increased by approximately 1.26 and 1.41%, respectively. These increments are close to the nominal mixture design 1% V_a

and 1.1% VMA differences between the control mixture and test mixture. The VMA nominal mixture design values for the control mixture and test mixture are 15.6 and 16.7%, respectively. However, the nominal V_a and VMA differences between the control and test mixtures were obtained using laboratory produced-laboratory compacted asphalt mixtures. QA data typically derives from plant produced-laboratory compacted or –field compacted asphalt mixtures.

The model also suggests that increasing the P_b will increase in-place density and decrease V_a. This result is intuitive considering the direct relationship of P_b with the amount of air voids in laboratory or field compacted asphalt mixtures. The reduced dataset SURE with AR(1) indicates that P_b is the most significant factor determining V_a. Thus, if substantial P_b variations occur during production, it becomes problematic to achieve the desirable V_a, regardless of the mixture type or aggregate passing the 2.36 mm sieve. However, this statement appears not to be valid under field conditions, where the variations involved with mixture type, amount of RAP, and amount of aggregate passing the 2.36 mm sieve prevail over the changes in P_b.

In this study, the amount of RAP material incorporated in the asphalt mixtures was found to be significant in estimating in-place density. The RAP parameter estimate indicates that increasing the quantity of recycled materials reduces in-place density. However, the effect of the aged binder available in recycled materials (i.e., RAP and RAS) on volumetric properties is poorly understood (NCAT, 2017). This issue creates uncertainties about how recycled materials affect field construction variability. Hence, more research should be devoted to better comprehending how recycled materials influence laboratory and field compaction.

As reported in Table 6.4, the percent of aggregate passing the 2.36 mm sieve significantly influences in-place density and laboratory V_a, and VMA. The model denotes that adding more fine aggregate can increase in-place density. However, if more sand material is added to the mixture to increase the amount of fines, lower V_a and VMA will be obtained. It should be highlighted that lowering the Va and VMA may substantially compromise asphalt mixture performance (Brown, 2009). As such, the modified mixture design used to produce the test mixture utilizes the Bailey method to systematically adjust the aggregate gradation without sacrificing performance (Vavrik et al., 2002; Hekmatfar et al., 2015).

In the Bailey method, the definition of coarse and fine aggregate is specifically defined to better determine the packing and aggregate interlock provided by the combination of aggregates in various sized mixtures (Vavrik et al., 2002). The sieve which defines coarse and fine aggregate

is known as the Primary Control Sieve (PCS). This control sieve is based on the Nominal Maximum Particle Size (NMPS) of the aggregate blend. For this study, a NMPS of 9.5 mm was used for both aggregate blends, control mixture, and test mixture. The corresponding PCS for a 9.5 mm NMPS aggregate blend is the 2.36 mm sieve. Thus, the model seemingly supports the use of the Bailey method to perform engineering adjustments in asphalt mixture design. However, it should be noticed that the mixture type variable is more significant than the variable indicating the percent of aggregate passing the 2.36 mm sieve. These results imply that modifications in gradation might not be enough to improve asphalt mixture volumetric properties. Other asphalt mixture design modifications might be required, such as lower laboratory compaction effort and adjusted V_a and P_{be} volumetric targets.

The data source indicator shows a volumetric property testing variability between the agency and contractor. Previous research using the same QA data reported a statistically insignificant difference between the agency's and contractor's sample means for in-place density and laboratory V_a and VMA (Montoya et al., 2018). This statistical result was drawn via unrelated t-tests, which is the traditional procedure to analyze QA data (LaVassar et al., 2009). As a result, insignificant mean differences were observed for the volumetric properties. However, the SURE model in Table 6.4 suggests that a significant difference between the measurements reported by the agency and contractor can be detected when taking other variables into account.

6.3.4 Comparisons between control mixture and test mixture

Table 6.5 shows the parameter estimates and statistical measures for the SURE, without and with AR(1), developed using the control mixture and test mixture datasets. The DW statistics for the SURE without AR(1) suggest the disturbances are serially correlated. The DW statistics are departed away from 2. This issue is because asphalt pavement construction QA data is divided into sublots. Thus, the measurements are typically correlated across sublots. In order to correct for serial correlation, the SURE with AR(1) were developed. In general, SURE with AR(1) provide more efficient parameter estimates, closer to 2 DW statistics, and higher adjusted R^2 values when compared to SURE without AR(1). Hence, SURE with AR(1) appears to mitigate asphalt pavement construction QA data deficiencies and limitations.

Table 6.5. Estimation results using the entire dataset.

Description	Control mixture dataset		Test mixture dataset	
	Parameter estimate (Standard error)			
	SURE without AR(1)	SURE with AR(1)	SURE without AR(1)	SURE with AR(1)
Eq. (1). Dependent variable: In-place density (%)				
Constant	64.10 (11.29)[a]	58.88 (7.40)[a]	95.21 (3.99)[a]	94.20 (3.33)[a]
P_b (%)	2.07 (1.47)	2.83 (0.98)[a]	1.69 (0.33)[a]	1.68 (0.28)[a]
RAP (%)	-	-	-0.81 (0.29)[a]	-0.74 (0.24)[a]
2.36 mm sieve (%)	0.47 (0.11)[a]	0.48 (0.07)[a]	-	-
Data source (Indicator)	-	-	0.87 (0.24)[a]	0.85 (0.22)[a]
Eq. (2). Dependent variable: V_a (%)				
Constant	7.71 (0.90)[a]	7.66 (0.87)[a]	37.64 (1.78)[a]	36.93 (2.17)[a]
P_b (%)	-	-	-1.78 (0.08)[a]	-1.84 (0.08)[a]
2.36 mm sieve (%)	-0.08 (0.03)[a]	-0.08 (0.03)[a]	-	-
0.300 mm sieve (%)	-	-	-2.26 (0.20)[a]	-2.13 (0.20)[a]
Data source (Indicator)	-0.32 (0.06)[a]	-0.31 (0.06)[a]	-1.04 (0.10)[a]	-1.05 (0.09)[a]
Eq. (3). Dependent variable: VMA (%)				
Constant	17.45 (0.63)[a]	17.43 (0.59)[a]	28.70 (1.42)[a]	27.73 (1.42)[a]
4.75 mm sieve (%)	-	-	0.05 (0.01)[a]	0.06 (0.01)[a]
0.300 mm sieve (%)	-	-	-1.75 (0.15)[a]	-1.70 (0.15)[a]
0.150 mm sieve (%)	-0.37 (0.10)[a]	-0.37 (0.09)[a]	-	-
Data source (Indicator)	-	-	-0.33 (0.07)[a]	-0.30 (0.07)[a]
Number of observations	19	19	20	20
DW statistic – Eq. (1)	2.687	2.101	2.331	2.144
DW statistic – Eq. (2)	2.127	1.984	1.446	1.770
DW statistic – Eq. (3)	2.243	1.967	1.929	1.979
ρ used for AR(1) – Eq. (1)	-	-0.42	-	-0.16
ρ used for AR(1) – Eq. (2)	-	-0.07	-	0.28
ρ used for AR(1) – Eq. (3)	-	-0.12	-	0.02
Adjusted R^2 – Eq. (1)	0.45	0.62	0.54	0.58
Adjusted R^2 – Eq. (2)	0.11	0.13	0.94	0.94
Adjusted R^2 – Eq. (3)	0.08	0.11	0.86	0.86

[a] Variables significant at the 99% confidence interval.
[b] Variables significant at the 95% confidence interval.
[c] Variables significant at the 90% confidence interval.

Considering that different design methods were used for the control and test mixtures, the observed contrasts between the control and test mixtures models are realistic. Overall, the SURE models are more robust for the test mixture than for the control mixture. Higher adjusted R^2 values were obtained for the test mixture compared to the control mixture. Furthermore, the SURE models developed using the test mixture dataset support the finding that more variability is explained under laboratory conditions than field conditions. The extent of knowledge provided by the control mixture SURE models to estimate V_a and VMA is limited. For example, the P_b was found insignificant to predict V_a in the control mixture SURE models. This outcome becomes an issue when selecting an optimum P_b that improves asphalt mixture durability and performance. Asphalt

mixture design aims to choose an optimum P_b for an aggregate structure to meet prescribed criteria (Roberts et al., 2002).

Although the control mixture seems not responsive to P_b in the laboratory, a 1% unit change in P_b appears to yield a unit change of 2.83% in in-place density under field conditions. In contrast, the results obtained for the test mixture dataset suggest that the sensitivities of in-place density and V_a with respect to P_b are comparable. Based on the parameter estimates, the unit changes in in-place density and V_a resulting from a 1% measurement unit change in P_b are 1.68 and 1.84%, respectively. These results suggest that the test mixture was less sensitive to field adjustments than the control mixture. An asphalt mixture less sensitive to P_b and aggregate gradation fluctuations is extremely advantageous from a construction standpoint. Regardless of the mixture design method employed (i.e., Superpave 5, regressed air voids, balanced mix), asphalt mixtures are susceptible to field variations during production and construction. Field variations are due to several factors, such as stockpile variability, breakdown, and aggregate asphalt binder absorption during production and construction (Cooley and Williams, 2013; Aschenbrener et al., 2017; Leckie and Beeson, 2018).

Another interesting insight provided by the test mixture SURE models is the significance of the amount of aggregate passing the 0.300 mm sieve to estimate V_a and VMA. As previously mentioned, the test mixture gradation was prepared using the Bailey method. This approach breaks the aggregate blend into three distinct portions, coarse aggregate, coarse portion of fine aggregate, and fine portion of fine aggregate. To define where to split the aggregate blend into portions, three predetermined control sieves are used, PCS, Secondary Control Sieve (SCS), and Tertiary Control Sieve (TCS). In this study, the PCS, SCS, and TCS are the 2.36-, 0.600-, and 0.150 mm sieves, respectively. Although priority was given to include the effects of these sieves in the test mixture models, the best-fitting SURE models were obtained using the 4.75- and 0.300 mm sieve variables. The addition of the 4.75 mm sieve variable in the model is reasonable because this sieve significantly contributes to determining the VMA in 9.5 mm NMPS mixtures, as specified by the Bailey method (Vavrik et al., 2002). Nevertheless, the 2.36- and 0.150 mm sieve variables were found significant in the control mixture models. These findings are noteworthy because the test mixture aggregate blend originates from the control mixture aggregate blend, but different compaction characteristics are observed in the laboratory and field.

Finally, the test mixture SURE models support a discrepancy between the in-place density, laboratory V_a, and VMA measurements of the agency and contractor. Conversely, the data source variable was found significant just in the V_a estimation for the control mixture. Additionally, the test mixture SURE models suggest that increasing the amount of recycled materials can reduce in-place density. RAP materials are typically stiffer than virgin materials. Thus, RAP material properties should be properly accounted for to prevent problems in the placement and compaction of asphalt mixtures (Copeland, 2011). This finding should bear further investigations to fully understand the influence of RAP materials in asphalt pavement volumetric properties.

6.4 Summary and Conclusions

Considering that a basic understanding of volumetric interactions of asphalt mixtures is important from laboratory mixture design and field construction standpoints (Brown, 2009), this study's findings contribute to the progress and sustainability of asphalt pavements. This paper demonstrates that SURE approaches can be used to estimate the effect of asphalt mixture design, materials proportions and properties, and data collection factors on in-place density and laboratory V_a, and VMA.

The main reason asphalt mixture volumetric properties are not commonly modeled is the limited variability of QA data. Asphalt pavement construction performance incentives are calculated using the mean and standard deviation of the volumetric properties. Therefore, asphalt paving projects are delivered with uniform material proportions and consistent asphalt mixture volumetric properties to maximize construction performance incentives. However, the variability of the datasets used for this study was adequate to develop robust, informative, and concise SURE models. The results of this study condensed the main aspects of a paving demonstration project using SURE models. Hence, SURE approaches could be helpful to analyze large and small asphalt mixture QA databases.

This research work corroborates that SURE models are more elegant in their formulation and sophisticated in their use of statistical techniques in comparison to single equation linear regression models (Glickman, 1977). Particularly, SURE approaches can explicitly account for the interaction among volumetric properties, contemporaneous correlation among unobserved factors, and serial correlation across sublots. A gain in the efficiency of parameter estimates was obtained by considering the contemporaneous and serial correlation in asphalt mixture QA data.

Future studies on the current topic are therefore recommended to validate the results presented herein. Additional data collection and modeling could provide further insight into asphalt mixture production, construction, and performance. The SURE models in this study can be extended by including mechanical and thermal performance parameters as dependent variables. Also, other production and construction aspects can be used as independent variables, such as mixing and compaction temperatures, hauling distance, compaction features, and lift thickness. Furthermore, increasing the number of observations could also improve and corroborate the amount of asphalt mixture variability captured by SURE approaches.

7. SUMMARY, CONCLUSIONS, AND RECOMMENDATIONS

7.1 Summary

This dissertation aimed to investigate the environmental tuning of asphalt pavement materials using PCMs. The main purpose of this study was to facilitate critical information that would enable research and technology to further the thermoregulation of asphalt pavements with suitable PCM formulations. First, Chapter 1 contextualized this investigation by providing background information on modifying asphalt pavements and the most typical modifiers used for such engineering adjustments. Various enhancing materials are added to asphalt binders and mixtures to change their properties, particularly rutting, and fatigue and thermal cracking. Certain materials are more effective at modifying the properties to provide improved field performance cost-effectively. However, PCMs pose characteristics to modify asphalt materials beyond the ones offered by conventional modifiers and adjust asphalt pavements properties to withstand environmental loads better.

As previously demonstrated in Chapter 2, the modification of asphalt materials with PCMs has been under investigation over the last decade. Although a considerable vast amount of information has been published, very little or no research has been successfully translated to field implementation. Through an extensive literature review, this dissertation identified that to encourage the tuning of asphalt pavements with PCMs, the benefits, design, and challenges related should be more fully exhibited and quantified.

The evidence presented in this dissertation fully demonstrated the beneficial capacity of a PCM asphalt pavement slab to melt snow and ice and prevent freeze-thaw cycles. The experimental and computational results in Chapter 3 showed that, indeed, PCMs could enhance the thermal response of asphalt pavements to adverse environmental conditions, leading to a considerable reduction in snow accumulation and ice formation at the pavement's surface. Overall, these findings support the use of PCMs in asphalt pavements to provide them with TES properties for better low-temperature management and in-service performance. Computational simulations helped to quantify the benefits of implementing this methodology at 100 locations in the US. This part of the study established the most quantifiable evidence to support the tuning of asphalt pavements with PCMs.

Chapter 4 investigated the inclusion of a μPCM in asphalt binders and mixtures to help reduce environmental damage at a bordering intermediate-high temperature (43°C) in asphalt pavement technology. Through rheology, thermoanalytical, thermal cycling, and mechanical testing, this chapter attempted to capture the μPCM effect and link the behavior between μPCM modified asphalt binders and mixtures. Thus, this investigation identified a novel approach using rheological measurements to determine when the μPCM latent heat effect occurs. An asphalt mixture design method was demonstrated to systematically incorporate a substantial portion of μPCM particles in a Reference Mixture. Additionally, the thermal and mechanical performances of μPCM modified asphalt mixtures were evaluated and corroborated that a significant reduction in pavement temperature can be obtained, but some mechanical performance issues should be considered. The findings extend the thermomechanical understanding of μPCM modified asphalt binders and mixtures.

Chapters 5 and 6 examined a case study that documents and analyzes the field implementation of a new mixture design method. The following steps in tuning asphalt pavements with PCMs will revolve around translating research into field implementation. As such, the information related to the case study presented herein was deemed relevant to this dissertation's topic. In particular, the field demonstration presented in Chapter 5 could be considered as input to manufacturing PCM formulations that could better withstand high temperatures during asphalt mixture production, placement, and compaction. The statistical approach provided in Chapter 6 could be helpful to adjust the volumetric, thermal, and mechanical properties of asphalt mixtures modified with PCMs based on reliable correlations.

7.2 Conclusions

This dissertation strengthens the concept that by modifying asphalt materials with PCMs, it should be possible to tune the resulting asphalt pavement to the environment, thereby mitigating or eliminating pavement damage due to the exposure of asphalt pavement surfaces to critical temperature fluctuations. Several conclusions have already been presented at the end of each chapter reviewing this study's research methods and results individually. The findings of this investigation increment the theoretical, empirical, and methodological knowledge related to the tuning of asphalt pavements with PCMs and are expected to drive this area of research. Collectively, the following conclusions can be drawn from the present study:

1. The environmental tuning of asphalt pavements using PCMs will require careful examination of the PCM and asphalt material properties under specific climatic conditions. For instance, this dissertation's experimental and computational results demonstrated that the phase transition temperature of PCMs and air voids content of asphalt mixtures could impact the thermal response of PCM modified asphalt materials. Additionally, after a meticulous design of a PCM modified asphalt product, the tuning benefits should be quantified under realistic environmental conditions, as they could determine the appropriateness of a PCM formulation for a specific location. Hence, quantifiable criteria should be developed and refined to support the addition of PCMs to a pavement design.
2. This dissertation experimentally proved an approach to measure the μPCM latent heat effect out of transient rheological experiments. Performing an energy balance on a viscoelastic material undergoing shear can be far from straightforward. During DSR testing, a body is supplied with mechanical energy. A complete energy balance would consider the resulting changes in kinetic, surface, potential, thermal, and all other forms of energy within the sample (Tschoegl, 1989), making it complicated to recognize the μPCM latent heat effect. This study's findings demonstrated that the μPCM latent heat effect could be identified using DSR equipment, and the data obtained from such measurements is relatable to the thermal response of μPCM tuned asphalt mixtures. The proposed G* Change Rate parameter is reliable regardless of the amount of μPCM and the imposed transient conditions (i.e., cooling-heating cycle rate and μPCM dosage).
3. Incorporating a substantial amount of μPCM particles in asphalt mixtures that could lead to significant temperature changes in the pavement structures calls for a systematic mixture design framework. The substitution of a portion of fine aggregates and mineral filler with μPCM particles seems a reasonable design method. This technique could be enhanced as μPCM particles are adjusted for paving purposes. The available μPCM particles and design method appear not to affect the intermediate- and low-temperature performances of asphalt mixtures, based on cyclic fatigue and SCB testing results. However, the high-temperature performance of asphalt mixtures is strongly

compromised with the inclusion of μPCM particles, which may be the most shocking result of this study.

4. The asphalt binder mechanical results corroborate that μPCM particles could behave like a conventional mineral filler if they suffer no damage during blending with asphalt materials. The μPCM particles stiffen the modified asphalt binders but do not represent a menace to the relaxation of the binder matrix. However, the asphalt binder and mixture mechanical results suggest ambivalent performance outcomes caused by the incorporation of μPCM in asphalt paving materials. This outcome is mainly because μPCM particles experienced higher PCM leakage during the process of asphalt mixtures' mixing and compaction than blending with asphalt binders. Although the PCM leakage hindered the thermal benefits of μPCM Mixtures, the differences in temperature between μPCM and non-μPCM modified mixtures were still considerable.
5. A field demonstration project exemplified the construction process that PCM formulations are expected to survive to translate this technology from the laboratory to the field. This dissertation demonstrated two methods to incorporate PCMs in asphalt pavements, PCMs embedded in pipes and μPCM particles. Both forms of PCM integration into asphalt pavements exhibited advantages and disadvantages. The case study illustrated that readily implemented methodologies entail minimal variations from traditional construction practices and yield significant ultimate performance results. This study made an effort to bridge the fundamental knowledge of PCM formulation and asphalt technology by comparing the performance of μPCM Mixtures with a competitive Reference Mixture used in the field. However, approaches for constructing asphalt pavements with PCMs are missing. These advancements could be further through material developments, construction practices, or both.
6. Asphalt mixtures are typically referred to as a matrix because the mixture components converge to fulfill specific properties, such as volumetric, mechanical, and thermal. This dissertation confirmed that such conception is applicable as mixture components and design and construction factors were fitted in a statistical matrix to predict volumetric properties simultaneously. Thus, the proposed statistical approach or similar technique could be extended to adjust the volumetric, mechanical, and thermal properties of μPCM modified asphalt materials at the same time.

7.3 Recommendations

Overall, this study recommends furthering the study of the environmental tuning of asphalt pavements using PCMs. The significance of this research study should not be limited to the design of asphalt pavements with PCMs to resist diurnal and seasonal temperature fluctuations better. The widespread implementation of PCM tuned asphalt pavements could benefit the pavement engineering industry and society. The environmental tuning of asphalt pavements could mitigate the urban heat island effects faced by roadways, reduce snow accumulation and ice formation on the surface of pavements. Furthermore, the thermoregulation of asphalt binders and mixtures to control the surface and inner temperatures of asphalt pavements could result in considerable energy, material, and cost savings. Consequently, the adaptation of asphalt pavement to the environment could impose positive impacts in various areas, such as electricity demand and transportation safety. Accordingly, this dissertation provides the following insights for future research:

1. Considerations for the environmental tuning of asphalt pavements are not new. Asphalt pavements materials are required to show good performance under specific local climatic conditions. Paving materials are selected to provide sufficient stiffness to resist rutting at expected high service temperatures and enough flexibility to endure fatigue and thermal cracking at intermediate and low service temperatures. However, this dissertation highlights the importance of the temperature dependency of asphalt materials. Specific transient conditions could produce higher mechanical efforts in asphalt materials that could cause higher impacts on the ultimate performance of asphalt pavements. Transient conditions also impact the PCM latent heat effect, shifting the temperature and intensity of PCM thermal energy peaks. Databases that predict the PCM latent heat effect regardless of the ambient temperature gradient or formulation of highly stabled PCMs are vital aspects to further the technology under discussion.
2. Stress relaxation in viscoelasticity is usually defined as an observed decrease in stress in response to strain generated in the structure (Tschoegl, 1989). The G* Change Rate proposed by this dissertation suggests that μPCM modified asphalt binders experience stress relaxation when the μPCM latent heat occurs, a thermal lag is observed. However, a countereffect in the viscoelastic flow of μPCM modified asphalt binders was found using the G* Change Rate analysis. Therefore, a natural progression of this work is to

quantify the relaxation benefits provided by the μPCM incorporation and possible causes and implications of the observed countereffect.

3. Although this study has progressed the design of μPCM mixtures, several assumptions still required validation. In particular, the mixture design approach suggests replacing a portion of fine aggregate and mineral filler with μPCM particles by volume. The proposed relationships to perform this replacement showed to be reliable when fabricating asphalt mixture specimens with the SGC. The calculated masses of mixture material were well-adjusted using such an approach to meet the volume required to compact the specimens to a constant height. Nevertheless, the specific gravity and absorption properties of the replaced materials and μPCM particles should be further characterized to enhance the mixture design procedure.
4. This study's field case shows a learning curve in implementing new paving materials and methodologies in asphalt technology. Future work encompasses construction field trial sections with asphalt pavements tuned with PCMs. Such a process could help identify and address PCM modified asphalt pavements' benefits, design, and challenges. The additional costs related to the use of PCMs will be hard to justify without reliable field performance histories. Naturally, PCM tuned asphalt materials would have to demonstrate first in the laboratory that they replicate the performance of traditional paving materials. For example, μPCM modified asphalt mixtures would have to show a similar Flow Number curve to a reference mixture without confining pressure. Statistical techniques could aid to speed enabling research that validates the use of PCM tuned asphalt pavements.
5. Although many aspects related to the tuning of asphalt pavements with PCMs are still in flux, the implementation of pavements with intrinsic thermal resistance properties is expected to evolve quickly. Therefore, despite its limitations, this research work adds understanding to this growing area of study and recommends closely monitoring emerging technologies that could help with the temperature management of pavements.

REFERENCES

Abhat, A. (1983). Low temperature latent heat thermal energy storage: Heat storage materials. *Solar Energy*, *30*(4), 313–332. https://doi.org/10.1016/0038-092X(83)90186-X

Abtahi, S. M., Sheikhzadeh, M., & Hejazi, S. M. (2010). Fiber-reinforced asphalt-concrete - A review. *Construction and Building Materials*, *24*(6), 871–877. https://doi.org/10.1016/j.conbuildmat.2009.11.009

Agyenim, F., Hewitt, N., Eames, P., & Smyth, M. (2010). A review of materials, heat transfer and phase change problem formulation for latent heat thermal energy storage systems (LHTESS). *Renewable and Sustainable Energy Reviews*, *14*(2), 615–628. https://doi.org/10.1016/j.rser.2009.10.015

Akkinepally, R., & Attoh-Okine, N. (2006). *Quality control and quality assurance of hot mix asphalt construction in Delaware*. Delaware Center for Transportation. Newark, DE. Retrieved from https://cpb-us-w2.wpmucdn.com/sites.udel.edu/dist/1/1139/files/2013/10/Rpt.-173-Quality-Control-and-QualityAssura-21ac6yk.pdf

Al-Khayat, H., Gurganus, C., Newcomb, D. E., & Sakhaeifar, M. S. (2020). Developing specification limits for hot mix asphalt properties and impact on pay factors. *Journal of Transportation Engineering, Part B: Pavements*, *146*(3), 05020002. https://doi.org/10.1061/JPEODX.0000185

Anastasopoulos, P. C., Mannering, F. L., & Haddock, J. E. (2012). Random parameters seemingly unrelated equations approach to the postrehabilitation performance of pavements. *Journal of Infrastructure Systems*, *18*(3), 176–182. https://doi.org/10.1061/(ASCE)IS.1943-555X.0000096

Anderson, D. A., Christensen, D. W., Bahia, H. U., Dongre, R., Sharma, M. G., Antle, C. E., & Button, J. (1994). *National Research Council, Report No. SHRP-A-369: Binder characterization and evaluation, volume 3: Physical characterization.* Strategic Highway Research Program. Washington, D.C. Retrieved from http://onlinepubs.trb.org/onlinepubs/shrp/SHRP-A-369.pdf

Ang, A., & Tang, W. (2007). *Probability concepts in engineering: Emphasis on applications in civil & environmental engineering*. New York: Wiley.

Anupam, B. R., Sahoo, U. C., & Rath, P. (2020). Phase change materials for pavement applications: A review. *Construction and Building Materials*, *247*, 118553. https://doi.org/10.1016/j.conbuildmat.2020.118553

Aschenbrener, T., Brown, E.R., Tran, N., & Blankenship, P.B. (2017). *Demonstration project for enhanced durability of asphalt pavements through increased in-place pavement density*. Publication National Center for Asphalt Technology Report 17-05. Auburn, AL. Retrieved from https://eng.auburn.edu/research/centers/ncat/files/technical-reports/rep17-05.pdf

Asphalt Institute Foundation. (2017). *STAR symposium report 2017*. Retrieved from https://bookstore.asphaltinstitute.org/STAR17report

Athukorallage, B., & James, D. (2016, November 11). Incorporating phase change materials to mitigate extreme temperatures in asphalt concrete pavements. *Volume 8: Heat Transfer and Thermal Engineering*. https://doi.org/10.1115/IMECE2016-67765

Athukorallage, B., Dissanayaka, T., Senadheera, S., & James, D. (2018). Performance analysis of incorporating phase change materials in asphalt concrete pavements. *Construction and Building Materials*, *164*, 419–432. https://doi.org/10.1016/j.conbuildmat.2017.12.226

Baetens, R., Jelle, B. P., & Gustavsen, A. (2010). Phase change materials for building applications: A state-of-the-art review. *Energy and Buildings*, *42*(9), 1361–1368. https://doi.org/10.1016/j.enbuild.2010.03.026

Baghaee Moghaddam, T., & Baaj, H. (2016). The use of rejuvenating agents in production of recycled hot mix asphalt: A systematic review. *Construction and Building Materials*, *114*, 805–816. https://doi.org/10.1016/j.conbuildmat.2016.04.015

Beckett, G., MacKenzie, J. A., & Robertson, M. L. (2001). A moving mesh finite element method for the solution of two-dimensional Stefan problems. *Journal of Computational Physics*, *168*(2), 500–518. https://doi.org/10.1006/jcph.2001.6721

Bian, X., Tan, Y. Q., Lv, J. F., & Shan, L. Y. (2012). Preparation of latent heat materials used in asphalt pavement and theirs' controlling temperature performance. *Advanced Engineering Forum*, *5*, 322–327. https://doi.org/10.4028/www.scientific.net/aef.5.322

Brasileiro, L., Moreno-Navarro, F., Tauste-Martínez, R., Matos, J., & Rubio-Gámez, M. del C. (2019). Reclaimed polymers as asphalt binder modifiers for more sustainable roads: A review. *Sustainability (Switzerland)*, *11*(3), 1–20. https://doi.org/10.3390/su11030646

Brown, E.R. (2009). *Hot mix asphalt materials, mixture design, and construction* (3rd ed.). Lanham, Md.: NAPA Educational Foundation.

Buddhavarapu, P., Prozzi, J. A., & Smit, A. de F. (2016). Pay factors based on observed field-performance data. *Journal of Transportation Engineering*, *142*(5), 04016016. https://doi.org/10.1061/(ASCE)TE.1943-5436.0000839

Bueno, M., Kakar, M. R., Refaa, Z., Worlitschek, J., Stamatiou, A., & Partl, M. N. (2019). Modification of asphalt mixtures for cold regions using microencapsulated phase change materials. *Scientific Reports*, *9*(1), 1–10. https://doi.org/10.1038/s41598-019-56808-x

Chen, M. Z., Hong, J., Wu, S. P., Lu, W., & Xu, G. J. (2011). Optimization of phase change materials used in asphalt pavement to prevent rutting. *Advanced Materials Research*, *219–220*, 1375–1378. https://doi.org/10.4028/www.scientific.net/AMR.219-220.1375

Chen, M., Wu, S., Wang, H., & Zhang, J. (2011). Study of ice and snow melting process on conductive asphalt solar collector. *Solar Energy Materials and Solar Cells*, *95*(12), 3241–3250. https://doi.org/10.1016/j.solmat.2011.07.013

Chen, M., Wan, L., & Lin, J. (2012). Effect of phase-change materials on thermal and mechanical properties of asphalt mixtures. *Journal of Testing and Evaluation*, *40*(5), 20120091. https://doi.org/10.1520/jte20120091

Chen, Y., Wang, H., You, Z., & Hossiney, N. (2020). Application of phase change material in asphalt mixture – A review. *Construction and Building Materials*, *263*, 120219. https://doi.org/10.1016/j.conbuildmat.2020.120219

Copeland, A. (2011). *Reclaimed asphalt pavement in asphalt mixtures: State of the practice*. Federal Highway Administration FHWA-HRT-11-021. McLean, VA. Retrieved from https://www.fhwa.dot.gov/publications/research/infrastructure/pavements/11021/11021.pdf

Cooley, L., & Williams, K. (2013). *Aggregate absorption in HMA mixtures*. Mississippi Department of Transportation FHWA/MS-DOT-RD-13-245. Jackson, MS. Retrieved from https://rosap.ntl.bts.gov/view/dot/27480

Durbin, J., & Watson, G. S. (1951). Testing for serial correlation in least squares regression. II. *Biometrika*, *38*(1/2), 159–178. https://doi.org/10.2307/2332325

Dutil, Y., Rousse, D. R., Salah, N. Ben, Lassue, S., & Zalewski, L. (2011). A review on phase-change materials: Mathematical modeling and simulations. *Renewable and Sustainable Energy Reviews*, *15*(1), 112–130. https://doi.org/10.1016/j.rser.2010.06.011

Esmaeeli, H. S., Farnam, Y., Haddock, J. E., Zavattieri, P. D., & Weiss, W. J. (2018). Numerical analysis of the freeze-thaw performance of cementitious composites that contain phase change material (PCM). *Materials and Design*, *145*, 74–87. https://doi.org/10.1016/j.matdes.2018.02.056

Ezzat, H., El-Badawy, S., Gabr, A., Zaki, E. S. I., & Breakah, T. (2016). Evaluation of asphalt binders modified with nanoclay and nanosilica. *Procedia Engineering*, *143*(Ictg), 1260–1267. https://doi.org/10.1016/j.proeng.2016.06.119

Fan, J., Liu, S., Meng, Q., & Song, F. (2021). Liquid thermal conductivity of three biodiesel compounds: Methyl myristate, methyl laurate and methyl caprate. *Journal of Chemical Thermodynamics*, *155*. https://doi.org/10.1016/j.jct.2020.106374

Farnam, Y., Esmaeeli, H. S., Zavattieri, P. D., Haddock, J., & Weiss, J. (2017). Incorporating phase change materials in concrete pavement to melt snow and ice. *Cement and Concrete Composites, 84*, 134–145. https://doi.org/10.1016/j.cemconcomp.2017.09.002

Federal Highway Administration (FHWA). (2016). *Strategies for improving sustainability of asphalt pavements*. Tech-Brief FHWA-HIF-16-012. Retrieved from https://www.fhwa.dot.gov/pavement/sustainability/hif16012.pdf

Gil, A., Oró, E., Peiró, G., Álvarez, S., & Cabeza, L. F. (2013). Material selection and testing for thermal energy storage in solar cooling. *Renewable Energy*, *57*, 366–371. https://doi.org/10.1016/j.renene.2013.02.008

Giuliani, F., Merusi, F., Polacco, G., Filippi, S., & Paci, M. (2012). Effectiveness of sodium chloride-based anti-icing filler in asphalt mixtures. *Construction and Building Materials*, *30*, 174–179. https://doi.org/10.1016/j.conbuildmat.2011.12.036

Gkritza, K., Karlaftis, M. G., & Mannering, F. L. (2011). Estimating multimodal transit ridership with a varying fare structure. *Transportation Research Part A: Policy and Practice*, *45*(2), 148–160. https://doi.org/10.1016/j.tra.2010.12.005

Glickman, N. (1977). *Econometric analysis of regional systems: Explorations in model building and policy analysis*. New York: Academic Press.

Gorkem, C., & Sengoz, B. (2009). Predicting stripping and moisture induced damage of asphalt concrete prepared with polymer modified bitumen and hydrated lime. *Construction and Building Materials*, *23*(6), 2227–2236. https://doi.org/10.1016/j.conbuildmat.2008.12.001

Greene, W. (2003). *Econometric analysis*. Upper Saddle River: Prentice Hall.

Guan, B., Ma, B., & Fang, Q. (2011). Application of asphalt pavement with phase change materials to mitigate urban heat island effect. *2011 International Symposium on Water Resource and Environmental Protection*, 2389–2392. https://doi.org/10.1109/ISWREP.2011.5893749

Guo, M., Liang, M., Jiao, Y., Zhao, W., Duan, Y., & Liu, H. (2020). A review of phase change materials in asphalt binder and asphalt mixture. *Construction and Building Materials*, *258*, 119565. https://doi.org/10.1016/j.conbuildmat.2020.119565

Habbouche, J., Hajj, E. Y., Sebaaly, P. E., & Piratheepan, M. (2020). A critical review of high polymer-modified asphalt binders and mixtures. *International Journal of Pavement Engineering*, *21*(6), 686–702. https://doi.org/10.1080/10298436.2018.1503273

Haddock, J. E., Rahbar-Rastegar, R., Pouranian, M. R., Montoya, M., & Patel, H. (2020). *Implementing the Superpave 5 asphalt mixture design method in Indiana*. Joint Transportation Research Program Publication No. FHWA/IN/JTRP-2020/12. West Lafayette, IN: Purdue University. https://doi.org/10.5703/1288284317127

Hassn, A., Aboufoul, M., Wu, Y., Dawson, A., & Garcia, A. (2016). Effect of air voids content on thermal properties of asphalt mixtures. *Construction and Building Materials*, *115*, 327–335. https://doi.org/10.1016/j.conbuildmat.2016.03.106

He, L. H., Li, J. R., & Zhu, H. Z. (2013). Analysis on application prospect of shape-stabilized phase change materials in asphalt pavement. *Applied Mechanics and Materials*, *357–360*, 1277–1281. https://doi.org/10.4028/www.scientific.net/AMM.357-360.1277

Hekmatfar, A., Shah, A., Huber, G., McDaniel, R., & Haddock, J. E. (2015). Modifying laboratory mixture design to improve field compaction. *Road Materials and Pavement Design*, *16*(sup2), 149–167. https://doi.org/10.1080/14680629.2015.1077003

Hekmatfar, A. (2016). *Improving the laboratory design of asphalt mixtures to enhance asphalt pavement durability*. Ph.D. dissertation, Purdue University. West Lafayette, IN.

Hohenbichler, M., & Rackwitz, R. (1982). First-order concepts in system reliability. *Structural Safety*, *1*(3), 177–188. https://doi.org/10.1016/0167-4730(82)90024-8

Huang, Y., Bird, R. N., & Heidrich, O. (2007). A review of the use of recycled solid waste materials in asphalt pavements. *Resources, Conservation and Recycling*, *52*(1), 58–73. https://doi.org/10.1016/j.resconrec.2007.02.002

Indiana Department of Transportation (INDOT). (2013a). *Basic design controls*. Indiana Design Manual, Chapter 40. Retrieved from https://www.in.gov/dot/div/contracts/design/Part%203/Chapter%2040%20-%20Basic%20Design%20Controls.pdf

Indiana Department of Transportation (INDOT). (2013b). *Hot mix asphalt paving*. Highway Technician Program Training Manual. Retrieved from https://erms.indot.in.gov/certifiedtechmanuals/View.aspx?contentId=DOT_5404003

Incropera, F. (2007). *Fundamentals of heat and mass transfer*. (6th ed. / Frank P. Incropera [and others]. ed.). Hoboken, NJ: John Wiley.

Jamekhorshid, A., Sadrameli, S. M., & Farid, M. (2014). A review of microencapsulation methods of phase change materials (PCMs) as a thermal energy storage (TES) medium. *Renewable and Sustainable Energy Reviews*, *31*, 531–542. https://doi.org/10.1016/j.rser.2013.12.033

Jin, J., Lin, F., Liu, R., Xiao, T., Zheng, J., Qian, G., Liu, H., & Wen, P. (2017). Preparation and thermal properties of mineral-supported polyethylene glycol as form-stable composite phase change materials (CPCMs) used in asphalt pavements. *Scientific Reports*, *7*(1), 1–10. https://doi.org/10.1038/s41598-017-17224-1

Jin, J., Xiao, T., Zheng, J., Liu, R., Qian, G., Xie, J., Wei, H., Zhang, J., & Liu, H. (2018). Preparation and thermal properties of encapsulated ceramsite-supported phase change materials used in asphalt pavements. *Construction and Building Materials*, *190*, 235–245. https://doi.org/10.1016/j.conbuildmat.2018.09.119

Jin, J., Liu, L., Liu, R., Wei, H., Qian, G., Zheng, J., Xie, W., Lin, F., & Xie, J. (2019). Preparation and thermal performance of binary fatty acid with diatomite as form-stable composite phase change material for cooling asphalt pavements. *Construction and Building Materials*, *226*, 616–624. https://doi.org/10.1016/j.conbuildmat.2019.07.305

Johnson, C.M. (2010). *Estimating asphalt binder fatigue resistance using an accelerated test method*. Ph.D. dissertation, University of Wisconsin-Madison. Madison, WI.

Kakar, M. R., Refaa, Z., Bueno, M., Worlitschek, J., Stamatiou, A., & Partl, M. N. (2019a). Investigating bitumen's direct interaction with Tetradecane as potential phase change material for low temperature applications. *Road Materials and Pavement Design*, *0629*. https://doi.org/10.1080/14680629.2019.1601127

Kakar, M. R., Refaa, Z., Worlitschek, J., Stamatiou, A., Partl, M. N., & Bueno, M. (2019b). Effects of aging on asphalt binders modified with microencapsulated phase change material. *Composites Part B: Engineering*, *173*(June). https://doi.org/10.1016/j.compositesb.2019.107007

Kakar, M. R., Refaa, Z., Worlitschek, J., Stamatiou, A., Partl, M. N., & Bueno, M. (2019c). Thermal and rheological characterization of bitumen modified with microencapsulated phase change materials. *Construction and Building Materials*, *215*, 171–179. https://doi.org/10.1016/j.conbuildmat.2019.04.171

Kheradmand, M., Castro-Gomes, J., Azenha, M., Silva, P. D., De Aguiar, J. L. B., & Zoorob, S. E. (2015). Assessing the feasibility of impregnating phase change materials in lightweight aggregate for development of thermal energy storage systems. *Construction and Building Materials*, *89*, 48–59. https://doi.org/10.1016/j.conbuildmat.2015.04.031

Kodippily, S., Yeaman, J., Henning, T., & Tighe, S. (2018). Effects of extreme climatic conditions on pavement response. *Road Materials and Pavement Design*, *0629*. https://doi.org/10.1080/14680629.2018.1552620

Kumalasari, I., Napiah, M., & Sutanto, M. H. (2018). A review on phase change materials incorporation in asphalt pavement. *Indonesian Journal of Science and Technology*, *3*(2), 171–179. https://doi.org/10.17509/ijost.v3i2.12762

Kutner, M. (2013). *Applied regression analysis*. Boston: McGraw-Hill Create.

Lane, G. (2018). *Solar heat storage. Volume I: Latent heat material* (CRC Revivals).

LaVassar, C., Mahoney, J., & Willoughby, K. (2009). *Statistical assessment of quality assurance-quality control data for hot mix asphalt*. Washington State Department of Transportation WA-RD 686.1. Olympia, WA. Retrieved from http://depts.washington.edu/trac/bulkdisk/pdf/686.1.pdf

Lazaridis, A. (1970). A numerical solution of the multidimensional solidification (or melting) problem. *International Journal of Heat and Mass Transfer*, *13*(9), 1459–1477. https://doi.org/10.1016/0017-9310(70)90180-8

Leckie, J., & Beeson, M. (2018). *HMA spec revisions and testing 2018* [Presentation]. Purdue Road School 2018. West Lafayette, IN: Purdue University. Retrieved from https://docs.lib.purdue.edu/roadschool/2018/presentations/37/

Leng, B., Chen, M., Zheng, S., & Wu, S. (2014). Theoretical and experimental studies on preparation of OMMT-based composite phase change materials used in asphalt pavement. *Key Engineering Materials*, *599*, 355–360. https://doi.org/10.4028/www.scientific.net/KEM.599.355

Lesueur, D., Petit, J., & Ritter, H. J. (2013). The mechanisms of hydrated lime modification of asphalt mixtures: A state-of-the-art review. *Road Materials and Pavement Design*, *14*(1), 1–16. https://doi.org/10.1080/14680629.2012.743669

Li, R., Xiao, F., Amirkhanian, S., You, Z., & Huang, J. (2017). Developments of nano materials and technologies on asphalt materials – A review. *Construction and Building Materials*, *143*, 633–648. https://doi.org/10.1016/j.conbuildmat.2017.03.158

Lin, F., Jin, J., Zheng, J., Shi, B., Huang, C, & Ren, T. (2017). Review on application and research in temperature-adjusting asphalt pavements based on phase change materials. *Materials China*, *36*(6), 467–472. https://doi.org/10.7502/j.issn.1674-3962.2017.06.11

Liston, L. C., Farnam, Y., Krafcik, M., Weiss, J., Erk, K., & Tao, B. Y. (2016). Binary mixtures of fatty acid methyl esters as phase change materials for low temperature applications. *Applied Thermal Engineering*, *96*, 501–507. https://doi.org/10.1016/j.applthermaleng.2015.11.007

Little, D. N., & Petersen, J. C. (2005). Unique effects of hydrated lime filler on the performance-related properties of asphalt cements: Physical and chemical interactions revisited. *Journal of Materials in Civil Engineering*, *17*(2), 207–218. https://doi.org/10.1061/(ASCE)0899-1561(2005)17:2(207)

Lo Presti, D. (2013). Recycled tyre rubber modified bitumens for road asphalt mixtures: A literature review. *Construction and Building Materials*, *49*, 863–881. https://doi.org/10.1016/J.CONBUILDMAT.2013.09.007

Ma, B., Ma, J., Wang, D., & Peng, S. (2011). Preparation and properties of composite shape-stabilized phase change material for asphalt mixture. *Applied Mechanics and Materials*, *71–78*, 118–121. https://doi.org/10.4028/www.scientific.net/AMM.71-78.118

Ma, B., Si, W., Ren, J., Wang, H. N., Liu, F. W., & Li, J. (2014). Exploration of road temperature-adjustment material in asphalt mixture. *Road Materials and Pavement Design*, *15*(3), 659–673. https://doi.org/10.1080/14680629.2014.885462

Ma, B., Zhou, X. Y., Liu, J., You, Z., Wei, K., & Huang, X. F. (2016). Determination of specific heat capacity on composite shape-stabilized phase change materials and asphalt mixtures by heat exchange system. *Materials*, *9*(5). https://doi.org/10.3390/ma9050389

Ma, B., Chen, S.-S., Wei, K., Liu, F.-W., & Zhou, X.-Y. (2019). Analysis of thermoregulation indices on microencapsulated phase change materials for asphalt pavement. *Construction and Building Materials*, *208*, 402–412. https://doi.org/10.1016/j.conbuildmat.2019.03.014

Ma, B., Chen, S., Ren, Y., & Zhou, X. (2020). The thermoregulation effect of microencapsulated phase-change materials in an asphalt mixture. *Construction and Building Materials*, *231*. https://doi.org/10.1016/j.conbuildmat.2019.117186

Mallick, R. B., Radzicki, M. J., Daniel, J. S., & Jacobs, J. M. (2014). Use of system dynamics to understand long-term impact of climate change on pavement performance and maintenance cost. *Transportation Research Record*, *2455*, 1–9. https://doi.org/10.3141/2455-01

Mansell, T. (2021, Jan. 21). Paving fundamentals – quality paving practices [Presentation]. *Workshop 1020: Bridging the Gap Between Paving Fundamentals and New Technology*. Transportation Research Board 2021 Annual Meeting.

Mogawer, W. S., Booshehrian, A., Vahidi, S., & Austerman, A. J. (2013). Evaluating the effect of rejuvenators on the degree of blending and performance of high RAP, RAS, and RAP/RAS mixtures. *Road Materials and Pavement Design*, *14*, 193–213. https://doi.org/10.1080/14680629.2013.812836

Montoya, M. A., Pouranian, M. R., & Haddock, J. E. (2018). Increasing asphalt pavement density through mixture design: A field project. *Asphalt Paving Technology*, *87*, 1–29. https://doi.org/10.12783/aapt2018/33800

National Asphalt Pavement Association (NAPA). (2014). *Fast facts*. Retrieved from https://www.asphaltpavement.org/PDFs/GovAffairs/NAPA%20Fast%20Facts%2011-02-14%20Final.pdf

National Center for Asphalt Technology (NCAT). (2017). Moving towards balanced mix design for asphalt mixtures. *Asphalt Technology New*, *29*(1), 1–5. Retrieved from https://www.eng.auburn.edu/research/centers/ncat/newsroom/2017-spring/balanced-mix.html

Oró, E., de Gracia, A., Castell, A., Farid, M. M., & Cabeza, L. F. (2012). Review on phase change materials (PCMs) for cold thermal energy storage applications. *Applied Energy*, *99*, 513–533. https://doi.org/10.1016/j.apenergy.2012.03.058

Oshone, M., Dave, E. V., Daniel, J. S., & Rowe, G. M. (2020). Assessment of various approaches to determining binder bending beam rheometer low temperature specification parameters from dynamic shear rheometer test. *Asphalt Paving Technology*, *aapt*. https://doi.org/10.12783/aapt2018/33811

Papagiannakis, A., & Masad, E. (2008). *Pavement design and materials*. Hoboken, N.J.: John Wiley.

Pauly, J., Kouakou, A. C., Habrioux, M., & Le Mapihan, K. (2014). Heat capacity measurements of pure fatty acid methyl esters and biodiesels from 250 to 390 K. *Fuel*, *137*, 21–27. https://doi.org/10.1016/j.fuel.2014.07.037

Pielichowska, K., & Pielichowski, K. (2014). Phase change materials for thermal energy storage. *Progress in Materials Science*, *65*, 67–123. https://doi.org/10.1016/j.pmatsci.2014.03.005

Pindyck, R., & Rubinfeld, D. (1998). *Econometric models and economic forecasts*. New York: McGraw-Hill.

Popescu, R., Deodatis, G., & Nobahar, A. (2005). Effects of random heterogeneity of soil properties on bearing capacity. *Probabilistic Engineering Mechanics*, *20*(4), 324–341. https://doi.org/10.1016/j.probengmech.2005.06.003

Pratas, M. J., Freitas, S., Oliveira, M. B., Monteiro, S. C., Lima, Á. S., & Coutinho, J. A. P. (2011). Densities and viscosities of minority fatty acid methyl and ethyl esters present in biodiesel. *Journal of Chemical and Engineering Data*, *56*(5), 2175–2180. https://doi.org/10.1021/je1012235

Prowell, B., Zhang, J., & Brown, E. R. (2005). *Aggregate properties and the performance of Superpave-designed hot-mix asphalt*. Transportation Research Board NCHRP Report 539. Washington. D.C. https://doi.org/10.17226/13844

Prozzi, J. A., & Hong, F. (2008). Transportation infrastructure performance modeling through seemingly unrelated regression systems. *Journal of Infrastructure Systems*, *14*(2), 129–137. https://doi.org/10.1061/(ASCE)1076-0342(2008)14:2(129)

Putman, B. J., & Amirkhanian, S. N. (2004). Utilization of waste fibers in stone matrix asphalt mixtures. *Resources, Conservation and Recycling*, *42*(3), 265–274. https://doi.org/10.1016/j.resconrec.2004.04.005

Rahman, M. T., Mohajerani, A., & Giustozzi, F. (2020). Recycling of waste materials for asphalt concrete and bitumen: A review. *Materials*, *13*(7). https://doi.org/10.3390/ma13071495

Rastogi, M., Chauhan, A., Vaish, R., & Kishan, A. (2015). Selection and performance assessment of Phase Change Materials for heating, ventilation and air-conditioning applications. *Energy Conversion and Management*, *89*, 260–269. https://doi.org/10.1016/j.enconman.2014.09.077

Rathod, M. K., & Kanzaria, H. V. (2011). A methodological concept for phase change material selection based on multiple criteria decision analysis with and without fuzzy environment. *Materials and Design*, *32*(6), 3578–3585. https://doi.org/10.1016/j.matdes.2011.02.040

Refaa, Z., Kakar, M. R., Stamatiou, A., Worlitschek, J., Partl, M. N., & Bueno, M. (2018). Numerical study on the effect of phase change materials on heat transfer in asphalt concrete. *International Journal of Thermal Sciences*, *133*(March), 140–150. https://doi.org/10.1016/j.ijthermalsci.2018.07.014

Ren, J., Ma, B., Si, W., Zhou, X., & Li, C. (2014). Preparation and analysis of composite phase change material used in asphalt mixture by sol-gel method. *Construction and Building Materials*, *71*, 53–62. https://doi.org/10.1016/j.conbuildmat.2014.07.100

Riehm, M., Gustavsson, T., Bogren, J., & Jansson, P. E. (2012). Ice formation detection on road surfaces using infrared thermometry. *Cold Regions Science and Technology*, *83–84*, 71–76. https://doi.org/10.1016/j.coldregions.2012.06.004

Roberts, F. L., Mohammad, L. N., & Wang, L. B. (2002). History of hot mix asphalt mixture design in the United States. *Journal of Materials in Civil Engineering*, *14*(4), 279–293. https://doi.org/10.1061/(ASCE)0899-1561(2002)14:4(279)

Roque, R., Yan, Y., & Lopp, G. (2020). *Evaluation of the cracking performance of asphalt binders at intermediate temperatures*. Florida Department of Transportation. Tallahassee, FL. Retrieved from https://fdotwww.blob.core.windows.net/sitefinity/docs/default-source/research/reports/fdot-bdv31-977-83-rpt.pdf

Rubio, M. C., Martínez, G., Baena, L., & Moreno, F. (2012). Warm mix asphalt: An overview. *Journal of Cleaner Production*, *24*, 76–84. https://doi.org/10.1016/j.jclepro.2011.11.053

Russo, F., Biancardo, S. A., Formisano, A., & Dell'Acqua, G. (2018). Predicting percent air voids content in compacted bituminous hot mixture specimens by varying the energy laboratory compaction and the bulk density assessment method. *Construction and Building Materials*, *164*, 508–524. https://doi.org/10.1016/j.conbuildmat.2017.12.174

Sakulich, A. R., & Bentz, D. P. (2012). Incorporation of phase change materials in cementitious systems via fine lightweight aggregate. *Construction and Building Materials*, *35*, 483–490. https://doi.org/10.1016/j.conbuildmat.2012.04.042

Santos, J., Pham, A., Stasinopoulos, P., & Giustozzi, F. (2021). Recycling waste plastics in roads: A life-cycle assessment study using primary data. *Science of the Total Environment*, *751*, 141842. https://doi.org/10.1016/j.scitotenv.2020.141842

Sassani, A., Ceylan, H., Kim, S., Arabzadeh, A., Taylor, P. C., & Gopalakrishnan, K. (2018). Development of carbon fiber-modified electrically conductive concrete for implementation in Des Moines International Airport. *Case Studies in Construction Materials*, *8*(October 2017), 277–291. https://doi.org/10.1016/j.cscm.2018.02.003

Sharma, A., Tyagi, V. V., Chen, C. R., & Buddhi, D. (2009). Review on thermal energy storage with phase change materials and applications. *Renewable and Sustainable Energy Reviews*, *13*(2), 318–345. https://doi.org/10.1016/j.rser.2007.10.005

Si, W., Zhou, X. Y., Ma, B., Li, N., Ren, J. P., & Chang, Y. J. (2015). The mechanism of different thermoregulation types of composite shape-stabilized phase change materials used in asphalt pavement. *Construction and Building Materials*, *98*, 547–558. https://doi.org/10.1016/j.conbuildmat.2015.08.038

Si, W., Ma, B., Ren, J., Hu, Y., Zhou, X., Tian, Y., & Li, Y. (2020). Temperature responses of asphalt pavement structure constructed with phase change material by applying finite element method. *Construction and Building Materials*, *244*. https://doi.org/10.1016/j.conbuildmat.2020.118088

Smith, M. (2009). *ABAQUS/Standard user's manual, Version 6.9*. Dassault Systèmes Simulia Corp.

Smith, B. C., & Diefenderfer, B. K. (2008). Comparison of nuclear and nonnuclear pavement density testing devices. *Transportation Research Record: Journal of the Transportation Research Board*, *2081*(1), 121–129. https://doi.org/10.3141/2081-13

Srivastava, V., & Giles, D. (1987). *Seemingly unrelated regression equations models: Estimation and inference*. New York: Dekker.

Tofallis, C. (2015). A better measure of relative prediction accuracy for model selection and model estimation. *Journal of the Operational Research Society*, *66*(8), 1352–1362. https://doi.org/10.1057/jors.2014.103

Tian, Y., Ma, B., Liu, F., Li, N., & Zhou, X. (2019). Thermoregulation effect analysis of microencapsulated phase change thermoregulation agent for asphalt pavement. *Construction and Building Materials*, *221*, 139–150. https://doi.org/10.1016/j.conbuildmat.2019.05.184

Tran, M., Turner, P., & Shambley, J. (2016). *Enhanced compaction to improve durability and extend pavement service life: A literature review*. Publication National Center for Asphalt Technology Report No. 16-02R. Auburn, AL. Retrieved from https://eng.auburn.edu/research/centers/ncat/files/technical-reports/rep16-02.pdf

Tschoegl, N. (1989). *The phenomenological theory of linear viscoelastic behavior: An introduction*. Berlin, Heidelberg: Springer Berlin Heidelberg.

Vavrik, W.R., Huber, G.A., Pine, W.J., Carpenter, S.H., & Bailey, R. (2002). *Bailey method for gradation in hot-mix asphalt mixture design*. Transportation Research Board of the National Academies E-C044. Washington, D.C. Retrieved from http://onlinepubs.trb.org/onlinepubs/circulars/ec044.pdf

Wang, H. (2010). Sparse seemingly unrelated regression modelling: Applications in finance and econometrics. *Computational Statistics & Data Analysis*, *54*(11), 2866–2877. https://doi.org/10.1016/j.csda.2010.03.028

Wang, Y. D., Underwood, B. S., & Kim, Y. R. (2020). Development of a fatigue index parameter, Sapp, for asphalt mixes using viscoelastic continuum damage theory. *The International Journal of Pavement Engineering*, 1–15. https://doi.org/10.1080/10298436.2020.1751844

Wang, Z., Xie, J., Gao, L., Liu, Y., & Tang, L. (2021). Three-dimensional characterization of air voids in porous asphalt concrete. *Construction and Building Materials*, *272*. https://doi.org/10.1016/j.conbuildmat.2020.121633

Washington, S., Karlaftis, M., & Mannering, F. (2011). *Statistical and econometric methods for transportation data analysis*. Boca Raton, FL: CRC Press.

Wei, G., Wang, G., Xu, C., Ju, X., Xing, L., Du, X., & Yang, Y. (2018). Selection principles and thermophysical properties of high temperature phase change materials for thermal energy storage: A review. *Renewable and Sustainable Energy Reviews*, *81*(March 2017), 1771–1786. https://doi.org/10.1016/j.rser.2017.05.271

Wei, K., Ma, B., & Duan, S. Y. (2019a). Preparation and properties of bitumen-modified polyurethane solid-solid phase change materials. *Journal of Materials in Civil Engineering*, *31*(8), 1–8. https://doi.org/10.1061/(ASCE)MT.1943-5533.0002795

Wei, K., Wang, Y., & Ma, B. (2019b). Effects of microencapsulated phase change materials on the performance of asphalt binders. *Renewable Energy*, *132*, 931–940. https://doi.org/10.1016/j.renene.2018.08.062

Williams, B.A., Willis, J.R., & Shacat, J. (2020). *Asphalt pavement industry survey on recycled materials and warm-mix asphalt usage: 2019*. Information Series 138 (9th edition). National Asphalt Pavement Association. Retrieved from https://trid.trb.org/view/1746439

Xu, H., Sze, J. Y., Romagnoli, A., & Py, X. (2017). Selection of phase change material for thermal energy storage in solar air conditioning systems. *Energy Procedia*, *105*, 4281–4288. https://doi.org/10.1016/j.egypro.2017.03.898

Yang, X., You, Z., Dai, Q., & Mills-Beale, J. (2014). Mechanical performance of asphalt mixtures modified by bio-oils derived from waste wood resources. *Construction and Building Materials*, *51*, 424–431. https://doi.org/10.1016/j.conbuildmat.2013.11.017

Yavuzturk, C., Ksaibati, K., & Chiasson, A. D. (2005). Assessment of temperature fluctuations in asphalt pavements due to thermal environmental conditions using a two-dimensional, transient finite-difference approach. *Journal of Materials in Civil Engineering*, *17*(4), 465–475. https://doi.org/10.1061/(ASCE)0899-1561(2005)17:4(465)

Yildirim, Y. (2007). Polymer modified asphalt binders. *Construction and Building Materials*, *21*(1), 66–72. https://doi.org/10.1016/j.conbuildmat.2005.07.007

Yusoff, N. I. M., Shaw, M. T., & Airey, G. D. (2011). Modelling the linear viscoelastic rheological properties of bituminous binders. *Construction and Building Materials*, *25*(5), 2171–2189. https://doi.org/10.1016/j.conbuildmat.2010.11.086

Zalba, B., Marín, J. M. a, Cabeza, L. F., & Mehling, H. (2003). Review on thermal energy storage with phase change: materials, heat transfer analysis and applications. *Applied Thermal Engineering*, *23*(3), 251–283. https://doi.org/10.1016/S1359-4311(02)00192-8

Zaumanis, M., Mallick, R. B., Poulikakos, L., & Frank, R. (2014). Influence of six rejuvenators on the performance properties of Reclaimed Asphalt Pavement (RAP) binder and 100% recycled asphalt mixtures. *Computers and Chemical Engineering*, *71*, 538–550. https://doi.org/10.1016/j.conbuildmat.2014.08.073

Zellner, A. (1962). An efficient method of estimating seemingly unrelated regressions and tests for aggregation bias. *Journal of the American Statistical Association*, *57*(298), 348–368. https://doi.org/10.1080/01621459.1962.10480664

Zhang, D., Chen, M., Wu, S., Liu, Q., & Wan, J. (2018). Preparation of expanded graphite/polyethylene glycol composite phase change material for thermoregulation of asphalt binder. *Construction and Building Materials*, *169*, 513–521. https://doi.org/10.1016/j.conbuildmat.2018.02.167